Dynamics of the Tsitsikamma current, with implications for larval transport of chokka squid (*Loligo reynaudii*) on the eastern Agulhas Bank

by

Lisa Hancke

Thesis submitted in fulfilment of the requirements for the

Master of Technology: Oceanography

in the Faculty of Applied Science at the

CAPE PENINSULA UNIVERSITY OF TECHNOLOGY

Supervisors:

Conrad Sparks

Michael John Roberts

Cape Town

February 2010

DECLARATION

I, Lisa Hancke, declare that the contents of this thesis represent my own unaided work, and that the thesis has not previously been submitted for academic examination towards any qualification. Furthermore, it represents my own opinions and not necessarily those of the Cape Peninsula University of Technology.

Hancke — February 2010

Signed — Date

ABSTRACT

The current dynamics along the Tsitsikamma coast is described from a combination of acoustic current measurements, satellite-tracked surface drifters and underwater temperature recordings made between November 2006 and March 2008. The Tsitsikamma coast is largely a Marine Protected Area (MPA) that protects a rich marine biodiversity. The nearshore currents are important in the dispersal of eggs and larvae of many marine species, including the paralarvae of the commercially caught chokka squid, *Loligo reynaudii*. Changes in the environment, including the currents, can affect the successful recruitment of chokka squid, and can bring about large annual fluctuations in biomass that creates economic uncertainty in the squid fishery. Results confirm the existence of a predominantly alongshore current off the Tsitsikamma coast. At Middelbank eastward flow was slightly dominant, with a percentage occurrence of 58% vs. 41% westward flow near the surface. The percentage eastward flow decreased with depth, with 41% vs. 58% westward flow near the seabed. At Thyspunt westward and eastward flow occurred at near equal percentages, but westward flow was slightly dominant throughout the water column. The alongshore current was strongest near the surface during eastward flow (maximum = 141 $cm.s^{-1}$; average = 27 $cm.s^{-1}$), while westward surface currents were weaker (maximum velocity = 78 $cm.s^{-1}$; average = 19 $cm.s^{-1}$). Current speed generally decreased with depth and opposing surface and bottom currents, associated with a thermal stratified water column, were occasionally recorded. The nearshore flow regime was characterised by frequent barotropic alongshore reversals that occurred year round. An increase in strong eastward episodes, and opposing surface and bottom currents during spring and summer months have implications for the dispersal of squid paralarvae during the summer and winter spawning seasons. In summer, the combination of strong eastward pulses in the current and upwelling at the capes favoured dispersal onto the midshelf of the Agulhas Bank. In winter, alongshore oscillations without the offshore displacement associated with upwelling, restricted offshore dispersal which caused surface particles to be retained inshore. Drifter trajectories show that both the eastward and westward nearshore current can link the inshore spawning grounds with the nursery grounds, offshore on the central Agulhas Bank; and that passive, neutrally buoyant material in the surface layer can reach the vicinity of the cold ridge in as little as eight days. The wind-driven processes of upwelling and coastal trapped waves (CTWs), and the influence of the greater shelf circulation are discussed as possible driving forces of variability in the currents off the Tsitsikamma coast. The occurrence of coastal trapped waves during thermal stratification appears to drive the jet-like, eastward pulses in the current, and results suggest that the propagation of CTWs may regulate and even enhance upwelling and downwelling along the Tsitsikamma coast.

ACKNOWLEDGEMENTS

I wish to thank the following institutes for their generous contribution towards this research that forms part of the South African Climate Change and Squid Programme:

- Marine and Coastal Management (MCM) for their financial and logistical support needed to maintain the network of oceanographic monitoring equipment on the Tsitsikamma coast.

- South African Squid Management and Industrial Association (SASMIA) for financial assistance with the field research carried out during the squid fishery's closed-seasons.

- National Research Foundation (NRF), who funded the satellite drifter project (THRIP project 3101).

- Bayworld Centre for Research and Education (BCRE) for financial and logistical support during my studies.

- Cape Peninsula University of Technology for their financial contribution in support of my attendance to the 6th South African Marine Science Symposium (SAMSS).

- SANParks, who supports the long-term oceanographic monitoring programme in the Tsitsikamma National Park, for providing accommodation during field research, and the management and employees of the Tsitsikamma National Park for preserving such a pristine establishment.

- Ray Norse from Norsewood Constructions, who assisted with the research and development of the surface drifters, and who constructed the drifters used in this study.

- The staff of Ocean Blue Adventures for their help with the deployment of drifters at Plettenberg Bay.

- South African Weather Services (SAWS) who provided the meteorological data.

I also want to thank the following individuals for their enthusiasm and support throughout this project:

- My supervisors, Mike Roberts and Conrad Sparks, for sharing ideas and reviewing the progress of this manuscript. I thank them for their patience and encouragement throughout my studies.

- Rick Harding, Marcel van den Berg, Niel Engelbrecht, Bradley Blows, Fiona Duncan, Tammy Morris, Darrel Anders, Niel van den Heever, Alistair Busby; the team of divers and skippers that helped with servicing the network of current meters and temperature recorders off the Tsitsikamma coast. Thanks for keeping me safe, both above and under water.

- The officers and crew of the *RS Algoa,* who assisted with the deployment, retrieval and servicing of the current meter moorings and with drifter deployments at Middelbank.

- Lloyd Duncan and Fiona Cuff for the development of the ADCP Analysis Software (ADAS) that saved me countless hours of data processing.

- Marcel van den Berg for his advice on the processing and analysis of ADCP data and for the SST data at the inshore locations.

- Willem Nel, who assisted with the interpolation of the drifter tracks.

- Wayne Goschen for assistance with the analysis and interpretation of the rotary spectra of the ADCP data.

- Michelle Slabber for the use of the electronic reference library.

- The staff at the Gilchrest Library at Marine and Coastal Management for their assistance with finding numerous references.

- Tony van Dalsen, who provided digital maps of the Robberg and Goukamma MPAs.

- And last, but not least, my friends and family. Thank you for believing in me and encouraging me every step of the way.

DEDICATION

For my dad

"The sea is everything. It covers seven tenths of the terrestrial globe. Its breath is pure and healthy. It is an immense desert, where man is never lonely, for he feels life stirring on all sides."

-Jules Verne, from 20 000 leagues under the sea-

"The weeks passed. We saw no sign either of a ship or of drifting remains to show that there were other people in the world. The whole sea was ours, and, with all the gates of the horizon open, real peace and freedom were wafted down from the firmament itself. It was as though the fresh salt tang in the air, and all the blue purity that surrounded us had washed and cleansed both body and soul. To us on the raft the great problems of civilized man appeared false and illusory – like perverted products of the human mind. Only the elements mattered. And the elements seemed to ignore the little raft. Or perhaps they accepted it as a natural object, which did not break the harmony of the sea but adapted itself to current and sea like bird and fish. Instead of being a fearsome enemy, flinging itself at us, the elements had become a reliable friend which steadily and surely helped us onward. While wind and waves pushed and propelled, the ocean current lay under us and pulled, straight toward our goal."

-Thor Heyerdahl, from Kon-Tiki

TABLE OF CONTENTS

LIST OF FIGURES

LIST OF TABLES

LIST OF APPENDICES

GLOSSARY

Abbreviations	
ADCP	Acoustic Current Doppler Profiler
EEZ	Exclusive Economic Zone
MPA	Marine Protected Area
SST	Sea surface temperature
TNP	Tsitsikamma National Park
UTR	Underwater temperature recorder
WTH	Western Transport Hypothesis

Terms	Definition
Eulerian measurements	Eulerian techniques measure the velocity of water at a fixed position. The velocity of flow can be measured using moored current meters or ship mounted current meters.
Jet current	A swift and narrow ocean current that is associated with high variability.
Lagrangian measurements	*Lagrangian techniques measure the position of a parcel of* water in the ocean by following it. The position can be determined using surface or subsurface drifters, or chemical tracers.
No-take marine reserve	A Marine Protected Area where all fishing activities are prohibited
Paralarvae	The planktonic life stage of cephalopods. In this study paralarvae are assumed to be passive drifting, neutrally buoyant biological matter with a lifespan of 30 days.

CHAPTER 1
GENERAL INTRODUCTION AND LITERATURE REVIEW

1.1 General introduction

1.1.1 Research problem

The Tsitsikamma coast, situated on the South African south coast (Figure 1.1), is home to a pristine marine ecosystem that has largely been protected from commercial and recreational exploitation since the establishment of the Tsitsikamma National Park (TNP) in 1964. The area is known for its breathtaking scenery that includes indigenous coastal forests, mountain fynbos, coastal river gorges, estuarine and marine systems. The TNP protects a rich marine biodiversity, including 202 fish species from 84 families (Buxton and Smale 1984, Wood *et al.* 2000), many of which are slow growing with a high degree of residency (Cowley *et al.* 2002, Brouwer *et al.* 2003). Chokka squid (*Loligo reynaudii*), a fast growing and highly mobile cephalopod, also spawns within the TNP (Sauer 1995) and, like most marine organisms, have planktonic larvae that are distributed over great distances by the currents.

A narrow, jet current has been observed off the Tsitsikamma coast (Roberts and van den Berg 2005). This current (from here on referred to as the Tsitsikamma current) is of interest given its role in the transport of marine eggs and larvae from the TNP to surrounding areas. The South African squid fishery is concentrated on the narrow eastern Agulhas Bank (Figure 1.1) where sexually mature individuals form large spawning aggregations in shallow (< 60 m) bays between Plettenberg Bay and Cape Padrone (Augustyn *et al.* 1994). Roberts (2005) showed that this discrete spawning location has bottom temperature and bottom dissolved oxygen ranges that favours the embryonic development of benthic squid eggs, and linked annual fluctuations in chokka squid biomass to variability in the Agulhas Bank ecosystem.

The inshore spawning grounds of chokka squid are situated to the west of an oceanographic feature known as the cold ridge (Figure 1.2). This body of cool water extends offshore across the central and eastern Agulhas Bank and has been described as an intermittent upwelling filament that originates at the Knysna–Tsitsikamma coast (Roberts 2005). It is more prominent during summer months (Boyd and Shillington 1994) and is associated with elevated copepod biomass (Verheye *et al.* 1994), which is the preferred food of newly hatch squid paralarvae (Augustyn 1994, Venter 1999) and considered essential to their early survival and recruitment.

The main spawning ground for chokka squid, inshore on the eastern Agulhas Bank, and the optimum feeding grounds for squid paralarvae, offshore on the central Agulhas Bank, are therefore separated by a distance of about 200 km. This geographical mismatch led to the

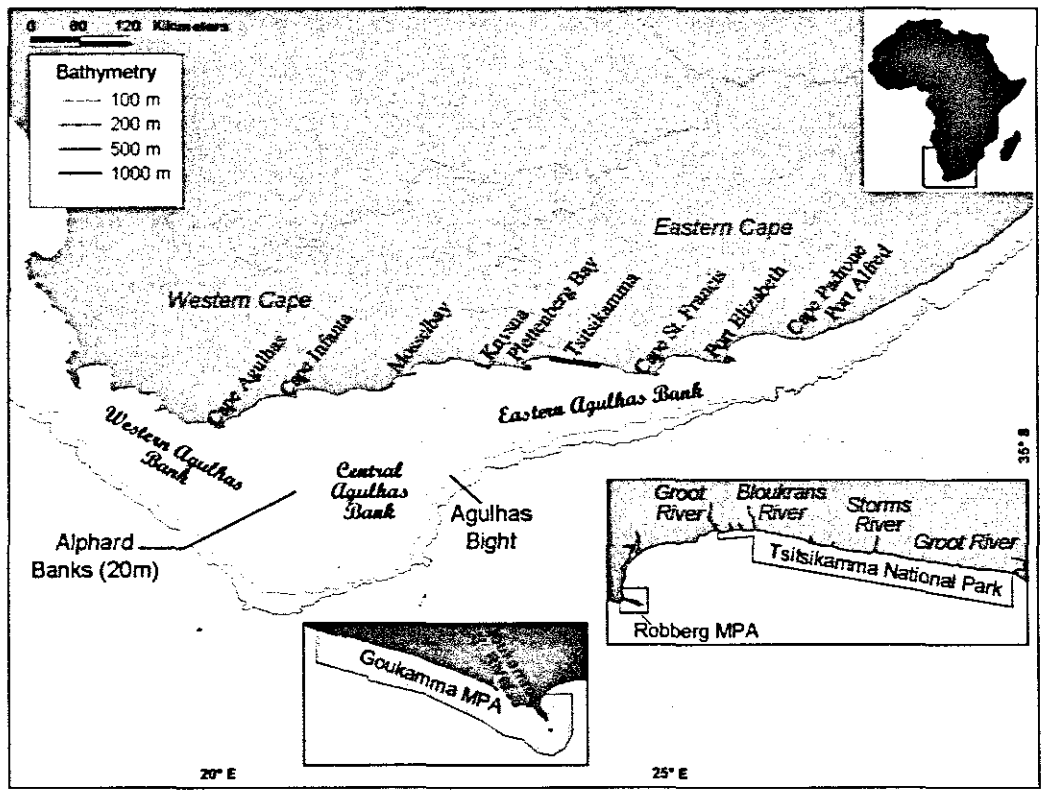

Figure 1.1: A map of the study area showing the coastal provinces of the Western and Eastern Cape, Marine Protected Areas near the Tsitsikamma coast (insets) and the bathymetry of the Agulhas Bank. The shelf break occurs between the 200 – 1000 m isobaths.

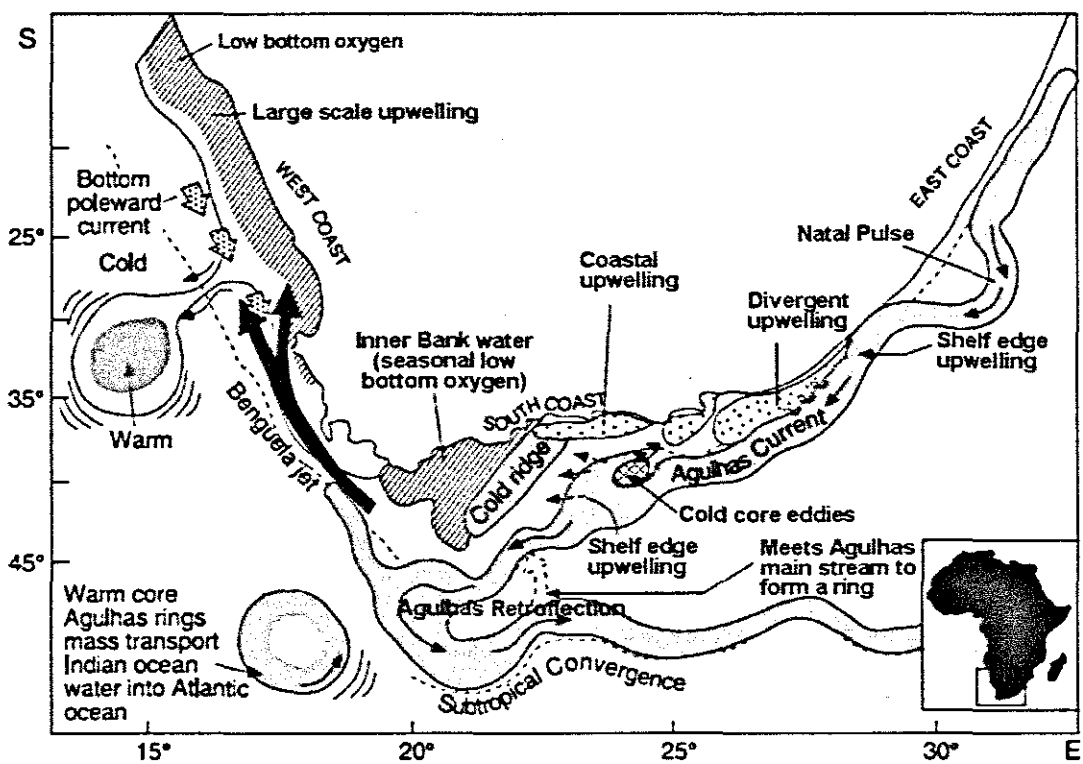

Figure 1.2: The main oceanographic features of South Africa and the Agulhas Bank. Adapted from Roberts (2005).

formulation of the Western Transport Hypothesis (WTH) (Roberts 2005), which states that newly hatched paralarvae improve their chances of survival by being transported westward to the copepod maximum by the net barotropic flow over the mid-shelf (Boyd *et al.* 1992).

Further investigation by Roberts and van den Berg (2005) analysed 12 months of current measurements made by an Acoustic Current Doppler Profiler (ADCP) moored in the TNP. Their results showed the existence of a strong (> 1 $m.s^{-1}$), intermittent current along the Tsitsikamma coast that flows mainly eastwards. This finding complicates the WTH (Roberts 2005), because an eastward current carries passively drifting paralarvae away from the food maxima at the cold ridge. Roberts and van den Berg (2005) subsequently revised the WTH to only be relevant during westward flow along the Tsitsikamma coast. They proposed that eastward flow moves squid paralarvae away from the optimum food source of the cold ridge, either resulting in a lengthier circulation on the eastern Agulhas Bank or continued transport towards Algoa Bay, from where paralarvae could be lost to the Agulhas Current.

1.1.2 Aims and objectives

This thesis continues the research of Roberts (2005) and Roberts and van den Berg (2005), investigating in detail the dynamics of the Tsitsikamma current from a combination of Eularian and Lagrangian current measurements. Three bottom-mounted ADCP moorings, deployed off the Tsitsikamma coast, provided data on the dynamics of the Tsitsikamma current. The deployment of Lagrangian drifters provided data on actual displacement and potential transport routes for squid paralarvae. Underwater temperature recorders (UTRs) were used to measure vertical and horizontal temperature gradients in the nearshore regions. These data allowed the dynamics of the Tsitsikamma current, including seasonality, driving forces and larval transport potential to be examined.

1.1.3 Key questions

The key questions addressed in this thesis are:

- What area is affected by the Tsitsikamma current, *i.e.*, what is the width of the current, where does it start and where does it end?
- Is the Tsitsikamma current seasonal?
- What are the driving forces of the Tsitsikamma current?
- Does the Tsitsikamma current link the inshore spawning grounds with the offshore nursery grounds in the vicinity of the cold ridge?
- How long does it take for passively drifting material to move from the Tsitsikamma coast to the region of the cold ridge?
- What are the implications of the Tsitsikamma current for the transport of paralarvae and the recruitment success of chokka squid on the eastern Agulhas Bank?

1.2 Literature review

1.2.1 Boundary currents

The Agulhas Current flows poleward along the east coast of South Africa and forms the western limb of the South Indian Ocean gyre. In the northern regions, the trajectory of the Agulhas Current is stabilized by the abrupt bathymetry of the continental slope (de Ruijter *et al.* 1999). Here the current is fast (> 2 $m.s^{-1}$) and the core is normally situated on the seaward side of the shelf break, about 40 - 50 km from shore (Schumann 1981). Occasionally, a solitary meander, called a Natal Pulse, originates in the Durban Bight (Lutjeharms and Roberts 1988) and moves downstream at approximately 20 km/day, displacing the current core up to 200 km offshore (Harris *et al.* 1978, Gründlingh 1979, Gründlingh 1986). Past Port Alfred, the continental shelf widens considerably and the southern Agulhas Current follows the shelf break away from the coast. The southern part of the Agulhas Current is distinctly different from the northern part and is characterised by a greater tendency to meander (Lutjeharms 2006). At the southern tip of the continental shelf the Agulhas Current undergoes a dramatic retroflection, flowing eastwards into the South Indian Ocean (Lutjeharms and van Ballegooyen 1988) as the Agulhas Return Current. At times the Agulhas Current continues west, past the African continent, and into the South Atlantic Ocean. Leakage of warm, saline Indian Ocean water into the cooler Atlantic Ocean occurs at the Agulhas Current Retroflection, with the periodic shedding of Agulhas Rings (Lutjeharms 1981, Gordon 1985, Lutjeharms and van Ballegooyen 1988).

The west coast of South Africa, including the western Agulhas Bank, is part of the Benguela upwelling system, one of the world's largest wind-driven upwelling systems (Parrish *et al.* 1983 cited by Boyd and Nelson 1998). In summer, strong air pressure gradients between the South Atlantic High pressure cell and a heat induced low, over the interior, creates south-easterly winds that drive upwelling along the west coast. To the south, the Benguela Current is fed by the South Atlantic Current (Shannon 2001) and by leakage from the Indian Ocean through Agulhas Rings (Lutjeharms and van Ballegooyen 1988). The Benguela Current is generally weak, with an average velocity of ~ 17 $cm.s^{-1}$ (Shannon 1985). Northward flowing jet currents (~ 75 $cm.s^{-1}$) develop in the frontal zones (Bang and Andrews 1974, Boyd *et al.* 1992) and increase the transport potential of the Benguela Current. A detailed overview of the principle characteristics of the Benguela Upwelling System is given by Shannon and Nelson (1996).

1.2.2 The Agulhas Bank

The Agulhas Bank is the large, triangular extension of the continental shelf where water from the warm Indian Ocean and the cold Atlantic Ocean meet. It is a dynamic region, strongly influenced by the proximity of the Agulhas Current. The Agulhas Bank is part of South

Africa's Exclusive Economic Zone (EEZ) and, besides its oil and gas fields, supports a high marine biomass and species diversity (Hutchings 1994). It is the spawning ground for small pelagics (Barange *et al.* 1998, van der Lingen *et al.* 2001, Armstrong *et al.* 1991) and the centre of abundance for numerous warm temperate species, including several endemic sparids (Hutchings *et al.* 2002). Chokka squid (*Loligo reynaudii*) is a key component in the Agulhas Bank ecosystem (Lipinski 1992) and one a major generators of income for people of the impoverished and drought stricken Eastern Cape.

1.2.2.1 Bathymetry

The Agulhas Bank is the broad (~ 800 km), shallow (< 200 m) part of the continental shelf that extends away from the South African shoreline in a roughly triangular shape (Figure 1.1). The shelf break occurs at the 200 m isobath, from where the bathymetry drops steeply to below 1000 m. The shallow Alphard Banks (21 °E) in the central region divides the Agulhas Bank into a relatively steep and narrow western side, and a wider eastern side with a more gradual shoreward gradient (Lutjeharms 2000). Approximately 60% of the Agulhas Bank consists of hard substratum, and high profile reefs are found both close inshore and extending offshore, south of Cape Agulhas (Hutchings 1994). At the eastern extremity of the Agulhas Bank, near Port Alfred, the shelf break is only about 35 km offshore. The continental shelf widens gradually in a westward direction and at its apex the shelf break is found approximately 250 km south of Cape Infanta.

1.2.2.2 Oceanography of the central and eastern Agulhas Bank

The influence of the Agulhas Current is greatest on the eastern extremity of the Agulhas Bank where the shelf is narrowest. A widening shelf leads the current away from the coast (Grūndlingh 1983, Schumann 1987). Meanders, eddies and attendant warm water plumes regularly form on the landward side of the southern Agulhas Current, because of the horizontal shear between the swift moving current core and the water over the adjacent shelf region (Lutjeharms 1981). These shear edge features often intrude onto the shelf along the southeastern side of the Agulhas Bank. Lutjeharms *et al.* (1989) showed that meanders in the Agulhas Current increase in size as they move downstream and that cyclonic eddies are generally concentrated in the eastward facing Agulhas Bight south of Mossel Bay. Associated plumes of warm, saline Agulhas Current water are known to extend over large parts of the Bank, even intruding into embayments on the south coast (Goschen and Schumann 1994).

The divergence of the Agulhas Current from the coast, north of Port Alfred, induces a semi-permanent upwelling cell (Walker 1986, Lutjeharms *et al.* 2000). Cold water (< 17 °C) from this area can persist at the sea surface for several weeks and may be advected westwards over large parts of the Agulhas Bank (Walker 1986) and into adjacent bays (Beckley 1988,

Shumann *et al.* 1988). Several of mechanisms have been proposed to account for shelf edge upwelling that lifts cold bottom water onto the Agulhas Bank. These include upslope veering of the bottom layer of the current due to sidewall friction (Hsueh and O'Brien 1971 as cited by Lutjeharms *et al.* 1989), cross current Ekman transport caused by sustained wind stress (Swart and Largier 1987), and vertical advection in cyclonic border eddies (Lutjeharms *et al.* 1989, Goschen and Schumann 1994).

The cold basal layer on the eastern Agulhas Bank slowly moves westward (Largier and Swart 1987) along the 100 m isobath (Lutjeharms 2006), spreading nutrient rich water over the Bank. At the same time warm Agulhas Current intrusions continuously feed the surface water on the shelf, creating a well mixed surface layer on top of the cold bottom layer. Schumann and Beekman (1984) observed seasonal differences in the vertical temperature structure over the Agulhas Bank with a deep, well mixed surface layer (0 – 80 m) and little variation in temperature in winter, and in contrast, intense thermoclines in the upper 80 m during summer months. The increased solar heating and a reduction in wind strength in summer helps to intensify stratification and has implications for the vertical distribution of phytoplankton (Carter 1987). With the onset of winter storms, the thermocline is broken down and a deep, well-mixed, surface layer returns.

Various authors including Lutjeharms *et al.* (1981), Walker (1986), Largier and Swart (1987) have noted the upward doming of the thermocline over the central Agulhas Bank and the resultant occurrence of a subsurface ridge of cold water, associated with increased biological production (Figure 1.3). Boyd and Shillington (1994) described this upwelling feature as an intermittent, subsurface ridge of cool water of variable width, and suggested that it is forced by the divergence of surface water related to the widening of the shelf between Port Elizabeth and Knysna. Walker (1986) used satellite observations to analyse upwelling on the south coast and found that abnormally high occurrence of easterly winds over the Agulhas Bank resulted in the advection of cold water tongues westward and offshore along the 100 m isobath. The link between cold ridge formation and wind-driven coastal upwelling was further supported by Roberts (2005) who described the cold ridge as an upwelling filament frequently found off Knysna. He showed that intense summer upwelling leads to greater cold ridge stability.

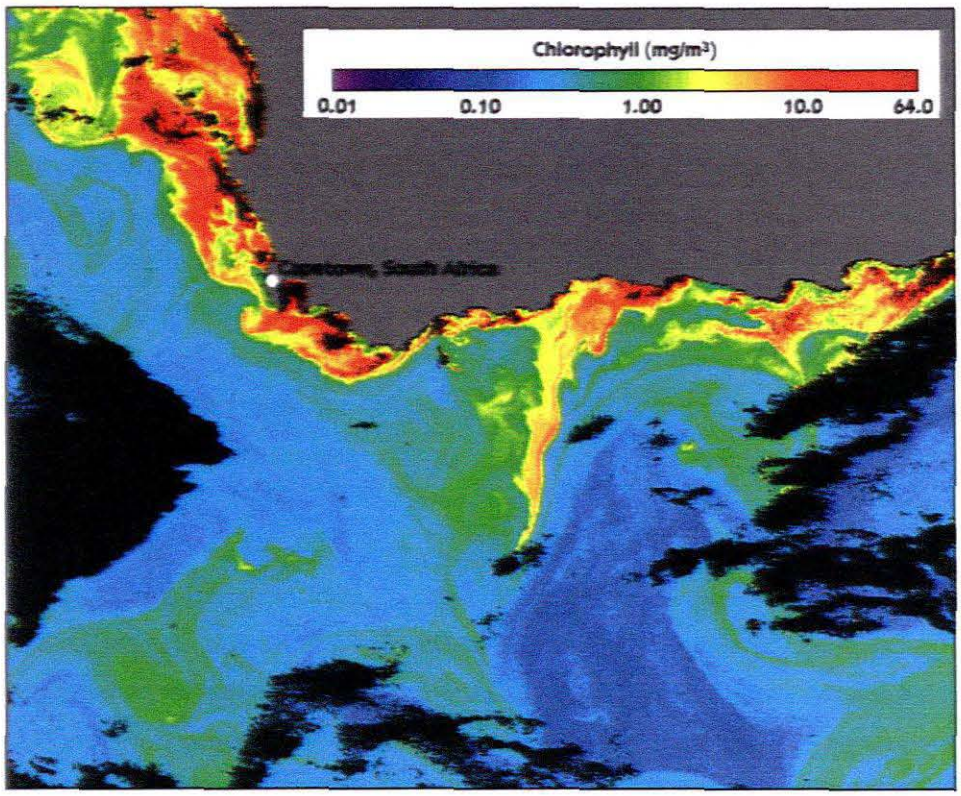

Figure 1.3: The cold ridge can be identified from satellite imagery by an elongated tongue of elevated chlorophyll on the central Agulhas Bank.

Wind-driven coastal upwelling occurs at prominent capes and headlands on the cape south coast, between Cape Seal at Plettenberg Bay and Cape Recife at Port Elizabeth (Schumann 1982). Upwelling occurs frequently during summer and autumn months when the percentage of easterly component winds increase (Schumann and Martin 1991, Jury 1994, Tilney *et al.* 1996). Easterly winds act on the surface layer of the ocean, deflecting water offshore because of Coriolis force — an apparent force that divert wind-driven currents to the left of the wind in the southern hemisphere. The result is a net movement of surface water at right angles to the direction of the wind, known as Ekman transport. Cold, dense, subsurface water is lifted towards the coast, to compensate for the offshore loss of surface water during Ekman transport. This newly upwelled water is rich in nutrients that drive primary productivity along the coast.

The thermocline separates the warm surface water (offshore) from the cold upwelled water (inshore). Longshore currents are generated at the frontal zone because of an offshore pressure gradient, and a cold longshore current is generally associated with upwelling along the south coast. Schumann (1982) explained how the difference in water depth between the northern (bayside) and southern (seaward) side of prominent capes creates a zone of divergence that enhances upwelling during easterly winds. Consequently, upwelling starts at the capes and progresses westwards with the alongshore upwelling current (Schumann 1982).

1.2.2.3 Shelf currents

The circulation on the Agulhas Bank is determined by local wind forcing and by the Agulhas Current (Schumann and Perrins 1983, Walker 1986). The mean flow over the greater part of the Agulhas Bank is in a south-westward direction (Boyd *et al.* 1992), parallel to the bathymetry and the trajectory of the southern Agulhas Current. Meanders and border eddies are regularly observed in the southern Agulhas Current and are thought to be caused by baroclinic instabilities (Wells *et al.* 2000). On the central and eastern Bank eastward flow occurs in cyclonic border eddies on the shelf edge and their associated reverse plumes (Lutjeharms *et al.* 1989, Boyd and Shillington 1994).

Currents on the central Bank are generally weak and there is evidence of cyclonic flow (Boyd *et al.* 1992) around the subsurface ridge of cold water (Swart and Largier 1987), offshore between Cape Agulhas and Mossel Bay, which retains and concentrates plankton in the area. This cyclonic flow is most intense in summer when easterly winds dominate (Hutchings 1994) and the cold ridge becomes quasi-permanent (Roberts 2005). Early studies of the circulation on the eastern Agulhas Bank suggest that there is a nearshore counter current between Mosselbay and Cape St. Francis (Shannon 1970, Boyd *et al.* 1992, Hutchings 1994,

Roberts and van den Berg 2005). This current is not always present and is variable throughout the year (Schumann 1987, Boyd and Shillington 1994).

1.2.3 Regional weather

1.2.3.1 Seasonal influences on South African weather patterns

South Africa is located in the subtropics and is influenced by atmospheric weather systems both from the tropics, to the north and from the temperate latitudes, to the south (Preston-Whyte and Tyson 1988). Air heated in the tropics moves south and descends at about 30 °S to form two semi-permanent high pressure cells, one on either side of the African continent. These anticlockwise rotating air-masses are known as the South Atlantic Anticyclone and the South Indian Anticyclone, respectively. Their centres have a seasonal latitudinal variation of approximately 6° (Preston-Whyte and Tyson 1988) that results in marked differences between summer and winter weather patterns over southern Africa (Figure 1.4). South of 30 °S, a band of low pressure cells, associated with cold fronts and strong westerly winds, circulate the globe from west to east. The effect of the westerly storm belt on the South African weather depends on the seasonal position of the South Atlantic Anticyclone and the South Indian Anticyclone.

In summer, the position of the South Atlantic Anticyclone, south of the African continent, (Figure 1.4a) creates a pressure gradient with the heat induced low over the interior of South Africa. This pressure gradient drives strong south-easterly and easterly winds along the South African seaboard. Occasional "bud-off" high pressure cells move eastward along the south coast, causing strong easterly winds, east off Cape Agulhas (Walker 1986) that prevail for periods of 3 – 5 days. When the high pressures systems and their associated easterly winds weaken, cold fronts from the westerly storm belt occasionally reach the African subcontinent, and travel eastwards along the south coast until they are deflected south by the Indian Ocean Anticyclone. Localised coastal lows originate on the west coast and travel from west to east around the coast ahead of these cold fronts. Both low pressure systems produce warm north-westerly winds before the front arrives, and southwesterly winds as the front passes. The southwesterly winds normally subside before the onset of an easterly wind, associated with the formation of the next high pressure system.

In winter, the South Atlantic and the South Indian Anticyclones move north, thus allowing the low pressure systems of the westerly storm belt to reach further into the interior of South Africa (Figure 1.4b). Cold fronts accompanied by strong north-westerly to westerly winds and rain move across South Africa from west to east, typically following a seven day weather sequence (Preston-Whyte and Tyson 1988) in the Western Cape.

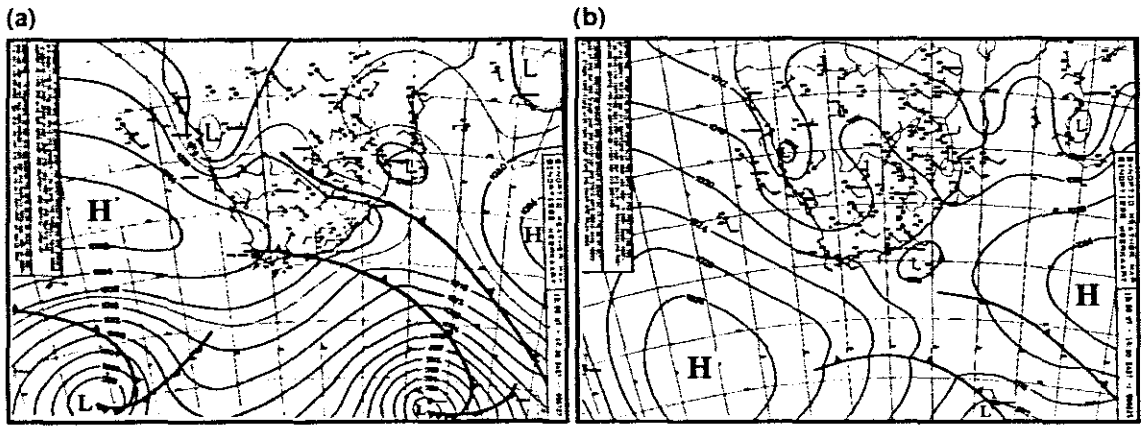

Figure 1.4: Seasonal synoptic charts, showing the position of the South Atlantic and Indian Ocean Anticyclones (a) during summer and (b) winter. (Adapted from Morgan 2010)

1.2.3.2 South coast climate

The Tsitsikamma coast is situated on the Cape south coast between two climatic regions: a Mediterranean climate with winter rainfall in the west, and a subtropical climate with summer rainfall in the east. The coast between these two regions has a temperate climate with warm summers and mild winters. The mean monthly air temperature recorded at Storms River Mouth over a 12 year period (1992 – 2003) ranged from a minimum of 10 - 18 °C and a maximum of 19 – 25 °C (Tsitsikamma National Park management plan 2006). Humid sea winds from the Indian Ocean bring rainfall on the weather side of the mountain slopes. An annual rainfall of 1000 mm falls throughout the year, with a lower rainfall from April to August. However, the region is currently experiencing the worst drought in more than 100 years thought to be associated with long-term climate change and below-normal sea temperatures on the Agulhas Bank (Jury and Levey 2006).

The wind along the south coast is predominantly alongshore. The principle axis is site specific and influenced by coastline topography and the land-sea interface (Schumann and Martin 1991). Westerly winds dominate throughout the year, while the occurrence of easterly winds increases during summer and autumn months, when the band of maximum anticyclonic activity has moved south (Taljaard 1972 cited by Schumann *et al.* 1982). Wind variability on the south coast occurs at shorter periods than on the west coast. Schumann (1999) found alongshore winds to fluctuate at periods ranging between two and six days on the south coast, while on the west coast variability occurred at periods between six and ten days. The greater variability along the south coast is attributed to smaller more localized coastal lows that are not associated with the cyclonic belt south of the continent (Schumann 1989). This increased variability along the south coast has implications for primary productivity associated with wind-driven, coastal upwelling (Schumann 1999).

1.2.4 South African squid fishery

The South African squid jig fishery is based in the impoverished south-eastern Cape and is one of the largest generators of employment and foreign revenue in the region (Augustyn 1990). Annual squid catches range between 2500 and 10 000 tons, with an annual catch average of approximately 7000 tons (Marine and Coastal Management, Commercial Squid Fisheries Data). The hand-line jig fishery is labour intensive and provides employment for nearly 3 000 people, including land based personnel. The majority of the catch is exported and the squid fishery generates about R180 million per year (DEAT Squid Policy 2005).

1.2.4.1 History

Until the mid-1980s almost all squid catches in South African waters were made by demersal trawlers (Augustyn 1986) from Asia, to satisfy the growing demand for the seafood delicacy, know as calamari. Foreign fishing activity was gradually phased out with the establishment of South Africa's Exclusive Economic Zone (EEZ) and excluded completely in 1993.

Large scale, local exploitation of the resource started in 1983 with the establishment of the lucrative hand-line jig industry in the Eastern Cape towns of St. Francis Bay and Jeffery's Bay. At first, fishing was done from ski boats and small deck boats. But bigger vessels with onboard freezers ranging up to 30 m soon joined the fleet, increasing the quality of the catch and the efficiency of the smaller boats (Augustyn 1986). In the early days, the fishery was largely unregulated and catches grew rapidly amongst fears that the resource could collapse under the increasing fishing effort (Augustyn 1986). A permit system, which limited the number of fishing vessels and crew operating in the fishery, was introduced in 1987, and in 1988 a comprehensive one month closed-season was introduced to protect female squid at the height of the spawning season in November (Augustyn *et al.* 1992). More recently, large fluctuations and a general decline in annual squid catches have led to additional closed fishing seasons in March/April and July/August (Government Gazette 2008) in an attempt to protect the spawning stock.

1.2.4.2 Biology and life cycle

Chokka squid (*Loligo reynaudii*) are distributed over most of the South African continental shelf, between the Namibian border on the west coast and Port Alfred on the southeast coast (Augustyn 1989). Most of the biomass is concentrated on the Agulhas Bank at depths shallower than 200 m (Roberts and Sauer 1994). The main spawning grounds are situated inshore on the south coast between Plettenberg Bay and Port Alfred (Augustyn 1990), where large schools of mature males and females aggregate in shallow bays to reproduce and lay benthic egg capsules. The squid jig fishery is also based here, with line fishermen targeting the spawning aggregations to maximize their catch.

Chokka is a short-lived species that completes its entire life cycle in less than 18 months (Augustyn and Roel 1998). The life history of chokka squid on the Agulhas Bank (Figure 1.5) is described in detail by Augustyn *et al.* (1992) and Augustyn *et al.* (1994). It includes a benthic egg phase, a passive and active planktonic phase and maturity at the age of about nine months (Roberts pers comms).

A summary of the life history of chokka squid is given below:

Eggs

The eggs of *Loligo reynaudii* are ovate (2.8 mm long and 2 mm wide) and yolky in appearance (Augustyn *et al.* 1994). About 120 eggs are arranged in a spiral within a gelatinous egg capsule (Augustyn 1989). These translucent egg capsules are soft, finger-shaped, and bright orange in colour (Figure 1.6a). Egg capsules are attached to the substratum and individual capsules are joined to form larger clusters. These clusters, or egg beds, can range in size from a few strands to more than 6 m in diameter (Augustyn *et al.* 1994). The preferred substrates for egg deposition appear to be low profile reef and fine sandy areas between reefs (Sauer *et al.* 1992). The hatching time of eggs depend on the water temperature. Laboratory experiments by Oosthuizen *et al.* (2002b) showed an optimum temperature range for embryonic development between 12 °C and 17 °C, with approximate hatching times of 50 days and 26 days respectively. Outside this optimal temperature range abnormal embryonic development occurred with mortality. Oosthuizen *et al.* (2002b) found that upwelling in the spawning areas has a negligible effect on the successful development of squid eggs.

Paralarvae

Knowledge of the natural behaviour of paralarvae is limited and most existing information comes from laboratory experiments (Vidal *et al.* 2002, Vidal *et al.* 2005, Oosthuizen *et al.* 2002a, Oosthuizen *et al.* 2002b, Martins in press). Newly hatched chokka squid or paralarvae, are not completely developed (Figure 1.6b) and appear to have a passive, planktonic existence (Augustyn *et al.* 1994). Starved hatchlings have enough internal yolk to survive for up to six days at 16 °C (Vidal *et al.* 2005), with longer survival rates expected at lower temperatures. Once the yolk is consumed their survival depends entirely on their ability to catch appropriate food. Paralarvae feed on copepods, mysids and other crustaceans of similar size (Augustyn *et al.* 1992).

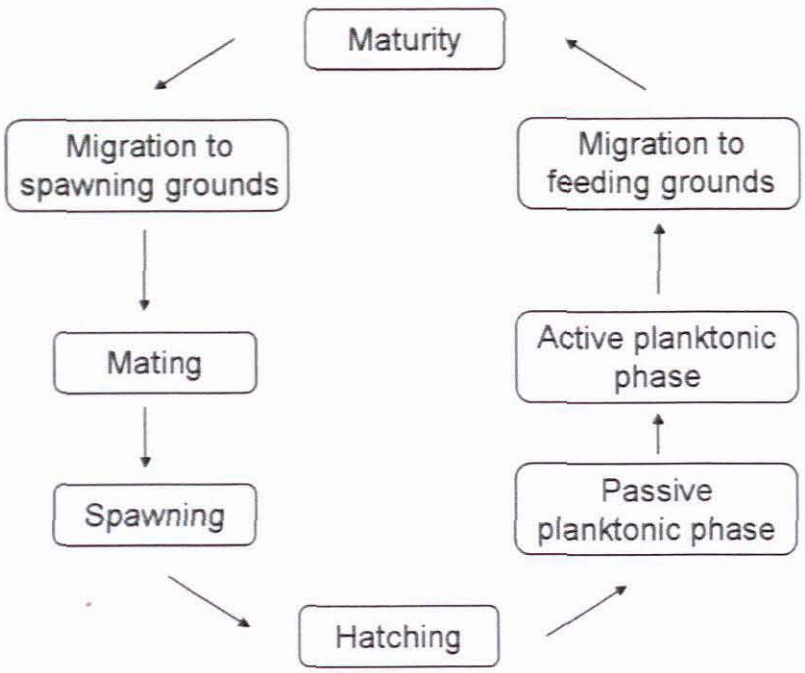

Figure 1.5: Schematic representation of the various phases of the life cycle of chokka squid. Recreated from Augustyn *et al.* (1992).

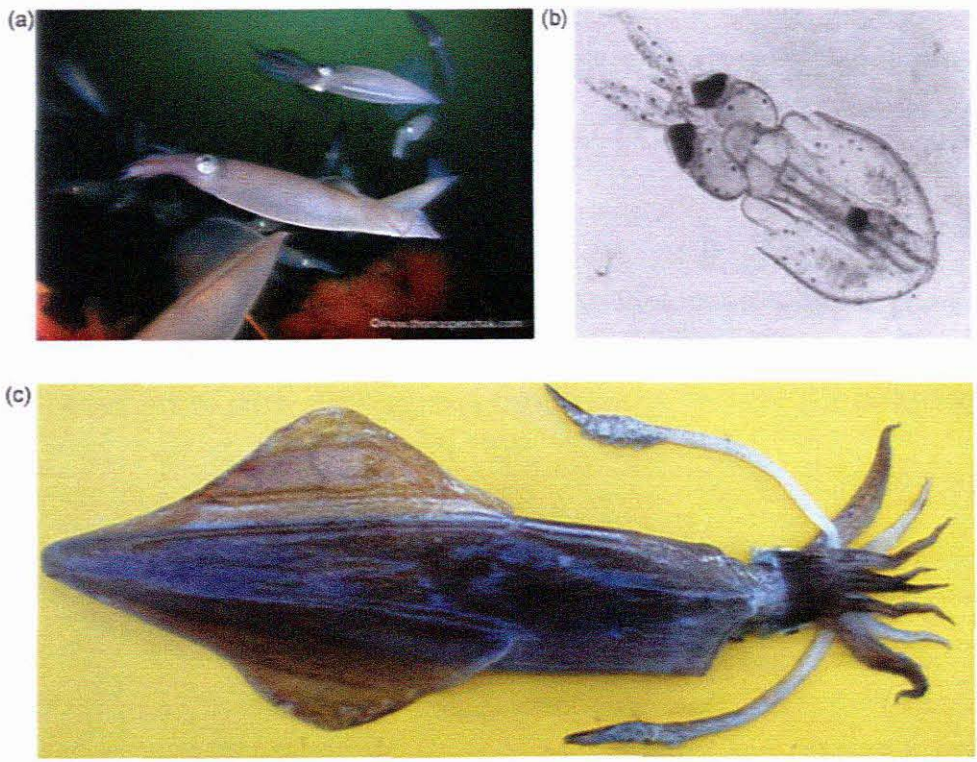

Figure 1.6: Some of the stages of the chokka squid (*Loligo reynaudii*) life cycle: (a) squid spawning above an egg bed, (b) a newly hatched squid paralarvae with internal yolk sac and (c) an adult squid.

It is not known when young squid begin to swim. Augustyn *et al.* (1992) assumed that horizontal movement is severely restricted during the first two months of existence. Squid paralarvae are negatively buoyant (Martins *et al.* in press) and in quiescent water, have to jet continuously to maintain their vertical position in the water column (Augustyn *et al.* 1992). However, new hatchlings in a laboratory experiment swam near the surface for two to three days before moving deeper (Vidal *et al.* 2005). It was thought that the initial buoyancy is derived by the greater yolk weight to body weight ratio of new hatchlings (Vidal *et al.* 2002).

Chokka squid paralarvae are distributed over large areas of the South African continental shelf, with the greatest concentrations near the upwelling zones at the coastal spawning grounds in the main summer spawning season (Augustyn *et al.* 1994). Surviving the early life stages depends on the prey catching ability and predator avoidance skills of squid paralarvae.

Juvenile and adult squid

Juvenile squid of 20 – 80 mm mantle length (ML) are present throughout the year on the south coast at depths between 30 m and 150 m (Augustyn *et al.* 1989). Juveniles feed on larger crustaceans and fish larvae (Augustyn *et al.* 1994), and by the time they reach a mantle length of 100 mm they feed almost exclusively on fish (Lipinski 1987). Size at maturity is highly variable and depends on the geographic location and the time of year (Augustyn 1990). Males can be mature at mantle lengths as small as 90 mm, or immature at 250 mm. In females the range is narrower at 100 – 180 mm ML (Augustyn 1989).

Spawning

Mature squid migrate inshore in sexually discreet schools (Sauer *et al.* 1992) to reproduce. On the spawning grounds, individuals pair up and move together to the substrate where the females deposit their egg capsules. Males outnumber females by a ratio of 2:1 (Sauer 1991) and lone sneaker males often intercept pairs moving to and from the communal egg bed. Squid are serial spawners (Melo and Sauer 1999). Histological analysis (Sauer and Lipinski 1990) suggests that individuals may spawn over a period of weeks to months. Sporadic spawning takes place throughout the year (Sauer 1991), but generally there are two peak periods, one in spring/early summer and another in autumn/winter (Augustyn *et al.* 1994).

CHAPTER 2
METHODS AND MATERIALS

2.1 Study area

The Tsitsikamma coast is located in the southern Cape, between Plettenberg Bay and Cape St. Francis (Figure 2.1). A large part of the coastline (*c.* 70 km) became protected in 1964 with the proclamation of the Tsitsikamma National Park (TNP), Africa's oldest and largest marine reserve (Robinson and de Graaff 1994). The marine section of the TNP covers an area of 340 km^2, extending from the high water mark up to three nautical miles (5.5 km) offshore between Groot Rivier (east) at Nature's Valley and Groot River (west) at Oubos. The relatively straight Tsitsikamma coastline is orientated in an east-west direction (primary axis at 100° - 280°) for more than 100 km, and is exposed to strong wave action. Sheer cliffs rise vertically to a height of about 180 m above sea level before the topography flattens onto a ravine cut coastal plateau that extends for approximately 8 km to the base of the Tsitsikamma Mountain Range (Toerien 1976). The sea cliffs continue below the water line and inside the TNP a depth of 90 m is found less than four nautical miles from shore.

Below this, the water depth decreases more gradually towards the shelf break at 200 m depth. The subtidal area of the TNP is a combination of soft bottom sediments (*c.* 79 %) and dispersed gravel platforms and rocky reefs (*c.* 21 %) (Flemming *et al.* 1986). In the east, at Cape Seal, a depth of 100 m is found only 4 km from shore. The distance between the 100 m isobath and the coastline gradually widens westward, to about 28 km at Knysna. Beyond the 100 m isobath, the water depth decreases more gradually towards the shelf break at 200 m. The bathymetry is more gradual in the west at Plettenberg Bay, and between Groot River (east) and the Tsitsikamma River. St Francis Bay is a shallow (< 50 m), log spiral bay situated on the eastern side of Cape St. Francis.

Middelbank (34° 02.72 S, 23° 52.51 E) is a prominent reef situated 3.7 km south of the Storms River mouth. The seaward side of the reef drops steeply from a shallow point of 23 m to 60 m, while the inshore side slopes more gradually to about 45 m (Roberts and van den Berg 2005). An Acoustic Current Doppler Profiler (ADCP) and a vertical array of underwater temperature recorders (UTRs) were deployed on the inshore side of the reef, at a depth of 36 m, allowing for the safe deployment and recovery of the instruments by SCUBA divers.

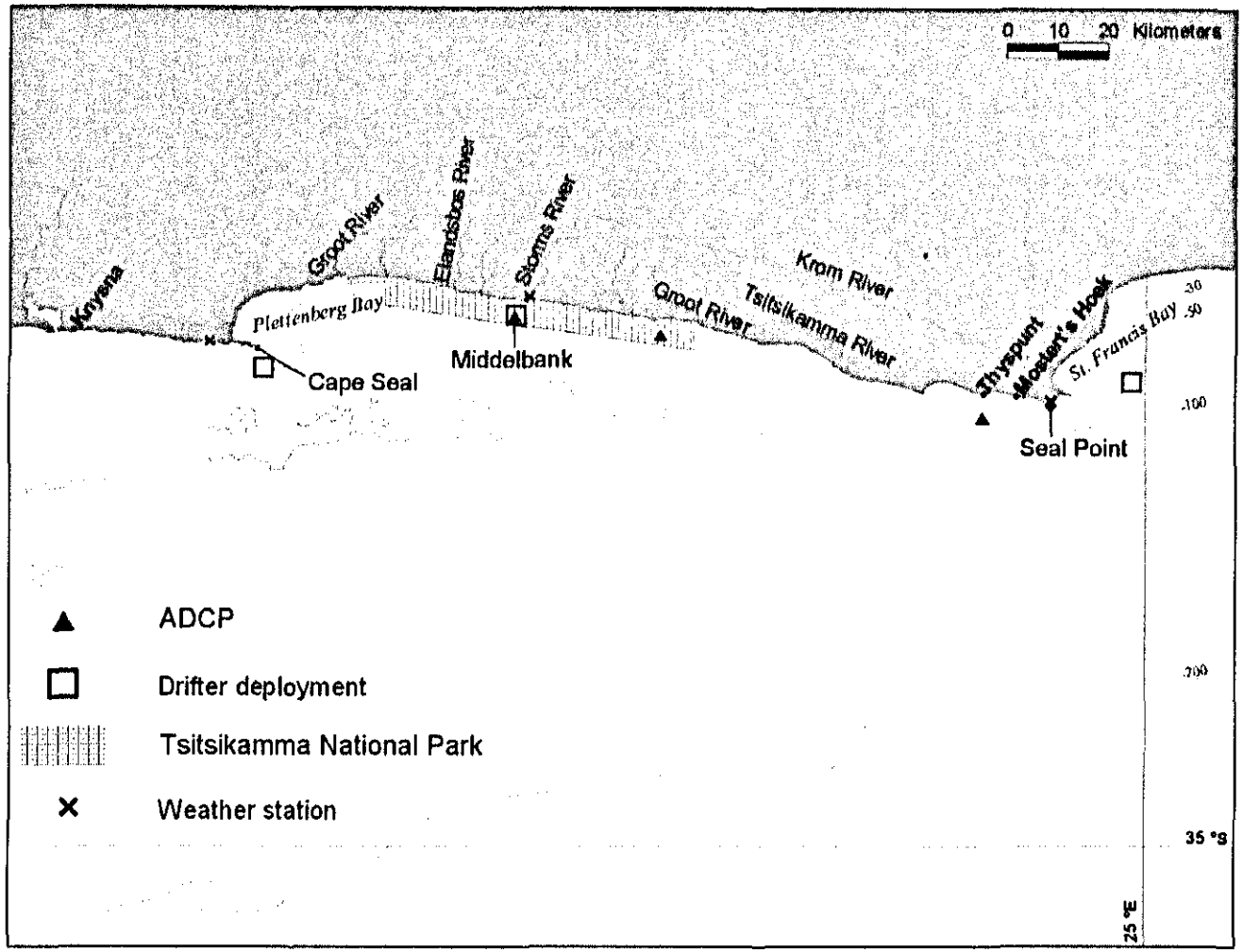

Figure 2.1: The study area on the eastern Agulhas Bank showing the drifter release sites, ADCP deployment positions, weather stations, bathymetry and the location of the Tsitsikamma National Park

2.2 Wind measurements

Hourly measurements of wind speed and direction were obtained from the South African Weather Service (SAWS) for three weather stations along the Tsitsikamma coast. The accuracy of wind direction is given as 10° and wind speed as 0.1 $m.s^{-1}$. The western most station at Plettenberg Bay (34° 05,634 S; 23° 19.734 E) is positioned on the top of a sea cliff, 139 m above sea level. The weather station at Tsitsikamma (34° 1.614 S; 23° 54.516 E) is at the foot of a sea cliff, 5 m above sea level, in an embayment created by the mouth of the Storms River. Neither the elevated position of the weather station at Plettenberg Bay, nor the sheltered position at Tsitsikamma is ideal, as the coastal topography may have influenced the wind measurements made at these locations. The eastern most station at Cape St. Francis (34° 12.00 S; 24° 49.974 E) is situated near the lighthouse at Seal Point, 7 m above sea level. It is the most exposed weather station of the three used in this study. Wind speeds are given in $m.s^{-1}$ and expressed in terms of the Beaufort wind scale (Appendix D).

Wind data were pooled into spring (September, October, November), summer (December, January, February), autumn (March, April, May) and winter (June, July, August) months to establish seasonal differences among stations. The classed frequency of wind speed and wind direction was graphed on stepped circular histograms (wind roses). Zero values for wind speed were excluded, as the wind vane could have been pointing in any direction during calm situations, and the associated direction is therefore meaningless.

Stick vectors were produced by plotting each measurement of wind speed and direction at time (z) as a vector. Wind measurements were first converted to the oceanographic standard by rotating the vectors 180° clockwise. The wind data was filtered with a New Hampshire Lanczos filter (97 weights and a 36 hour quarter power point) to remove high frequency oscillations (Schumann 1999) and rotated 90° clockwise to highlight the principle east-west component of the wind.

2.3 ADCP measurements

2.3.1 Principle of operation

An Acoustic Current Doppler Profiler (ADCP) is a type of sonar that measures water velocities over a range of depths. It transmits sound bursts, called pings, into the water column. Suspended particles, transported by the currents, produce echoes which are returned to the ADCP. Current velocity is calculated from the Doppler shift of these particles that undergoes a change in frequency as the particles move away or towards the ADCP. The Teledyne ADCP has four acoustic beams that measure at 20° angles from a central axis. The ADCP collects high-resolution time series of currents at user defined depths, called bins,

throughout the vertical water column. The technology has been used since the 1980s and is now considered an essential tool in the study of currents worldwide.

2.3.2 ADCP deployments

Three RDI Teledyne 600 kHz ADCPs were deployed along the Tsitsikamma coast, between the drifter deployment sites at Storms River and St. Francis Bay (Figure 2.1). The instruments were configured to sample the vertical water column in 2 m bins at 30 minute intervals using an ensemble size of 120 pings, with one ping per second. The quality of the data in each bin was assessed, and only bins with > 75% good readings were included in the analysis. This typically eliminates the first 5 m below the surface due to interference from waves, tides and atmospheric processes.

ADCP-1 was moored in the centre of the Tsitsikamma National Park, on the shoreward side of Middelbank (34° 02.72 S, 23° 52.51 E), in 36 m of water. The instrument recorded data for the duration of the drifter study (November 2006 – March 2008) and was serviced twice a year by SCUBA divers to retrieve the data and replace the batteries. ADCP-2 (referred to as TNP-east in this study) was positioned inside the TNP, 5 km from the eastern boundary (34° 04.7955 S; 24° 08.190 E), at a depth of 61 m. ADCP-3 was positioned 56 km east of ADCP-2, at Thyspunt (34° 13.653 S; 24° 42.637 E), in 68 m of water. The ADCPs at TNP-east and at Thyspunt were deployed from the *RS Algoa* and recovered by means of an acoustic release mechanism at three to four month intervals. Deployment duration at TNP-east (ADCP-2) was from 10 March 2007 to 9 July 2007 (121 days) and from 8 December 2007 to 28 March 2008 (111 days) at Thyspunt (ADCP-3).

2.3.3 ADCP data processing and data products

Data from specific depth bins were selected to represent the current at the surface, mid-water and at the bottom. The bin selection depended on the depth of the mooring at each ADCP deployment site. Additional bins were selected from TNP-east and Thyspunt to compare the currents at corresponding depths between these sites. A summary of deployment details and the selected bins at each mooring site is given in Table 2.1.

Current direction was calculated according to the circular co-ordinate system in which an angle (θ) is measured clockwise from the positive y-axis, which corresponds to north on a compass rose. Magnetic deviation was corrected for by subtracting 25° from the recorded direction, so that the positive y-axis indicates true north. The ADCP data were processed with RDI Teledyne support software and locally developed software.

The following data products were produced:

Polar histograms

At a specified depth, the occurrence of data (given as a percentage of the total) is divided into 16 sectors for direction (each representing 22.5° of the total) and 10 bins for speed ($cm.s^{-1}$). Speed bins, are presented on the radial axis and were selected to include maximum velocities, while out of range velocities were excluded.

Stick vectors

Each measurement of current speed and direction at time (z) is represented by a vector. Direction is given in the oceanographic sense and measured clockwise from the positive y-axis (true north), while the x-axis represents time. The stick vectors were rotated 90° clockwise to highlight the principle east-west component of the current measurements.

U and v components

Each vector of speed and direction was divided into u- and v-components by calculating the sine and cosine of the vector with basic trigonometric functions. The data were orientated to align with the Tsitsikamma coastline (-10°) so that the u-component corresponds to the alongshore current, with positive values representing eastward flow and negative values westward flow. Similarly, the v-component corresponds to cross-shelf currents with positive values representing northward flow and negative values southward flow.

Spectral analysis

The rotary spectra of the Middelbank ADCP data were calculated to examine the frequencies of variability in the current. The method decomposes a velocity vector into a clockwise and anti-clockwise rotating component (Mooers 1973), and calculates the energy for each rotating vector. Missing data were interpolated using a moving average. The dataset was also visually checked to eliminate any obvious errors and to ensure a uniform sampling frequency. Data from the surface (7 m) and bottom (31 m) bins were filtered to one-hour values and to twelve-hour values to highlight variability at periods less than 24 hours, and greater than 24 hours, respectively. The rotary analysis was done at a bandwidth of 0.001 cph (cycles per hour) with 42 cph degrees of freedom and a Nyquist Frequency of 0.041 cph. Significant peaks in the spectral energy were calculated at the 95% confidence limits of 0.675 and 1.575 for the lower and upper intervals respectively.

Table 2.1: ADCP deployment details, including the depths selected for statistical analysis, at three sites along the Tsitsikamma coast.

	Middelbank	TNP-east	Thyspunt
Start date	1 Nov 2006	10 Mar 2007	8 Dec 2007
End date	31 Mar 2008	9 Jul 2007	28 Mar 2008
Duration (days)	517	121	111
Latitude	34° 02.72 S	34° 04.79 S	34° 13.65 S
Longitude	23° 52.51 E	24° 08.19 E	24° 42.63 E
Mean water depth (m)	34.8	54.9	69.5
Max water depth (m)	36.2	55.9	70.9
Tidal range (m)	2.6	1.9	1.2
Depth of surface bin (m)	7	7	7
Depth of midwater bin (m)	19	31	31
Depth of bottom bin (m)	31	51	65

2.4 Surface drifters

2.4.1 Design

Satellite-tracked drifters were used to measure the near surface currents along the Tsitsikamma coast. The drifters were manufactured locally, following guidelines from the Global Drifter Program (Sybrandy and Niiler 1992; Sybrandy *et al.* 2005) that meet the standards of the World Ocean Circulation Experiment (WOCE). The design has a drag area ratio > 40, which improves its water following capability and minimizes wind induced slip

The drag area ratio of a drifter is defined as the ratio of the drag area of the drogue over the drag of the non-drogue elements (Sybrandy *et al.* 2005). Slip is the horizontal motion of a drifter that differs from the lateral motion of currents averaged over the drogue depth. Slip is largely caused by wind on the surface float; drag on the float and tether, and rectification of surface waves (Niiler *et al.* 1987; Geyer 1989). Minimal tension between the surface float and drogue and a large drag area ratio are the most important design characteristics that minimize slip (Niiler *et al.* 1987). As long as the drogue remains attached to the drifter, the downwind slip is estimated at 0.7 $cm.s^{-1}$ per 10 $m.s^{-1}$ of wind speed (Niiler and Paduan 1995). If the drogue becomes detach form the surface float, it will slip downwind at a speed of 8.6 $cm.s^{-1}$ per 10 $m.s^{-1}$ of wind (Pazan and Niiler 2001).

A drifter is made up of three components (Figure 2.2):
(1) A spherical surface float (Ø = 38 cm) provides buoyancy and houses the satellite communicator and batteries, (2) a thin wire tether (length = 5 m) connects the surface float to a sub-surface drogue and (3) a holey-sock drogue (Ø = 90 cm) anchors the drifter to a layer of water at the required depth. The drogue is a cylindrical tube of fray resistant material made up of several segments (total length = 5.4 m). Paired holes are cut into each segment, rotating at 90° between consecutive segments. The holes act like dimples on a golf ball by disrupting the formation of organized lee vortices (Lumpkin and Pazoz 2006), thus optimizing the drogue's water following capability. The drogue is held open by plastic rings. Weight is added to the bottom ring to ensure rapid sinking upon deployment and to maintain the drogue's vertical orientation in the water column. The drogue, centred at 8 m, effectively integrates the currents between 5 - 10 m below the surface.

2.4.2 Data accumulation and processing

A GPS device in the surface float transmits the drifter's position, together with a date and time, via the Inmarsat Indian Ocean Region Satellite to a ground station from where the data can be accessed over the internet. Each drifter time series was visually edited to remove bad data before applying a piecewise polynomial interpolation (Sanders and Chrysikopoulos 2004) and then sampled at regular one hour intervals. A time series was separated into

segments when communication was lost for more than 24 consecutive hours. The drifter trajectories were terminated when drifters moved outside of the study area. Hourly drift velocity was calculated from the interpolated time series, while u- and v- components were derived to show the alongshore and on/offshore movement of drifters.

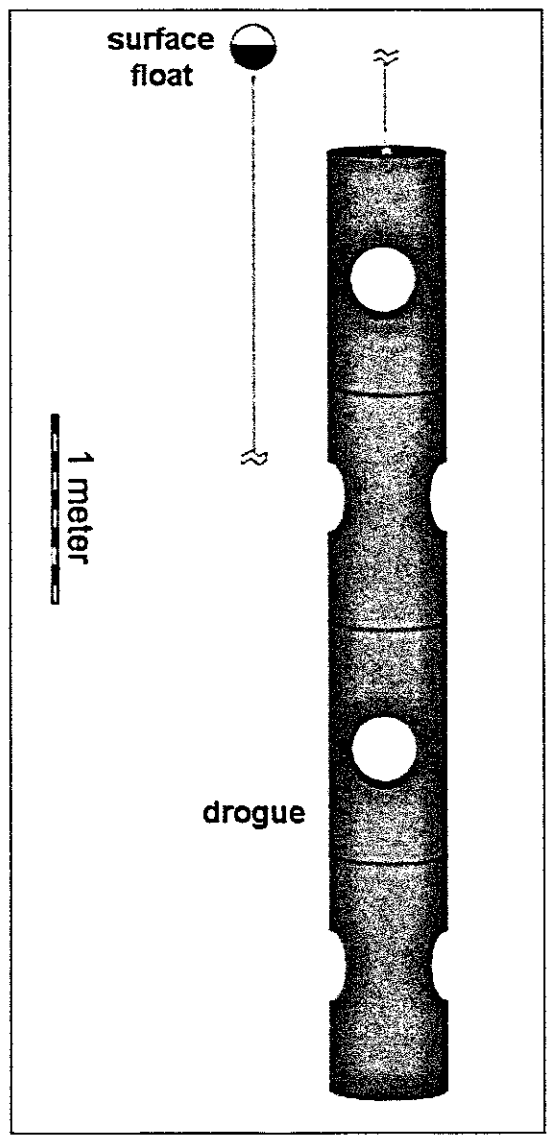

Figure 2.2: A drifter with holey sock drogue drawn to scale (Lumpkin and Pazos 2006). Most of the tether length is excluded from the diagram.

2.4.3 Drifter deployment

Fifteen satellite drifters were deployed along the Tsitsikamma coast between November 2006 and March 2008 (Table 2.2). Deployments were made year-round, but the majority coincided with summer and winter months when fieldwork was conducted in the region. Drifters were deployed in less than 100 m of water at Plettenberg Bay, Middelbank, and St Francis Bay (Figure 2.1), either in groups or individually. The release of drifters was restricted by the timing of fieldtrips, the availability of ships of opportunity and by weather conditions. This allowed for two group deployments of three drifters (deployments 1 and 4) and one group deployment of six drifters (deployment 3). The remaining three drifters were released as single deployments (deployments 2, 4 and 6).

During group deployment 1 (November 2006) three drifters were released along a transect perpendicular to the coast, off the Storms River mouth. A drifter was released directly above the ADCP moored at Middelbank, and two more drifters, 1.9 km apart, further along the transect. The deployments were made from an inflatable workboat, within 20 minutes of each other.

Group deployment 3 was made up of six drifters, released at three sites along the Tsitsikamma coast, over ten days in June 2007. Simultaneous deployments were made at Plettenberg Bay and Middelbank and at St. Francis Bay and Middelbank to investigate continuity in the currents. Single deployments were also made at Middelbank (n = 1), St. Francis Bay (n = 1) and Plettenberg Bay (n = 2). Releases at St. Francis Bay and Middelbank were done from the inflatable workboat, while a commercial whale watching operator assisted with deployments in Plettenberg Bay.

Group deployment 4 was made in November 2007, with three deployments over two consecutive days. Drifter 47 was released at Middelbank and drifter 48, four nautical miles (7.4 km) further offshore, 20 minutes later. Drifter 41 was released in St. Francis Bay the following day.

In March 2007, December 2007 and March 2008 single deployments were made at Middelbank from vessels of opportunity, *i.e.* the *RS Algoa* and the *RS Elen Kuswayo*. The details of the drifter deployments, along with lifespan and presumed reasons for failure are summarized in Table 2.2.

Table 2.2: Deployment and recovery details of drifters (n = 15) deployed along the Tsitsikamma coast between 2006 and 2008. Presumed failure types are (1) beached and recovered, (2) beached not recovered, (3) drifted beyond study area and (4) unknown reason.

		Deployment details				Last report in study area				
Deployment no.	Drifter no.	Date/time	Lat (S)	Long (E)	Area	Date/time	Lat (S)	Long (E)	Days in study area	Failure type
1	27	22-Nov-06 12:55	-34.0448	23.8778	Middelbank	03-Dec-2006 18;59	-34.1366	24.4348	11	1
1	29	22-Nov-06 13:03	-34.0603	23.8692	Middelbank	25-Nov-2006 03:26	-34.1865	24.5373	3	1
1	31	22-Nov-06 13:12	-34.0759	23.8619	Middelbank	30-Nov-2006 18:54	-34.1701	24.4842	8	1
2	32	04-Mar-07 09:55	-34.0468	23.8738	Middelbank	05-Mar-2007 23:21	-34.1541	24.4534	2	2
3	228	13-Jun-07 09:41	-34.0445	23.8682	Middelbank	30-Jun-2007 19:00	-34.9584	22.1867	17	3
3	227	13-Jun-07 11:00	-34.1197	23.4622	Plettenberg Bay	05-Jul-2007 08:00	-34.9332	22.1776	22	3
3	36	14-Jun-07 09:05	-34.0451	23.8726	Middelbank	15-Jun-2007 17:56	-34.0045	23.7614	1	2
3	37	17-Jun-07 12:50	-34.1623	24.9769	St. Francis Bay	09-Jul-2007 03:12	-34.1094	24.3756	22	2
3	40	20-Jun-07 10:08	-34.1626	24.9765	St. Francis Bay	29-Jul-2007 14:45	-34.0778	24.2411	39	2
3	38	20-Jun-07 17:00	-34.0427	23.8633	Middelbank	18-Jul-2007 04:00	-34.9039	22.1729	27	3
4	47	17-Nov-07 08:45	-34.0441	23.8737	Middelbank	29-Nov-2007 11:16	-34.541	22.9661	12	3
4	48	17-Nov-07 09:06	-34.1108	23.8658	Middelbank	20-Nov-2007 19:33	-34.3842	23.3292	3	4
4	41	18-Nov-07 16:37	-34.1736	24.9089	St. Francis Bay	21-Nov-2007 00:33	-34.2325	24.6971	2	4
5	43	04-Dec-07 15:47	-34.0456	23.8776	Middelbank	16-Dec-2007 11:09	-34.8684	22.0391	12	3
6	46	11-Mar-08 16:00	-34.0441	23.8737	Middelbank	26-Mar-2008 23:07	-34.8264	22.175	15	3

2.5 Sea temperature

A vertical array of underwater temperature recorders (UTRs), moored in 36 m of water at Middelbank (34° 02.66 S; 23° 52.60 E), provided data on the stratification of the water column. The thermistor array recorded hourly water temperature at approximate depths of 12 m, 19 m, 27 m, and 35 m between November 2006 and March 2008. Two UTRs, positioned in approximately 10 m of water at Storms River Mouth (34° 01.37 S; 23° 53.98 E) and at Mostert's Hoek (34° 11.84 S; 24° 46.46 E) monitored the nearshore water temperature, as well as alongshore temperature gradients. All temperature measurements were made at one hour intervals to an accuracy of 0.01 °C.

CHAPTER 3
RESULTS

3.1 Wind analysis

During the study period the wind was predominantly westerly along the Tsitsikamma Coast. There were, however, differences in the directional distribution between sites (**Figure 3.1**). West-southwesterly (WSW) winds dominated at Cape St. Francis, with an occurrence of nearly 25%. At the Tsitsikamma weather station southwesterly (SW) winds occurred most frequently (19%); followed by north-northeasterly (NNW) winds (12%). This large on-offshore component at Tsitsikamma can be attributed to the channelling of the land-sea breeze through the Storms River gorge. The wind direction at Plettenberg Bay was more variable, with west-southwesterly (WSW) winds slightly dominant (14%). Wind speeds greater than 12 $m.s^{-1}$ were only recorded at Cape St Francis, during both westerly and easterly conditions.

Changes in the alongshore wind direction at Plettenberg Bay, Tsitsikamma, and Cape St. Francis were well correlated (Figure 3.2). There was however a lag in the change of wind direction towards Cape St. Francis, with the westward movement of the wind systems. Generally, the wind was strongest at Cape St Francis. Wind speeds at Tsitsikamma and Plettenberg Bay were similar, with measurements at Plettenberg Bay slightly stronger.

The seasonal analysis of the wind field (Appendix A) shows an increase in easterly component winds at all three weather stations during spring, summer and autumn months. At Cape St. Francis and Tsitsikamma easterly winds had an offshore component, being mainly from the direction east-northeast (ENE). At Plettenberg Bay easterly winds was slightly onshore, from the direction east-southeast (ESE). The occurrence of easterly winds peaked in summer, with frequencies of 33%, 30% and 38% of the total at Plettenberg Bay, Tsitsikamma and Cape St. Francis respectively. However, westerly winds remained dominant throughout the study period.

3.2 ADCP measured currents

3.2.1 Middelbank

The current at Middelbank was predominantly alongshore; either eastward or westward (Figure 3.3), with the principal axis was aligned to the coast (100° - 280°). The basic statistics of the velocity components at Middelbank (Table 3.1) shows that near the surface (7 m), eastward flow occurred with a frequency of 58% and westward flow with a frequency of 41%. Midwater (19 m), eastward flow (54%) and westward flow (45%) were nearly equal. Near the

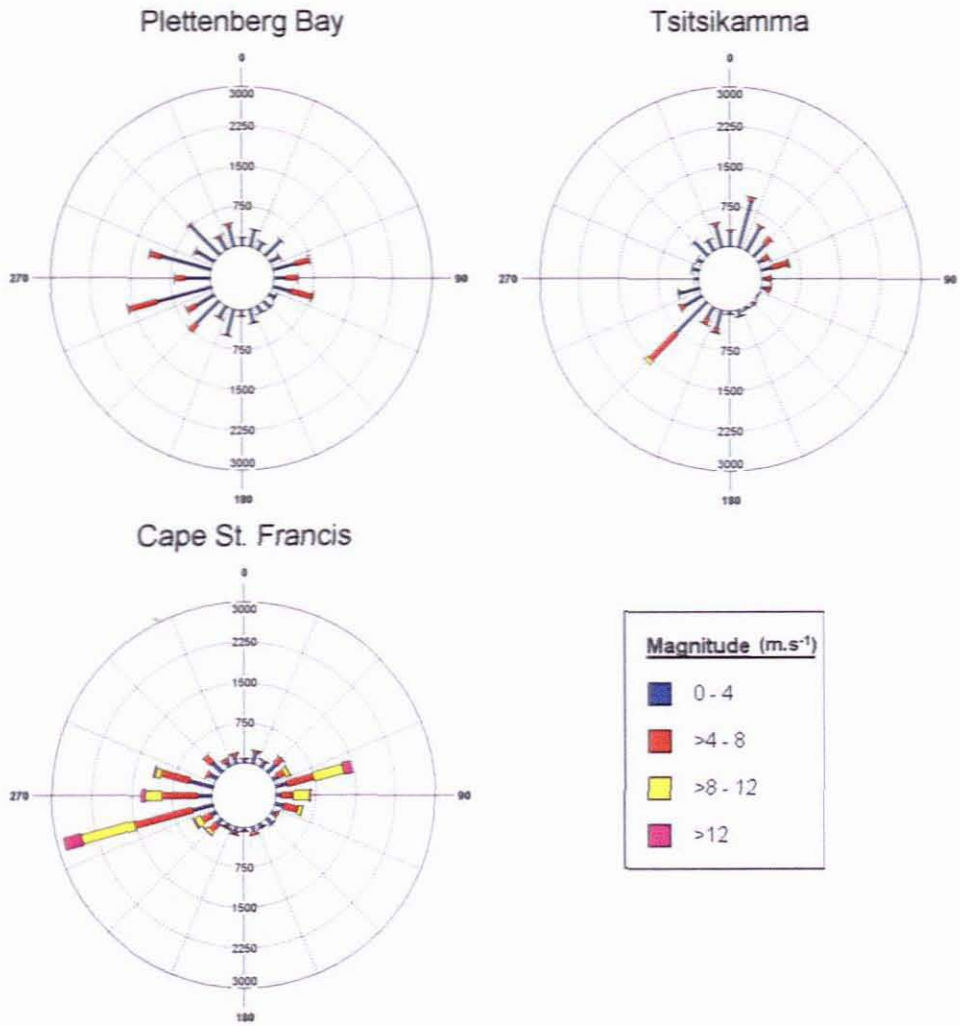

Figure 3.1: Wind distributions at three weather stations along the Tsitsikamma coast between November 2006 and March 2008. Direction is given in the meteorological standard.

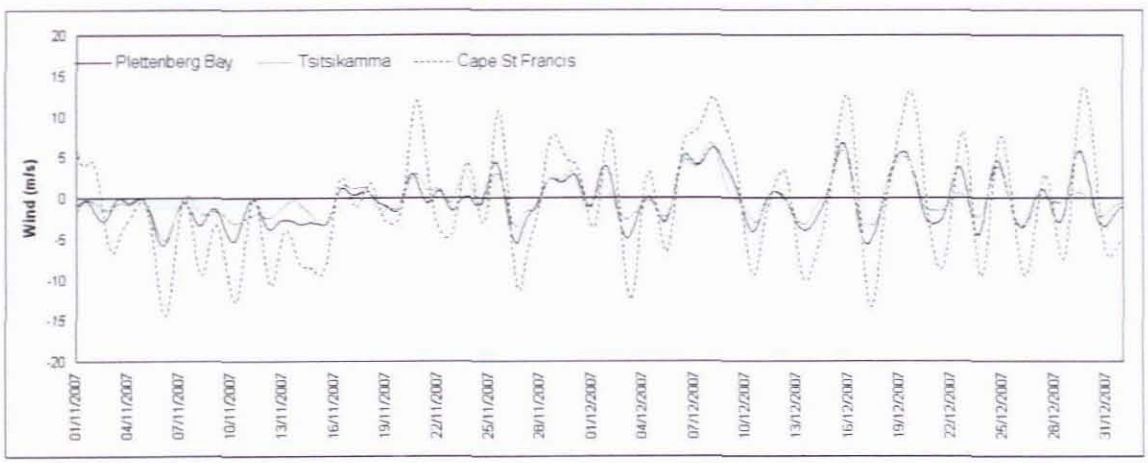

Figure 3.2: Alongshore winds recorded at Plettenberg Bay, Tsitsikamma and Cape St. Francis during November and December 2007. Positive values represent wind with an easterly component, and negative values wind with a westerly component.

seabed (31 m), eastward flow had a frequency of 41% and westward flow a frequency of 58%. Current velocity generally decreased with depth and a maximum surface velocity of 141 cm.s^{-1} was recorded during an eastward current on 11 February 2007. The maximum surface velocity coincided with the maximum velocity mid-water (120 cm.s^{-1}), and near the seabed (59 cm.s^{-1}), as shown in Appendix B1 and B2. Average alongshore velocities were 27 cm.s^{-1} (east) and 19 cm.s^{-1} (west) at the surface (7 m); and 9 cm.s^{-1} (east) and 11 cm.s^{-1} (west) near the seafloor (31 m).

Cross-shelf currents were less dominant than the alongshore currents (Figure 3.3). The direction of surface (7 m) and bottom (31 m) flow differed (Table 3.1), with offshore flow dominant (60%) to a depth of 19 m, and onshore flow dominant near the seabed at 31 m (62%). The onshore and offshore velocities were however similar. Maximum velocities were recorded during onshore flow at the surface (39 cm.s^{-1}) and at the bottom (26 cm.s^{-1}), and during offshore flow midwater (36 cm.s^{-1}). The average cross-shelf velocities were 5 cm.s^{-1} (north) and 7 cm.s^{-1} (south) at the surface (7 m); and 3 cm.s^{-1} (north) and 2 cm.s^{-1} (south) at the seabed (31 m).

Table 3.1: Statistics of ADCP measured velocity components at Middelbank during the study period (1 November 2006 and 31 March 2008). In the u-component positive values denote eastward flow and negative values westward flow. In the v-component positive values denote northward (onshore) flow and negative values southward (offshore) flow.

		Middelbank	
		u-component	v-component
7m	Maximum + (cm.s^{-1})	141	39.3
	Maximum - (cm.s^{-1})	78	36.3
	Average + (cm.s^{-1})	26.9	5.1
	Average - (cm.s^{-1})	19.2	6.4
	Percentage + (%)	58	39
	Percentage - (%)	41	60
19m	Maximum + (cm.s^{-1})	119.5	24.8
	Maximum - (cm.s^{-1})	61.9	35.6
	Average + (cm.s^{-1})	20.9	3.4
	Average - (cm.s^{-1})	16.8	4.2
	Percentage + (%)	54	39
	Percentage - (%)	45	60
31m	Maximum + (cm.s^{-1})	58.6	25.9
	Maximum - (cm.s^{-1})	50.7	21.9
	Average + (cm.s^{-1})	9.1	2.7
	Average - (cm.s^{-1})	11	2.3
	Percentage + (%)	41	62
	Percentage - (%)	58	37

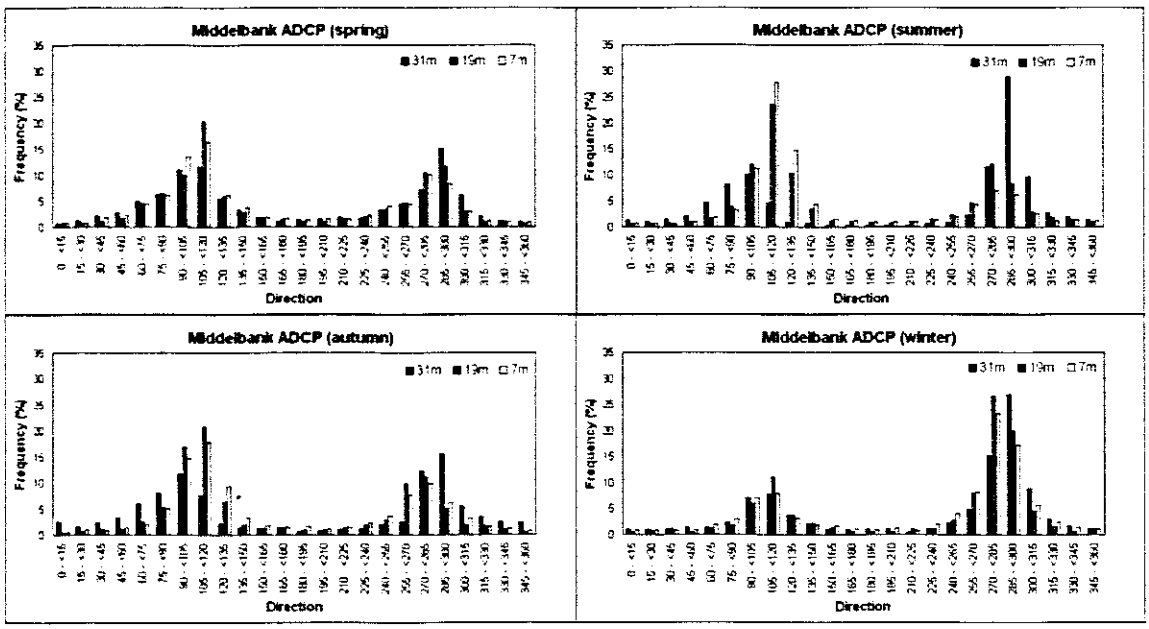

Figure 3.3: Seasonal distributions of the current direction at Middelbank at three depths (7 m, 19 m and 31 m) between November 2006 and March 2008

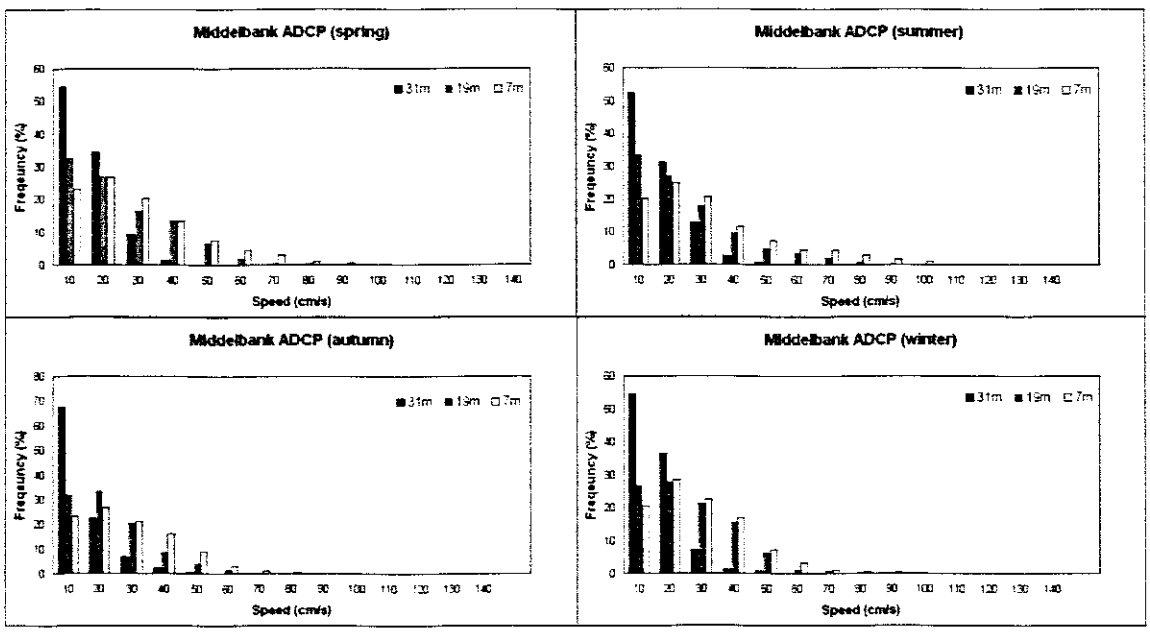

Figure 3.4: Seasonal distributions of current speed at Middelbank at three depths (7 m, 19 m and 31 m) between November 2006 and March 2008.

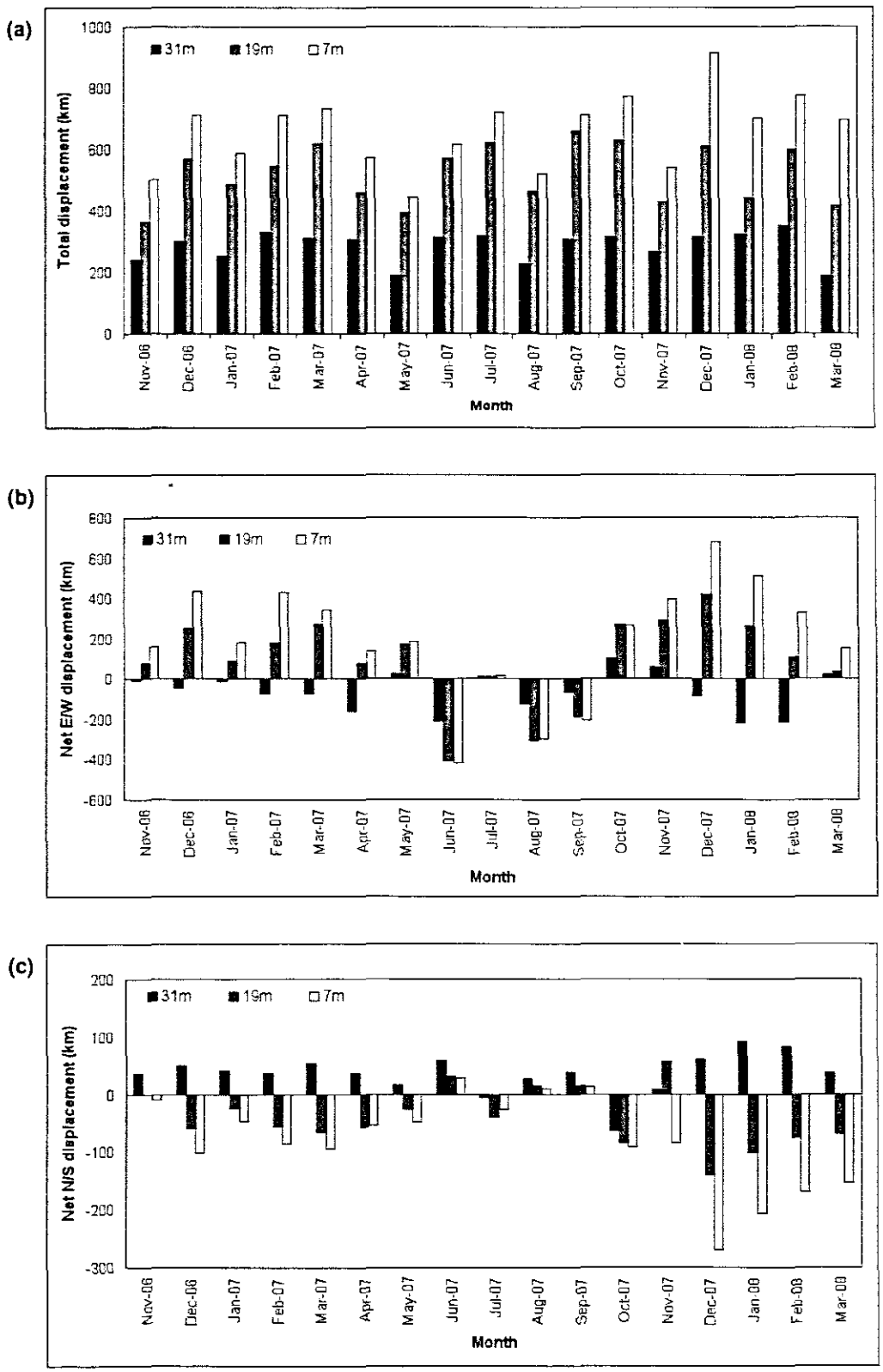

Figure 3.5: Monthly (a) total displacement, (b) net east-west displacement and (c) net north-south displacement from Middelbank at three respective depths.

Seasonal histograms of the current direction at Middelbank (Figure 3.3) show surface and bottom currents flowing in opposite directions in spring, summer and autumn. In spring and autumn, eastward flow dominated over westward flow at the surface (7 m) and midwater (19 m). At the same time, bottom currents (31 m) were evenly divided between eastward and westward flow. In summer, eastward flow dominated near the surface and midwater, and westwards flow dominated near the bottom. In contrast the current was predominately westward throughout the water column during winter months. Currents speeds greater than 100 $cm.s^{-1}$ occurred mostly in summer and only during eastward flow (Figure 3.4). The 100 $cm.s^{-1}$ threshold was exceeded once in spring (29 September 2007) and once in winter (27 – 28 July 2007), both during eastward flow.

Displacement potential was greatest near the surface and generally decreased with depth. The maximum total displacement distances were achieved near the surface during the summer months (Figure 3.5a). Monthly net displacement distances in the alongshore and cross-shelf components are given in Figure 3.5b and Figure 3.5c, respectively. The greatest net displacement distances were attained at the surface during summer months (direction east of Middelbank). The same months were associated with offshore (southward) displacement at the surface and onshore (northward) displacement near the bottom. June, August and September 2007 were the only months when net displacement at all three depths were west of Middelbank. At the same time onshore displacement occurred at all three depths, being greatest near the bottom (31 m). During July 2007, net displacement at the surface only 17 km east of Middelbank, despite a large total displacement (722 km) during the same time.

Spectral analysis of the current at Middelbank show significant peaks at a range of frequencies. The M_2 semi-diurnal frequency of 12.42 hours is prominent in the 1 hour filtered time series, especially near the surface (Figure 3.6a) where the anti-clockwise rotation had more energy. The energy-spectra near the bottom show the same peak (Figure 3.6b), but at a slightly lower level. Significant peaks were not found at the inertial period of 21.4 hour at either depth. The 12 hour-filtered series at 7 m (Figure 3.6c) and at 31 m (Figure 3.6d) show significant energy at periods of 18 days, 8 days, 4 days and 3.3 days, with the peaks more prominent at the greater depth.

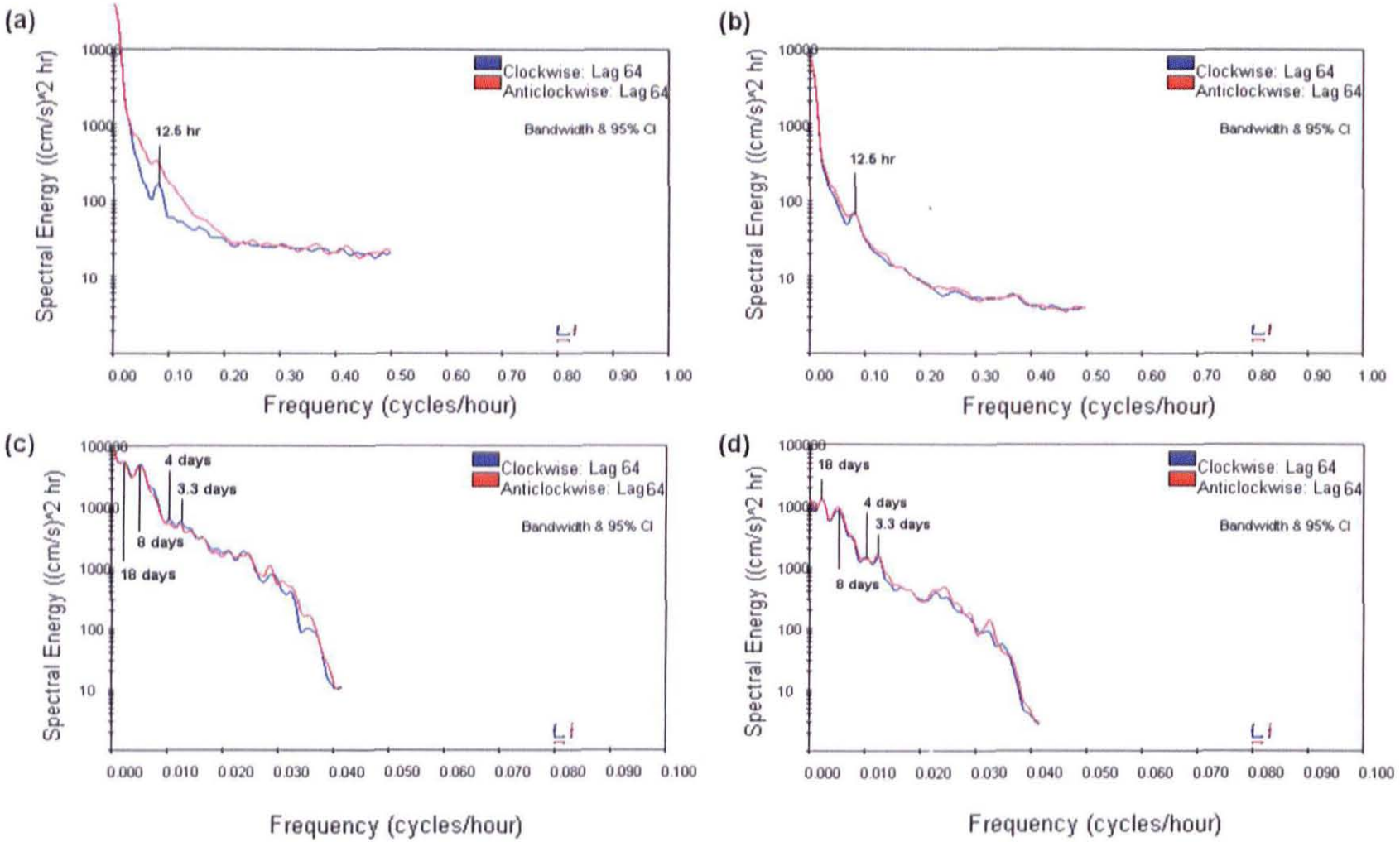

Figure 3.6: Clockwise and anticlockwise rotary spectra for the ADCP deployment at Middelbank. Values filtered to 1 hr averages at (a) 7 m and (b) 31 m show peaks at the M2 tidal period of 12.5 hr. Values filtered to 12 hr averages at (c) 7 m and (d) 31 m show various peaks at the longer periods, with peaks more prominent at 31m.

3.2.2 TNP-east

The ADCP at TNP-east measured a current that was similarly, predominantly alongshore with the main flow direction towards the east, aligned with coast (Figure 3.7). The strongest currents were recorded near the surface (7 m), during eastward flow (maximum = 69 $cm.s^{-1}$; average = 16 $cm.s^{-1}$). Alongshore velocities decreased with depth (Table 3.2) and near the seabed (51 m) peak velocity was recorded during eastward flow (max = 40 $cm.s^{-1}$; average = 9 $cm.s^{-1}$). The occurrence of westward (opposed to eastward) flow increased from 39% at the surface to 45% at the bottom.

Onshore (northward) and offshore (southward) flow occurred at equal percentages, with an average of 53% offshore flow throughout the water column. Cross-shelf velocity generally decreased with depth and maximum velocities were recorded during offshore flow at all depths, except at the surface (Table 3.2), where onshore flow was strongest (maximum = 31 $cm.s^{-1}$; average = 6 $cm.s^{-1}$).

Polar histograms (Figure 3.7a and b), from concurrent measurements made at Middelbank and TNP-east over a four month period, show differences in the distributions of the currents at the two sites. At Middelbank the surface current (7 m) was stronger and westward flow occurred more frequently than at TNP-east. The current direction at Middelbank was also more concentrated along the main axis (100° - 280°), while at TNP-east the current was weaker and offshore flow occurred with greater frequency. At Middelbank, the bottom current (31 m) was predominantly westwards (maximum = 48 $cm.s^{-1}$), while at TNP-east the bottom current (51 m) was mostly eastward (max = 40 $cm.s^{-1}$). Differences in the u- and v-components between the two sites are summarised in Table 3.2.

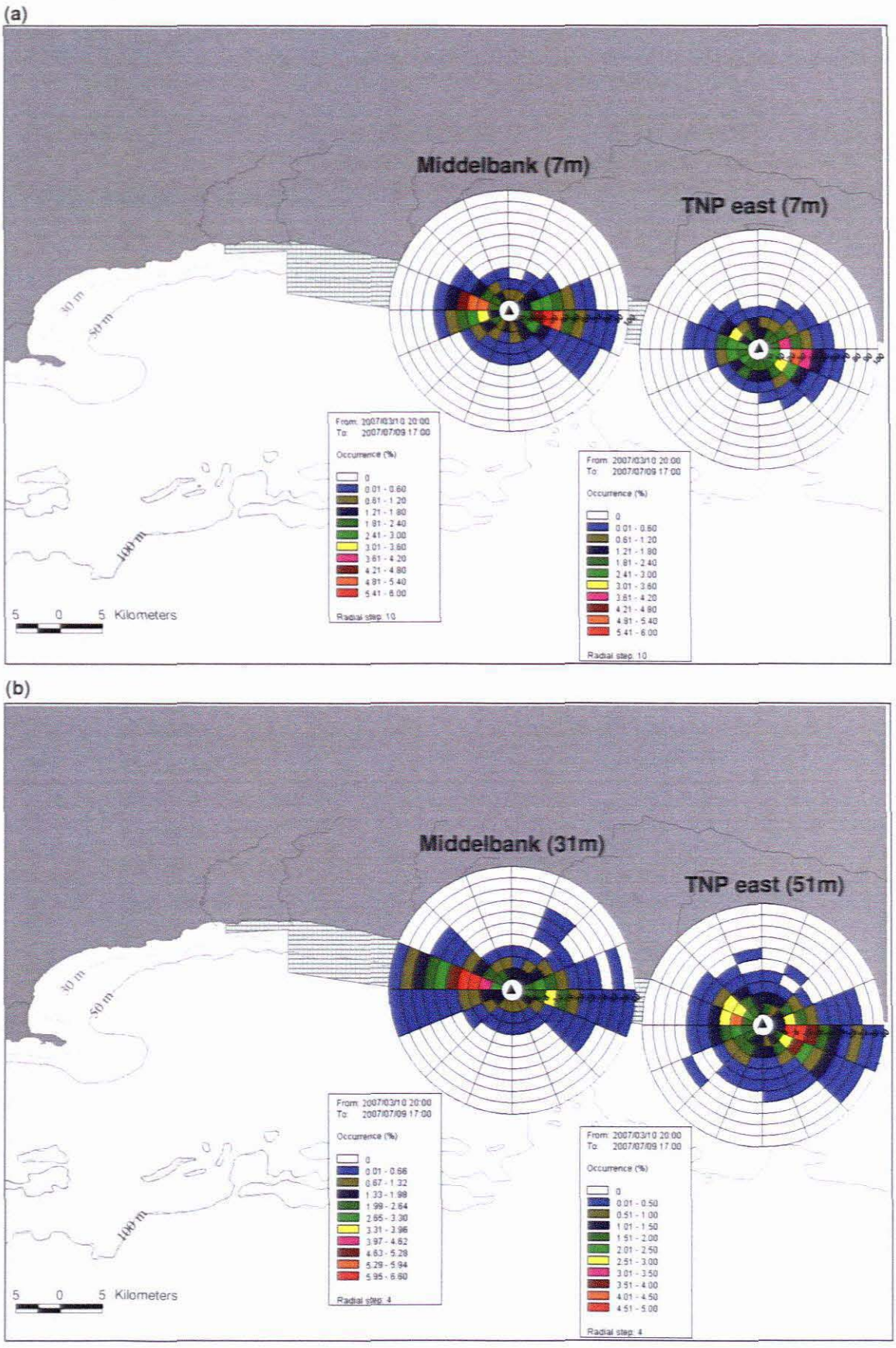

Figure 3.7: Polar histograms of (a) surface and (b) bottom currents at Middelbank and TNP-east between 10 March 2007 and 9 July 2007. Black triangles are the ADCP deployment positions.

Table 3.2: Statistics of the alongshore (u) and cross-shelf (v) velocity measured at Middelbank and at TNP-east between 10 March 2007 and 9 July 2007. In the u-component positive values denote eastward flow and negative values westward flow. In the v-component positive values denote northward (onshore) flow and negative values southward (offshore) flow.

		u-component		v-component	
		Middelbank	TNP-east	Middelbank	TNP-east
7m	Maximum + ($cm.s^{-1}$)	81.9	68.5	28	31.1
	Maximum - ($cm.s^{-1}$)	56	51	35	30.7
	Average + ($cm.s^{-1}$)	20.5	15.9	5.05	6.1
	Average - ($cm.s^{-1}$)	18.8	10.3	5.83	6.4
	Percentage + (%)	51	61	45	47
	Percentage - (%)	49	39	54	53
19m	Maximum + ($cm.s^{-1}$)	60.7	58	22	17.3
	Maximum - ($cm.s^{-1}$)	51.7	42	20	35.5
	Average + ($cm.s^{-1}$)	17.3	13.3	3.3	3.9
	Average - ($cm.s^{-1}$)	17.9	9.8	4.2	4.2
	Percentage + (%)	52	60	43	44
	Percentage - (%)	47	40	56	56
31m	Maximum + ($cm.s^{-1}$)	40.9	51.9	23	15.6
	Maximum - ($cm.s^{-1}$)	47.8	36	12	19
	Average + ($cm.s^{-1}$)	7.3	11.5	2.4	3
	Average - ($cm.s^{-1}$)	11.6	9.3	2	3.2
	Percentage + (%)	38	53	60	49
	Percentage - (%)	61	47	39	51
51m	Maximum + ($cm.s^{-1}$)	-	39.8	-	17.9
	Maximum - ($cm.s^{-1}$)	-	24	-	20.6
	Average + ($cm.s^{-1}$)	-	8.8	-	3.1
	Average - ($cm.s^{-1}$)	-	6	-	3.5
	Percentage + (%)	-	54	-	46
	Percentage - (%)	-	45	-	54

3.2.3 Thyspunt

At Thyspunt the current was mainly alongshore, with westward and eastward flow occurring at nearly equal percentages (Table 3.3). At the surface (7 m), the principal axis (~ 282°) was parallel to the coast (Figure 3.8a); while the current near the seafloor (65 m) was orientated more towards the coast with the principal axis at 303° (Figure 3.8b). The highest velocities were recorded during westward flow at the surface (7 m) (maximum = 85.9 cm.s^{-1}; average = 24.4 cm.s^{-1}), while eastward (surface) flow was somewhat slower (maximum = 78.0 cm.s^{-1}; average 17.1 cm.s^{-1}). Alongshore flow near the seafloor (65 m) reached maximum velocities of 36.9 cm.s^{-1} (west) and 35.3 cm.s^{-1} (east) and average velocities of 12.7 cm.s^{-1} (west) and 9.7 cm.s^{-1}(east).

The cross-shelf current at Thyspunt was less dominant that the longshore component (Figure 3.8a, b). At the surface (7 m), onshore (northward) flow occurred more frequently and attained higher velocities (maximum = 43.3 cm.s^{-1}; average = 9.0 cm.s^{-1}) than offshore flow (maximum = 32.0 cm.s^{-1}; average = 6.8 cm.s^{-1}) (Table 3.3). Near the seabed (65 m), onshore (northward) velocities (maximum = 16.8 cm.s^{-1}; average = 4.0 cm.s^{-1}) and offshore (southward) velocities (maximum = 18.4 cm.s^{-1}; average = 3.0 cm.s^{-1}) were similar.

Polar histograms from concurrent hourly measurements at Middelbank and at Thyspunt show differences between the surface (Figure 3.8a) and bottom (Figure 3.8b) currents at the two sites. The surface current at Middelbank was almost exclusively eastward, the direction concentrated between 90° and 135°. At Thyspunt, the current flowed either east or west. Westward flow was slightly dominant and eastward flow was directed onshore (between 45° and 90°), towards Seal Point at Cape St. Francis. The surface current (7 m) at Thyspunt attained maximum velocity (85.9 cm.s^{-1}) during westward flow on 15 January 2008, while maximum surface velocity at Middelbank (104.3 cm.s^{-1}) was recorded during eastward flow on 27 February 2008.

Bottom currents at Middelbank (31 m) and at Thyspunt (65 m) were predominantly westward (Figure 3.8b), but the current direction at Thyspunt was more variable. Circular concentration (r) indicates the dispersion (or variability) of circular measurements. It ranges from zero, when there is so much dispersion that a mean angle cannot be calculated, to one, when all data are concentrated in the same direction. The circular concentration (r) for the bottom current at Middelbank and Thyspunt was calculated at 0.86 and 0.46 respectively, giving confirmation that the flow direction of the bottom current was more variable at Thyspunt than at Middelbank. Statistics of the velocity components at Middelbank and at Thyspunt are summarized in Table 3.3.

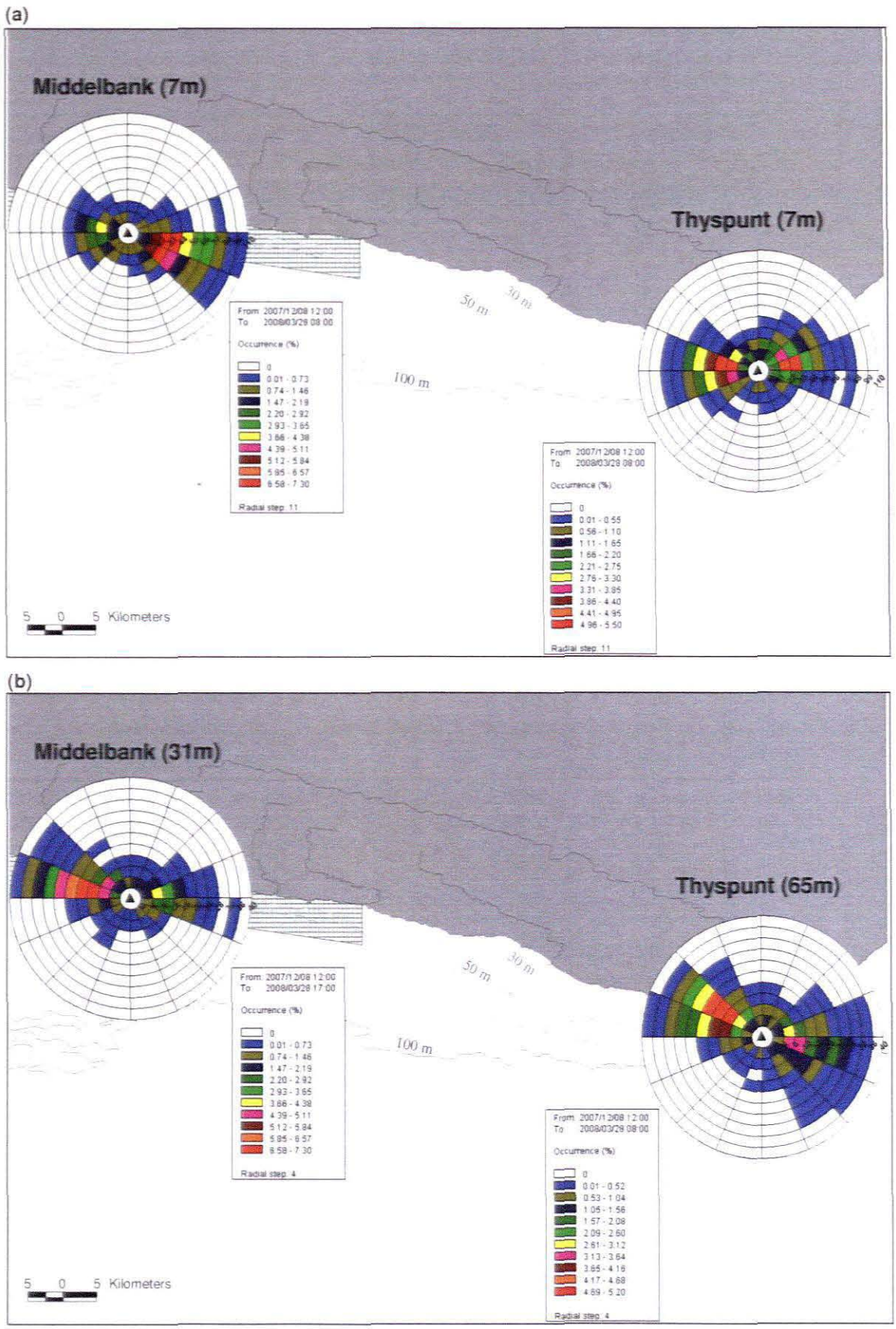

Figure 3.8: Polar histograms of (a) surface and (b) bottom currents at Middelbank and Thyspunt between 8 December 2007 and 28 March 2007. Black triangles are the ADCP deployment positions.

Table 3.3: Statistics of the alongshore (u) and cross-shelf (v) velocity measured at Middelbank and Thyspunt between 8 December 2007 and 28 March 2008. In the u-component positive values denote eastward flow and negative values westward flow. In the v-component positive values denote northward (onshore) flow and negative values southward (offshore) flow.

		u-component		v-component	
		Middelbank	Thyspunt	Middelbank	Thyspunt
7m	Maximum + ($cm.s^{-1}$)	104.3	78	23.8	43.3
	Maximum - ($cm.s^{-1}$)	53.6	85.9	36.3	32
	Average + ($cm.s^{-1}$)	31.9	17.1	4.2	9
	Average - ($cm.s^{-1}$)	17.3	24.4	7.5	6.8
	Percentage + (%)	70	45	25	62
	Percentage - (%)	30	55	75	38
19m	Maximum + ($cm.s^{-1}$)	87.7	67.1	20	29
	Maximum - ($cm.s^{-1}$)	47.9	73.6	20.3	26.7
	Average + ($cm.s^{-1}$)	20.8	17.7	3.1	6
	Average - ($cm.s^{-1}$)	13.5	22.2	4.7	5.1
	Percentage + (%)	62	46	32	46
	Percentage - (%)	38	54	67	54
31m	Maximum + ($cm.s^{-1}$)	35.8	57	13.2	16.2
	Maximum - ($cm.s^{-1}$)	47.9	53.5	10.4	30
	Average + ($cm.s^{-1}$)	6.9	14	2.7	4
	Average - ($cm.s^{-1}$)	12.1	18.9	1.5	4.1
	Percentage + (%)	32	43	78	55
	Percentage - (%)	68	56	21	44
65m	Maximum + ($cm.s^{-1}$)	-	35.3	-	16.8
	Maximum - ($cm.s^{-1}$)	-	36.8	-	18.4
	Average + ($cm.s^{-1}$)	-	9.7	-	4
	Average - ($cm.s^{-1}$)	-	12.7	-	3
	Percentage + (%)	-	42	-	71
	Percentage - (%)	-	58	-	28

3.2.4 Currents during upwelling

Data from the ADCP and the thermistor array, moored at Middelbank, were used to assess the currents during coastal upwelling events. The 13 upwelling episodes selected for the analysis (Appendix C2) were associated with a relatively weak (< 50 $cm.s^{-1}$) and short-lived westward current. Near the surface, westward flow generally persisted while cold water was being upwelled, and eastward flow returned with the relaxation of the upwelling process (Figure 3.9c). Typical progressive (surface) displacement distances during short period upwelling (~ 2 days) events ranged from 5 – 90 km west, and 1 -15 km south of Middelbank. During the more substantial upwelling events recorded in April 2007, February 2008 and March 2008, westward surface flow persisted at Middelbank for between six and nine days, resulting in progressive displacement distances between 130 – 140 km west, and 10 – 25 km south of Middelbank. Offshore, surface flow (Figure 3.9d) was brief and not only linked to the westward upwelling current, but also to eastward flow that occurred before and after upwelling events.

Bottom currents during upwelling at Middelbank were westward, as in the surface layer (maximum velocities ~ 40 $cm.s^{-1}$; average velocities ~ 14 $cm.s^{-1}$). Westward flow generally started at the onset of a decrease in bottom temperature and lasted until the peak of the upwelling, when eastward flow returned (Figure 3.9c). Near-bottom progressive displacement distances, west of Middelbank were between 30 and 60 km during short-period upwelling, and between 90 and 200 km during longer period events. At Middelbank, cross-shelf flow varied considerably, even when upwelling was in progress, and the onshore compensation current could not be clearly defined (Figure 3.9d). Onshore flow was usually stronger (maximum velocities ~ 10 $cm.s^{-1}$; average velocities ~ 3 $cm.s^{-1}$), but on occasion, offshore flow attained higher velocities. Typical progressive displacement distances were < 5 km north of Middelbank, with maximum distances between 20 -25 km offshore during substantial upwelling.

At Thyspunt the effect of upwelling on the surface current was similar, turning it west and offshore. However, during upwelling, westward flow at Thyspunt was stronger than at Middelbank (maximum velocities > 50 $cm.s^{-1}$; average velocities > 20 $cm.s^{-1}$) and generally lasted longer. During the substantial upwelling event recorded on 12 February 2008 (Appendix C2) the westward surface current at Thyspunt persisted for thirteen days (maximum velocity = 84 $cm.s^{-1}$; average velocity = 31 $cm.s^{-1}$), resulting in progressive displacement distances 330 km west, and 74 km south of Thyspunt.

The westward, upwelling current at Thyspunt did not always correspond to a westward current at Middelbank (Appendix B1). At Thyspunt a westward bottom current was closely

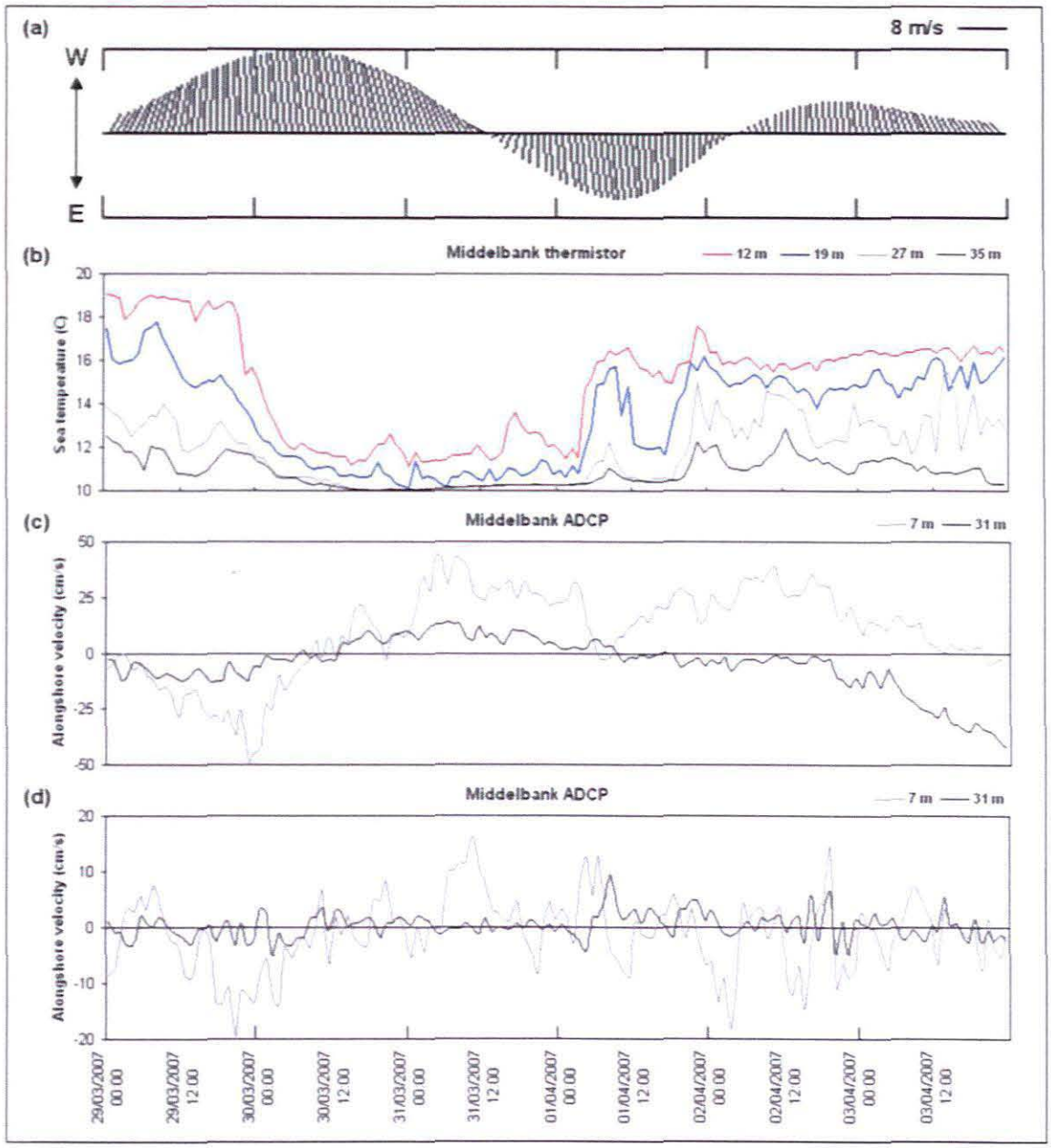

Figure 3.9: The current during an upwelling event at Middelbank. (a) Stick vectors of the wind at Cape St. Francis, (b) sea temperature from the thermistor array at Middelbank at four depths, (c) alongshore surface and bottom currents at Middelbank where positive values denote eastward flow and negative values westward flow, and (d) cross-shelf currents at Middelbank where positive values denote northward flow and negative values southward flow.

correlated with easterly winds and a decrease in sea surface temperature, inshore at Mostert's Hoek. The current near the seabed normally turned west a few hours before the cold water was recorded at the inshore location, and persisted until the peak of the upwelling event (maximum velocities ~ 30 $cm.s^{-1}$; average velocities ~ 13 $cm.s^{-1}$). Westward flow had a strong onshore component (maximum velocities ~ 12 $cm.s^{-1}$; average velocities ~ 5 $cm.s^{-1}$), in compensation for upwelling, that lasted for the duration of the westward upwelling current. Theoretical displacement distances near the seabed were 10 - 35 km west and 5 - 15 km north of Thyspunt, during upwelling events that lasted from one to four days. During bigger events (five to nine days) distances between 65 -160 km west, and 25 -30 km north of Thyspunt were possible.

During the upwelling event in March 2008 baroclinic currents persisted for eight days at Middelbank (Figure 3.20). The current was west in the water upper water column (7 – 30 m), but east near the seabed (> 30 m). At the same time, also during upwelling conditions, the current at Thyspunt was mainly west in the upper water column (7 – 30 m) and onshore at the bottom (30 – 60 m).

3.3 Drifter deployments

The seven drifter deployments were treated as case studies and the drifter trajectories are described below in terms of the coastal wind conditions, ADCP measured currents, and vertical and alongshore sea temperature gradients. Results from the drifter deployments are given in chronological order.

3.3.1 Deployment 1

Three drifters were deployed on 22 November 2006, in a line perpendicular to the coast, off the Storms River Mouth (Figure 3.10). Drifter 27 was released directly above the ADCP at Middelbank, and drifter 29 and 31 one nautical mile apart, further offshore. The weather station at Tsitsikamma failed to record data during deployment 1 and data from the weather station at Cape St. Francis was used instead. The drifters, deployed during gentle westerly winds (Figure 3.12a) and downwelling conditions at Middelbank (Figure 3.12b), moved east after deployment. Drifter 27, released above the Middelbank ADCP, attained the highest average velocity during the first 24 hours, while average daily velocity decreased with distance released offshore (Figure 3.11). Average (eastward) velocity during the first 24 hours was 45 $cm.s^{-1}$, 33 $cm.s^{-1}$ and 17 $cm.s^{-1}$ respectively for drifters 27, 29 and 31.

Drifters 31 and 29 recorded onshore flow in the early hours of 23 November, and again on 24 November, during westerly winds (Figure 3.12a) and downwelling at Middelbank (Figure 3.12b). This onshore movement was strongest in the trajectory of drifter 31, released furthest offshore (Figure 3.10). The drifters stayed parallel to the coast, apart from the onshore movement, and eastward drift was interrupted by three short-lived westward reversals. The alongshore components of hourly drift velocity and the wind velocity (Figure 3.11) show that east-west variability were synchronized in all three drifter trajectories, and that a change in wind direction generally preceded each alongshore change in drift direction.

The wind changed to fresh easterly on 25 November (Figure 3.12a), before the start of the first westward reversal (R1 in Figure 3.12). The three drifters were separated by ~ 43 km with drifter 27, released inshore, positioned near Thyspunt, and drifter 31, released furthest offshore, 9 km beyond the east boundary of the TNP (Figure 3.11). At the same time, drifter 29 washed ashore 8 km east of the Tsitsikamma River, near Tsitsikamma Point. From 25 – 27 November the drifters (27 and 31) moved west along the coast during easterly winds. The movement of drifter 27, located on the eastern side of the study area between the Tsitsikamma River and Thyspunt, was exaggerated compared to drifter 29 (i.e. greater velocities), but alongshore changes in direction were synchronised (Figure 3.11). Eastward drift resumed on 27 November during a change in wind direction to westerly, and persisted

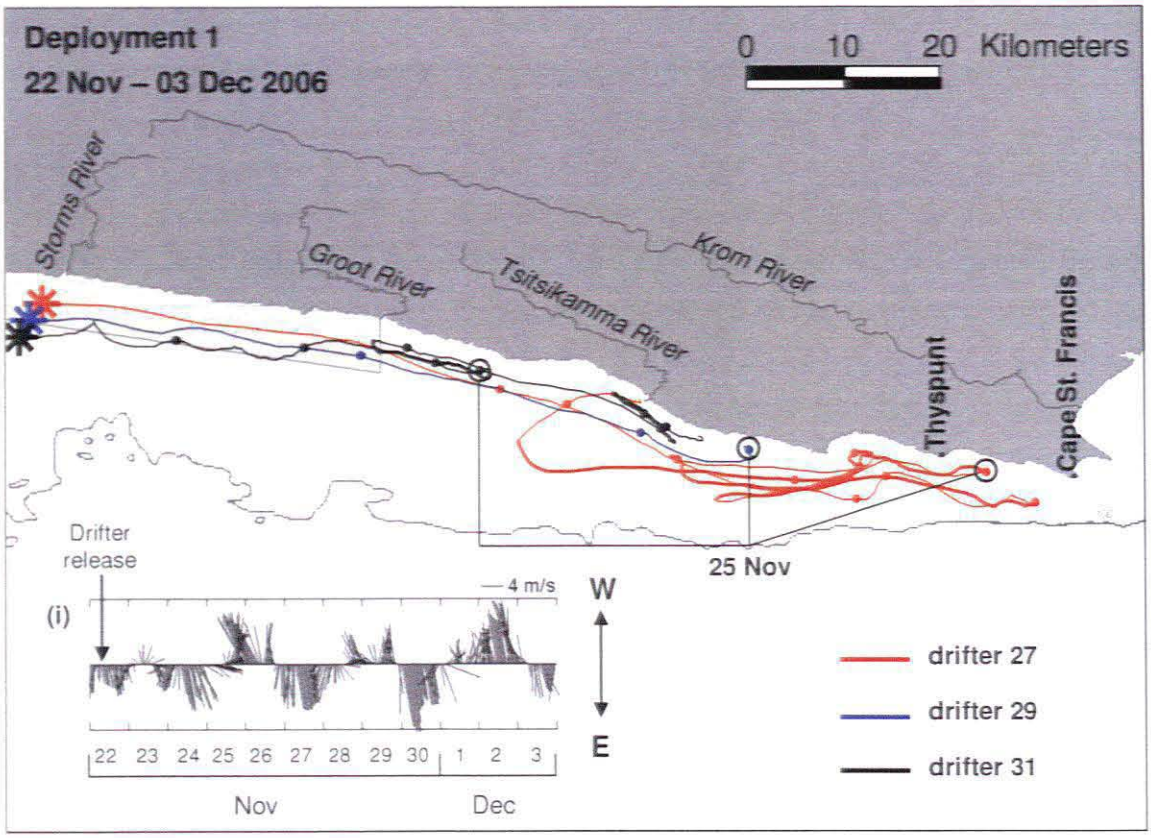

Figure 3.10: The trajectories of the drifters (n = 3) released during deployment 1 (November 2006). Drifter movement is away from the asterisk, coloured dots indicate daily ticks and bold lines represent displacement with a westward component. Inset (i) shows stick vectors of the wind at Cape St. Francis during drifter deployment 1.

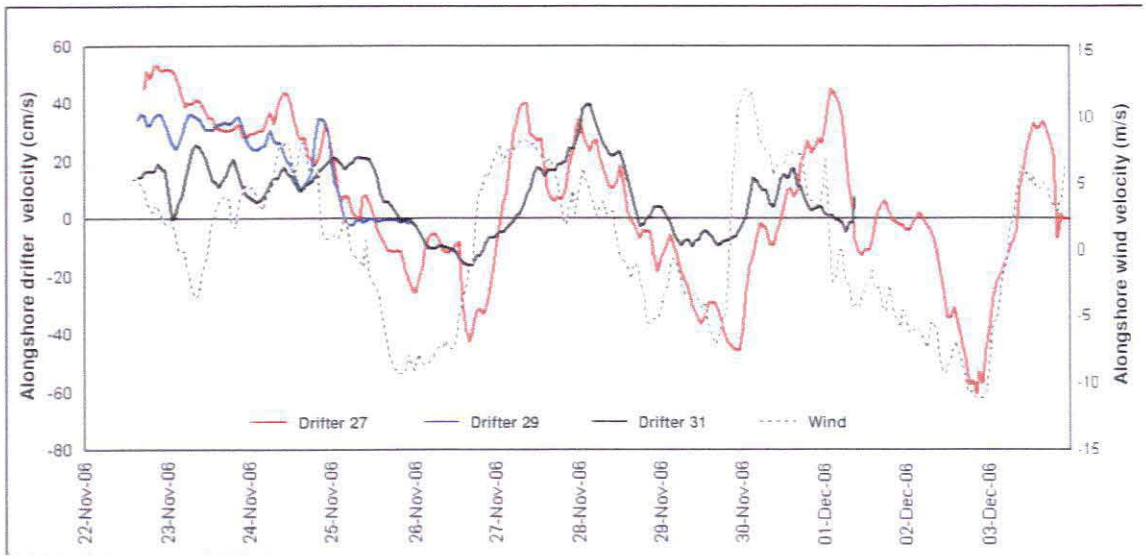

Figure 3.11: Alongshore velocity of each drifter (solid lines) and the wind at Cape St. Francis (dashed line) during deployment 1. Positive values denote eastward flow and negative values denote westward flow. Drift velocity is given in cm.s-1 and wind velocity in $m.s^{-1}$. The wind direction was converted to the oceanographic standard.

until the afternoon of 28 November. Similarly, drifters 27 and 31 recorded another two westward reversals during periods of easterly winds, from 28 - 30 November and from 1 - 3 December (R2 and R3 in Figure 3.12), before all three had washed ashore.

The ADCP at Middelbank recorded an above average, eastward current (maximum velocity = 49.6 $cm.s^{-1}$) on 22 November (Figure 3.12 c – d), when the drifters were released off Storms River. The surface current weakened but stayed eastward until 25 November (Figure 3.12c). During the time of the east-west drifter reversals (R1, R2, and R3 in Figure 3.12) the current at Middelbank was weak (< 20 $cm.s^{-1}$) and was mostly westward. The ADCP measured surface current turned west with each period of easterly wind (R1, R2, and R3 in Figure 3.12), and although weaker than the drifter velocities, corresponded to westward displacement in the drifter trajectories.

The three drifters released during deployment 1 washed ashore east of Storms River within 11 days after deployment (Figure 3.10). The inshore drifter (27) travelled furthest, with a total displacement of 247 km in 11 days. Drifters 29 and 31 travelled total distances of 66 km in 3 days and 102 km in 8 days, before washing ashore near the Tsitsikamma River. Net displacement distances were similar, despite the differences in the total distance covered by each drifter. All three washed up within ~ 10 km of each other (52 km, 63 km and 59 km east of Middelbank for drifter 27, 29 and 31 respectively).

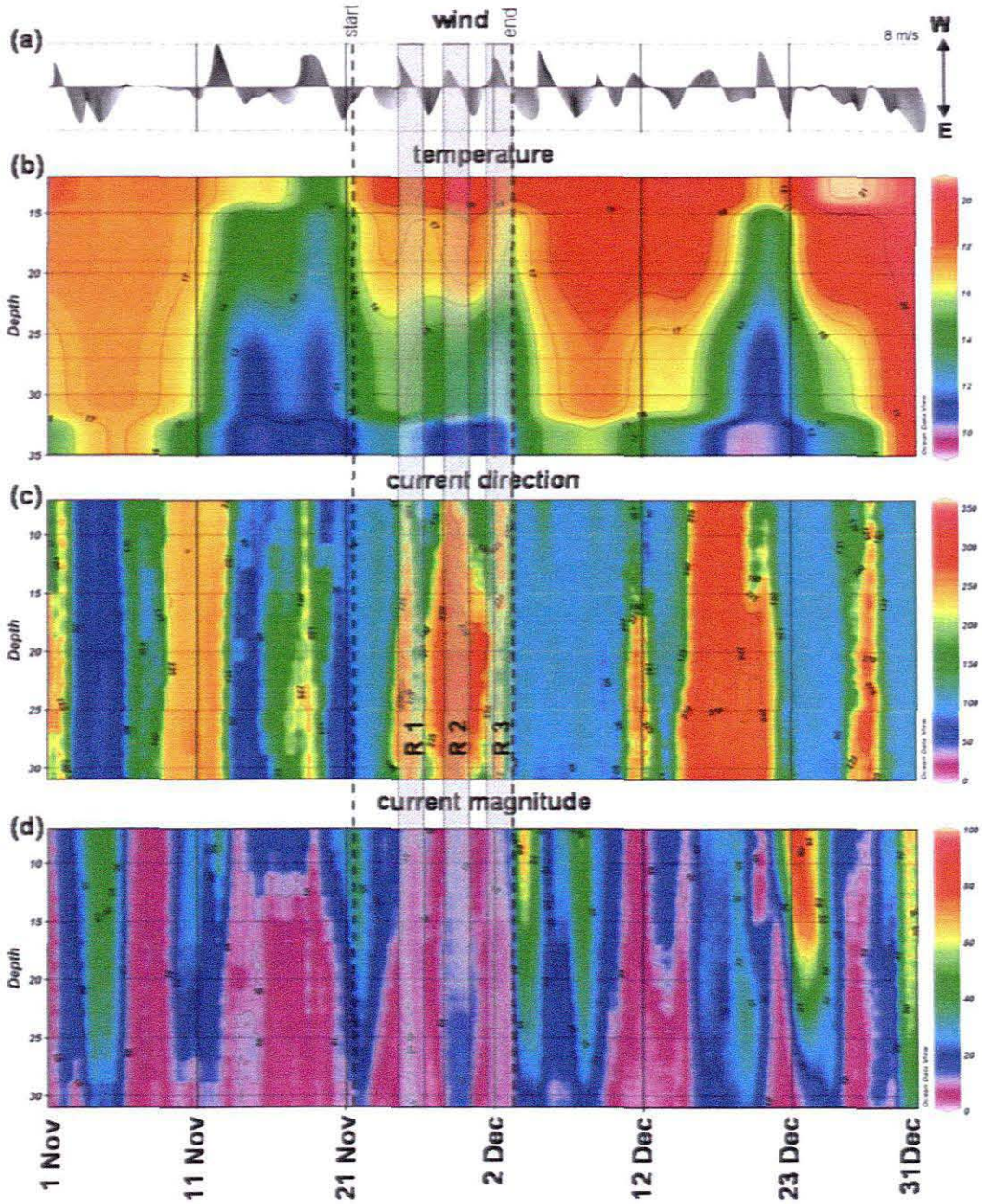

Figure 3.12: Data collected during November and December 2006. (a) Filtered wind vectors from the Cape St. Francis weather station, (b) sea temperature measurements from the thermistor array at Middelbank, (c) current direction and (d) current magnitude measured by the ADCP at Middelbank. The dashed lines indicate the start and end of the drifter deployment 1, and the shaded bars (R1, R2, and R3) indicate periods of westward displacement recorded by the drifters.

3.3.2 Deployment 2

Drifter 32 was released at Middelbank on 4 March 2007, during a period of strong westerly winds (Figure 3.14a) and isothermal conditions (Figure 3.14b). Drifter 32 moved east (Figure 3.13) in strengthening westerly winds, and attained a maximum hourly velocity of 72 $cm.s^{-1}$ before crossing the eastern boundary of the TNP. The average drift velocity during the first 24 hours was 53 $cm.s^{-1}$, and decreased to 16 $cm.s^{-1}$ during the last 12 hours of the deployment (Figure 3.13). Subsequently, the drifter washed ashore near the Tsitsikamma River, 54 km east of Middelbank (Figure 3.13), during moderating southwesterly winds (Figure 3.13 inset i), having travelled a total distance of 55 km in 38 hours.

The Middelbank ADCP (Figure 3.14 c – d) confirms a strong eastward current (63.8 $cm.s^{-1}$) at the time of the drifter deployment on 4 March. The eastward current persisted until 7 March, when the current throughout the water column turned west. The change in current direction was timed perfectly with a change in wind direction from westerly to easterly (Figure 3.14). The easterly winds prevailed until 10 March and was associated with a decrease in water temperature at 35 m form 21 °C to 10 °C (Figure 3.14b) and an onshore current component (Figure 3.14c).

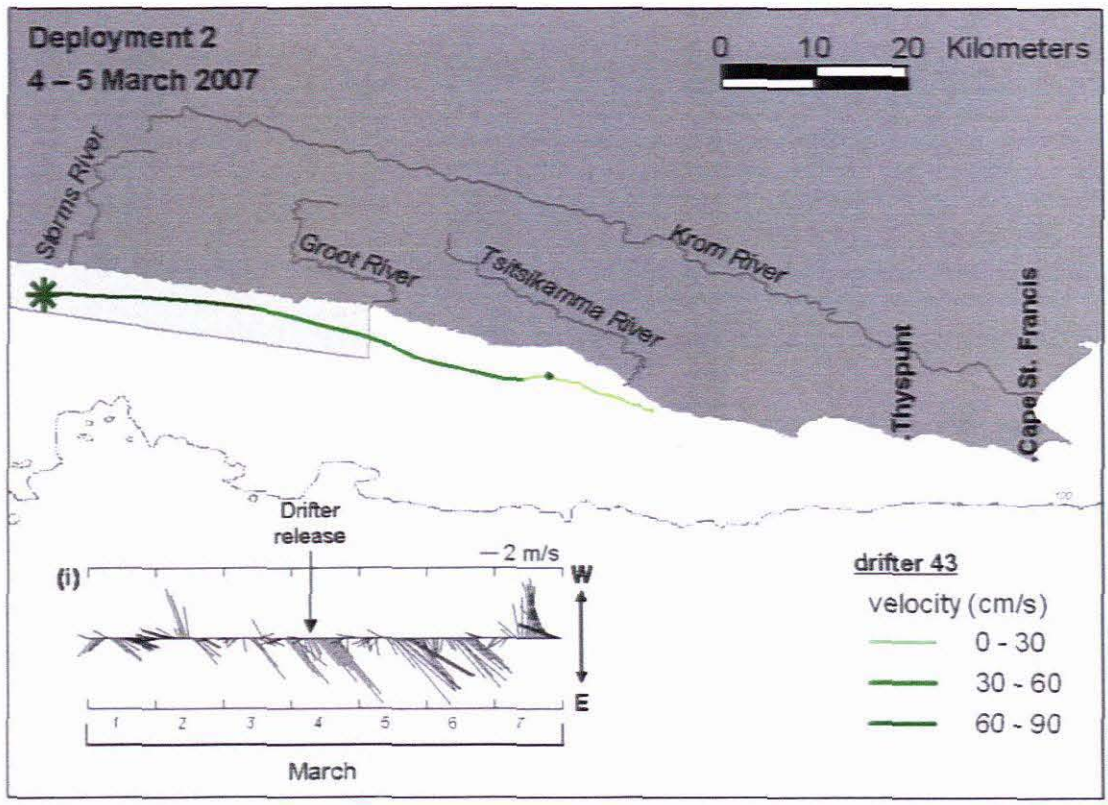

Figure 3.13: The trajectory of drifter 32 released during deployment 2. Drifter movement is away from the asterisk and drift velocity is colour coded according to the legend. Black dots indicate daily ticks. Inset (i) shows unfiltered stick vectors of the wind at Tsitsikamma during the time of drifter deployment 2.

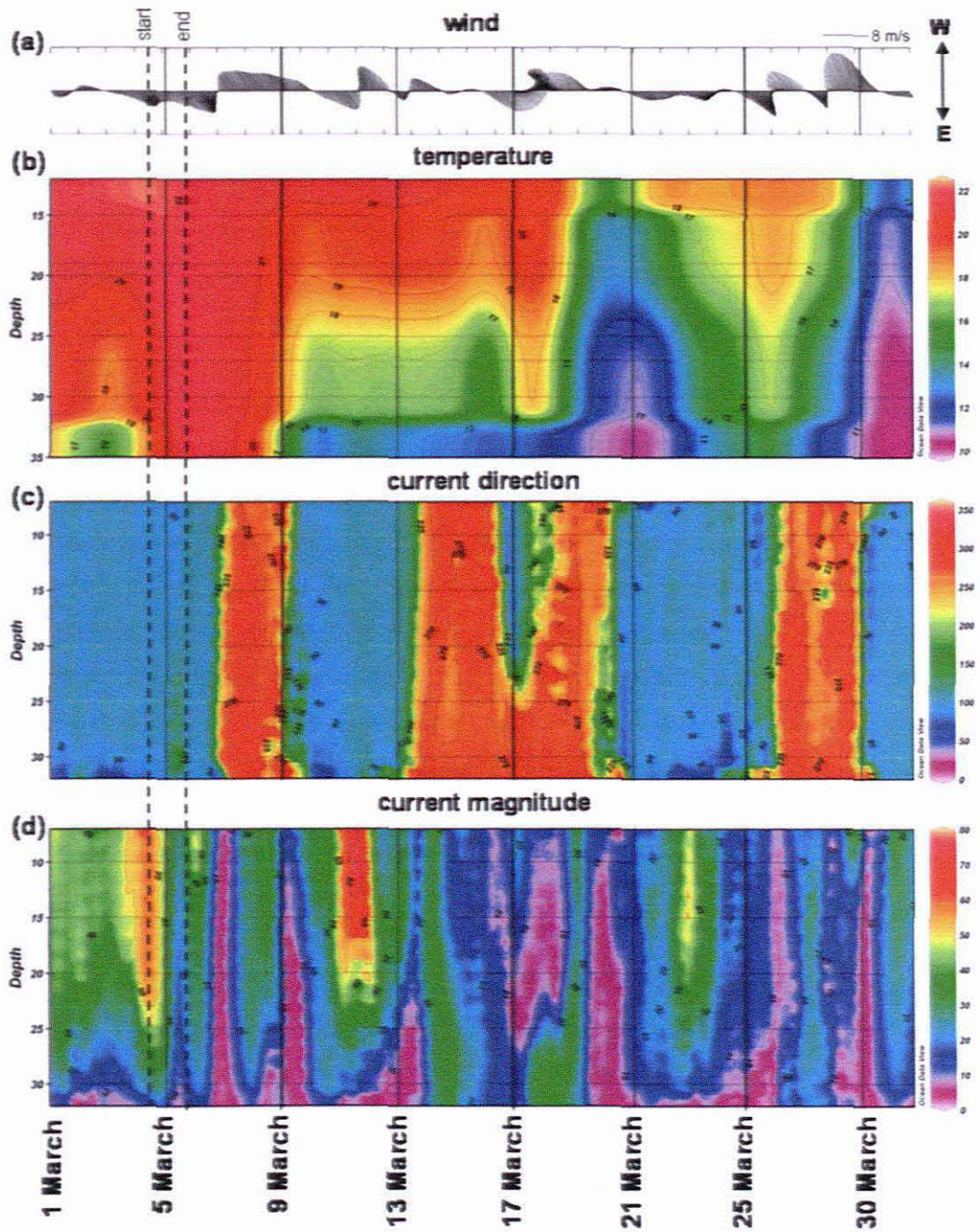

Figure 3.14: Data collected during March 2007. (a) Filtered wind vectors from the Tsitsikamma weather station, (b) sea temperature measurements from the thermistor string at Middelbank, (c) current direction and (d) current magnitude measured by the ADCP at Middelbank. The dashed lines indicate the start and end of drifter deployment 2.

3.3.3 Deployment 3

Drifter deployment 3 was made in June 2007 when eight drifters were released along the Tsitsikamma coast over a ten day period. Simultaneous deployments took place at Plettenberg Bay and Middelbank, and St. Francis Bay and Middelbank, to investigate continuity in the Tsitsikamma current. Single deployments were made at Middelbank (n = 1), St. Francis Bay (n = 1), and Plettenberg Bay (n = 2). Two drifters were excluded from the analysis because of a technical malfunction (229) and bad data quality (33). The remaining drifters (n = 6) were followed for a period of one month after deployment and their trajectories separated into four weekly periods (Figure 3.15 a - d), starting from the date of release of the first drifter (13 June).

During deployment 3 the water column at Middelbank was isothermal (Figure 3.16b) and the drifters measured a predominantly westward current along the Tsitsikamma coast. From Middelbank, drifters moved west along towards Cape Seal, staying parallel to the coast, and inshore of the 100 m depth contour. Eastward reversals interrupted the westward current on three occasions. These reversals occurred concurrently in several drifters, often resulting in closed trajectories. Some drifters moved eastwards along the coast between Knysna and Storms River Mouth. The drifters also measured clockwise and anti-clockwise circulation of St. Francis Bay, and high east-west variability between Knysna and Cape Seal, and between the Tsitsikamma River and Seal Point. Drifter deployment 3 is described in detail below with emphasis on the synchronised reversals.

Week 1

Two drifters were released simultaneously, at Middelbank (228) and Plettenberg Bay (227) on 13 June. At the time of deployment the wind was calm (Figure 3.16a) and the water column at Middelbank isothermal (Figure 3.16b). Drifter 228 moved west of Middelbank, staying parallel to the coast (Figure 3.15a). It reached a maximum hourly velocity (49 $cm.s^{-1}$) south of Cape Seal, on 16 June, during light westerly winds. Drifter (227) moved west of Cape Seal, and then inshore towards Knysna, from where it performed two consecutive cyclonic rotations. During the second rotation westward drift was characterised by offshore displacement (16 June) and eastwards drift by onshore displacement (17 -18 June) resulting in a closed trajectory (Figure 3.15a).

Drifter 36 was deployed on the morning of 14 June at Middelbank. Southwesterly winds strengthened and reached a maximum speed of 6 $m.s^{-1}$ in the afternoon. Drifter 36 slowly moved west (< 30 $cm.s^{-1}$) along the coast, against the wind. It washed ashore at the mouth of the Elandsbos River, about 15 km west of Middelbank, on 15 June 2007 (Figure 3.15a), during a gentle (3 – 6 $m.s^{-1}$) southwesterly winds.

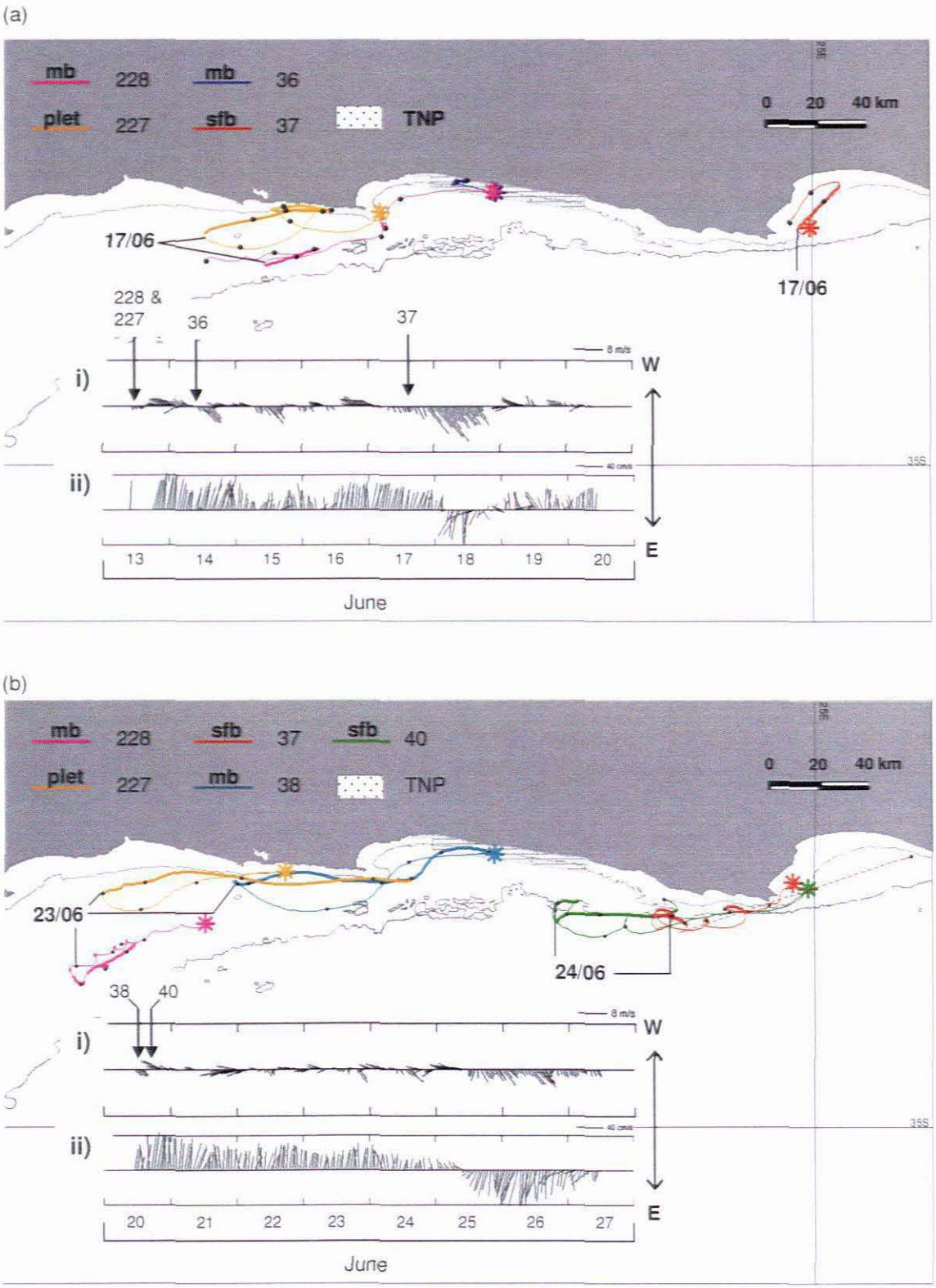

Figure 3.15: Drifter trajectories during (a) week 1, (b) week 2 (c) week 3 and (d) week 4 of deployment 3 (June – July 2007). Drifter movement is away from the asterisk and bold lines represent displacement with an eastward component. Dates indicate the time of concurrent reversals, while black dots are daily ticks. The insets are (i) unfiltered stick vectors of the wind at Tsitsikamma and (ii) and unfiltered current measurements in the surface layer (7m) at Middelbank.

Drifter 37, deployed on 17 June in St. Francis Bay, slowly moved west, towards Cape St. Francis (daily average speed = 10 $cm.s^{-1}$), while southwesterly winds gained strength (Figure 3.15a). The southwesterly wind reached gale force speeds (~ 19 $m.s^{-1}$) on the evening of 17 June and on 18 June. Drifter 37 changed direction from west to northeast after the onset of this strong southwesterly wind, to align with the wind direction (Figure 3.15a). It (drifter 37) recorded a maximum hourly velocity of 43 $cm.s^{-1}$ on 18 June, when southwesterly wind speeds were still in excess of 10 $m.s^{-1}$. When the westerlies moderated, on 18 June, the drifter changed direction to southwest, performing a complete anticlockwise circulation of St Francis Bay in the process (Figure 3.15a). By the end of week one drifter 37 travelled a total distance of ~ 51 km and was positioned just 5.5 km from where it was released three days earlier, highlighting a semi-enclosed circulation in the area.

Drifters 228 and 227, positioned south of Knysna, and drifter 37, in St. Francis Bay, experienced simultaneous eastward drift during the episode of strong to gale force southwesterly winds on 17 – 18 June (Figure 3.15a). The Middelbank ADCP also recorded an eastward current on 18 June (Figure 3.15 inset i and ii). Figure 3.16 c and d show that the eastward current recorded on 18 June was barotropic, being present throughout the water column. Maximum velocity recorded by the ADCP was 50 $cm.s^{-1}$ and 33 $cm.s^{-1}$ at the surface (7 m) and near the seabed (31 m), respectively.

Week 2

Five drifters were active across the study area during week two and moved west between 20 – 23 June. On 23 June, drifters 228, 227, and 38, located west of Knysna, changed direction to eastward (Figure 3.15b). The reversal started in the west and progressed eastward, with drifter 227 and 228 turning around first, followed by drifter 38. The Middelbank ADCP recorded an eastward reversal in the current on 25 June (Figure 3.15 inset ii) that lasted for 60 hours. The reversal occurred throughout the water column (Figure 3.16c) and maximum velocity at the surface and near the seabed were 67 $cm.s^{-1}$ and 41 $cm.s^{-1}$ respectively. At the time of the eastward reversal the wind at Tsitsikamma changed to southwesterly (Figure 3.15 inset i), reaching light to moderate (1 – 5 $m.s^{-1}$) speeds. Each drifter's trajectory during week 2 is described in more detail below:

Drifters 40 and 37 moved west, from St. Francis Bay around Seal Point, between 20 – 24 June (Figure 3.15b). Both drifters (37 and 40) continued to travel west against moderate (north) westerly winds and performed regular clockwise rotations. Drifter 37 experienced a break in transmission that lasted for 36 hours and reported again on 27 June, east of St. Francis Bay. Drifter 40 moved eastwards between 24 – 26 June.

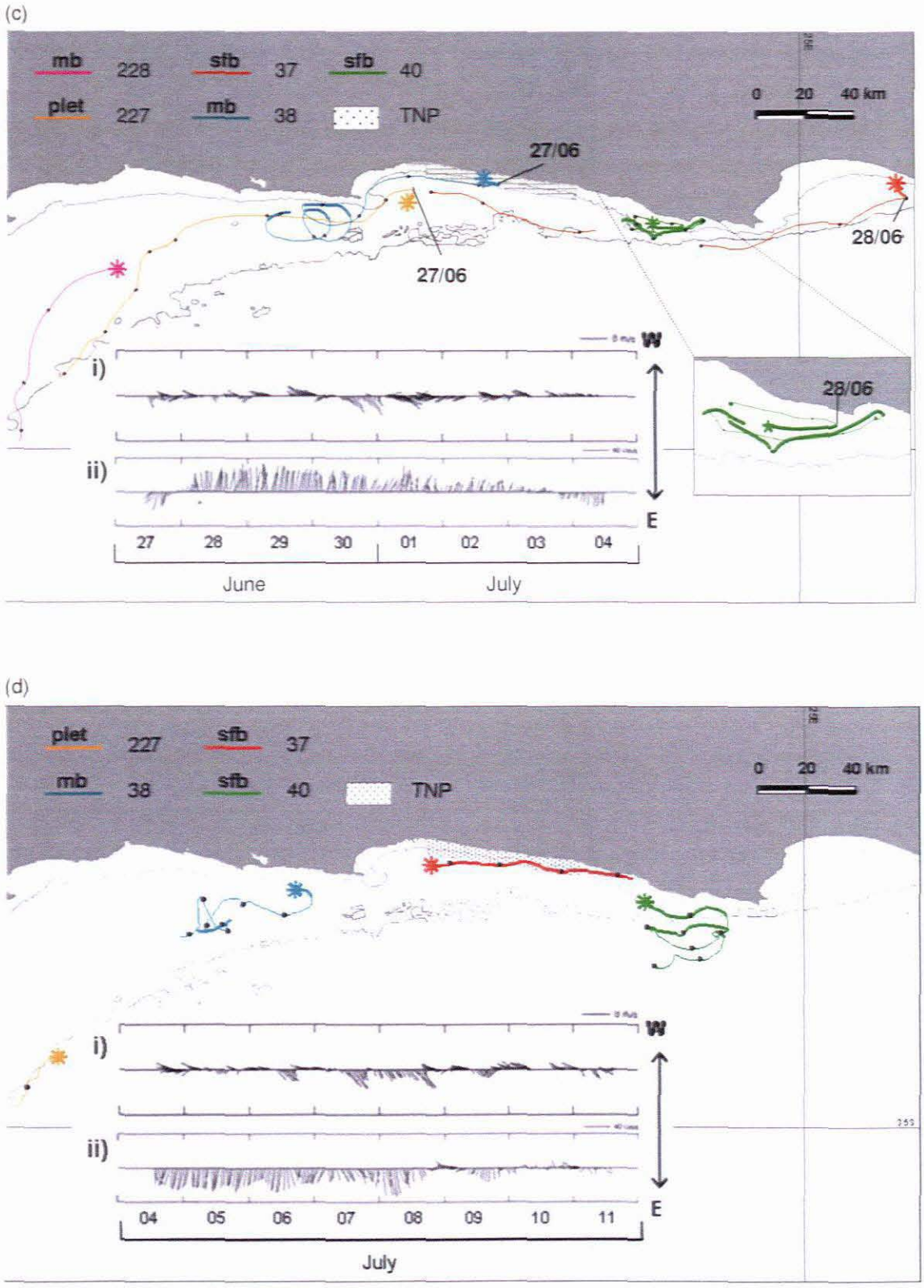

Figure 3.14: The trajectories of drifters during (c) week 3 and (d) week 4 of deployment 3. Drifter movement is away from the asterisk and bold lines represent displacement with an eastward component. Dates indicate the time of concurrent reversals, while black dots are daily ticks. The insets are (i) unfiltered stick vectors of the wind at Tsitsikamma and (ii) and unfiltered current measurements in the surface layer (7m) at Middelbank.

Drifter 38, released at Middelbank during gentle offshore winds, moved ~ 95 km west towards Knysna (Figure 3.15b). It stayed parallel to the coast and reached a maximum a velocity of 53 $cm.s^{-1}$ soon after deployment on 20 June. The winds gained strength to moderate offshore on 21 June, and the drifter continued west. Drift velocity decreased from 50 $cm.s^{-1}$ on 22 June, to < 1 $cm.s^{-1}$ on 23 June, during light and variable winds. Drifter 38, positioned 13 km southwest of Knysna, turned east and followed the coastline towards Storms River. The winds changed to moderate westerly between 25 – 27 June (Figure 3.15b inset i). On 25 June, drifter 38 accelerated eastwards (61 $cm.s^{-1}$) as it moved pass Cape Seal, and on 27 June it was positioned only 1.5 km from its release site in the TNP, creating a completely closed trajectory (Figure 3.15b). Drifter 38 travelled a distance of 190 km in seven days, maintaining a daily average speed of 27 $km.day^{-1}$.

The eastward reversal, described above, was also observed in the trajectories of drifters 228 and 227 (Figure 3.15b). On 23 June, drifter 227 was moving west about 15 km offshore, between Mossel Bay and Plettenberg Bay. It turned east and accelerated to 60 $cm.s^{-1}$ as it drifted pass Cape Seal. At the same time, drifter 228 was moving southwest, about 40 km offshore between Mossel Bay and Plettenberg Bay. Drifter 228 turned east between 23 -26 June, closely following the 100 m isobath (SW – NE), and resumed south-westward drift on 27 June.

Week 3

The drifters resumed their westward drift during the third week of deployment 3 (Figure 3.15c). The reversal again happened from west to east across the study area, and started on the last day of week 2 (June 26), when drifter 228 turned west on the midshelf region of the Agulhas Bank (Figure 3.15b). Eighteen hours later, drifter 227, located directly east of Cape Seal; and drifter 38, located near Middelbank, both turned west in light offshore winds (Figure 3.15c inset i). A westward current was confirmed by the Middelbank ADCP (Figure 3.15c inset ii), which recorded the change in direction throughout the water column on 28 June (Figure 3.16c).

After the reversal, drifters 228 and 227 continued southwest and offshore along the 100 m depth contour (Figure 3.16c), reaching maximum velocities of 47 $cm.s^{-1}$ and 68 $cm.s^{-1}$ respectively. Drifter 288 left the study area and moved further offshore, but remained on the Agulhas Bank. It returned to the Tsitsikamma coast in mid-August without its drogue.

Drifter 38 moved west from Middelbank towards Knysna, staying parallel to the coast (Figure 3.15c). It then performed three clockwise rotations west of Cape Seal (Figure 3.15c), during a period of altering easterly and westerly winds recorded at Plettenberg Bay.

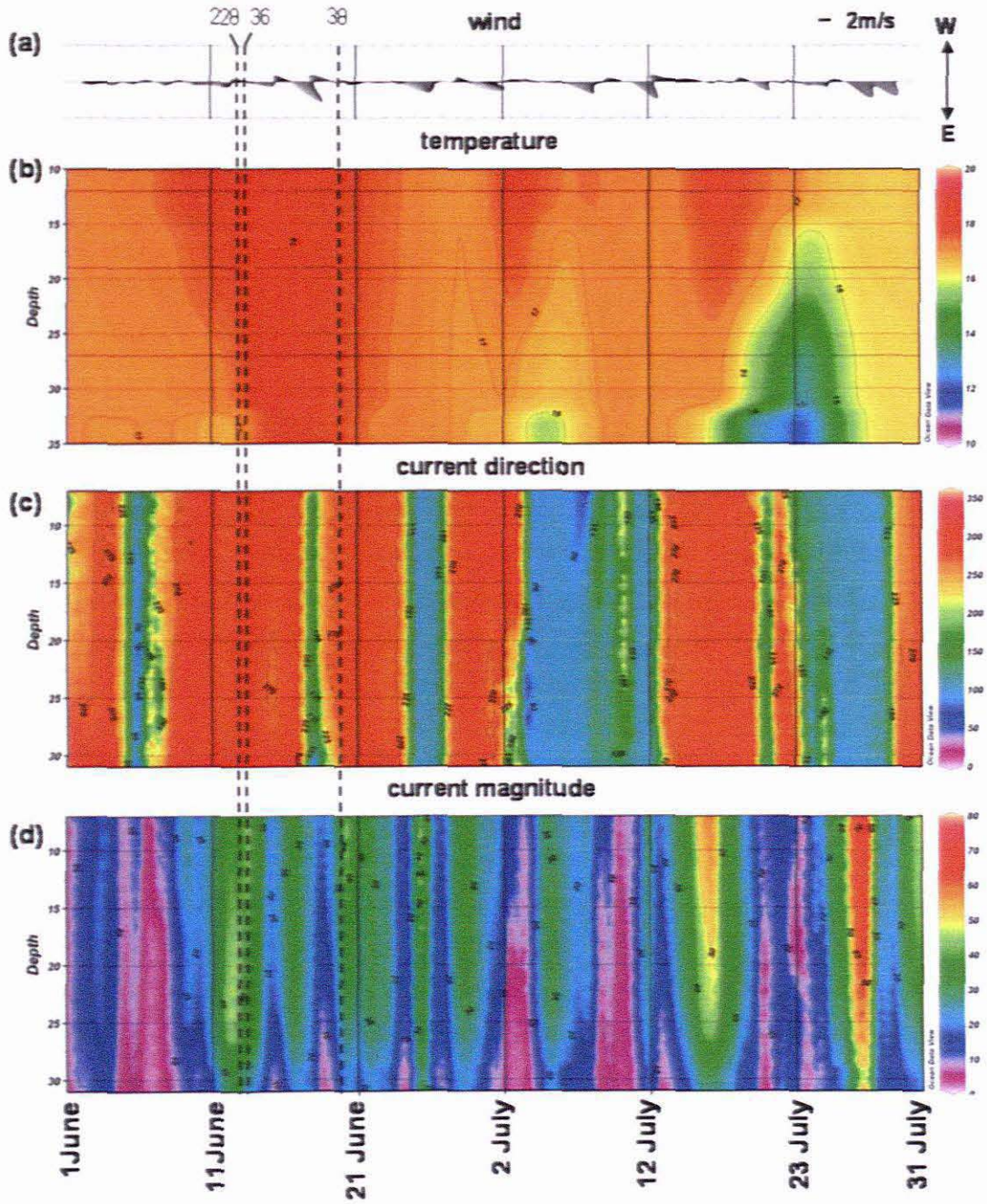

Figure 3.16: Data collected during June and July 2007. (a) Filtered wind vectors from the Tsitsikamma. weather station, (b) sea temperature measurements from the thermistor string at Middelbank, (c) current direction and (d) current magnitude measured by the ADCP at Middelbank. The dashed lines indicate the time of drifter deployment at Middelbank.

Drifter 40 remained in the area between Thyspunt and the Tsitsikamma River during week 3, as its direction changed between eastward and westward (Figure 3.15c map inset). Current measurements from the ADCP at TNP-east also indicate a surface current that fluctuated between eastward and westward during this period (Appendix B1). Drifter 37, positioned on the eastern side of St. Francis Bay, turned west on 28 June (Figure 3.15c) and moved about 170 km west along the 100 m depth contour, reaching a maximum velocity of 88 $cm.s^{-1}$. Communication with drifter 37 was lost for nearly two days, but drifter 40, located nearby, gave confirmation of a westward current. Drifter 37 continued west and stayed inshore of the 100 m depth contour (Figure 3.15c), while its velocity decreased to just 5 $cm.s^{-1}$ on 4 June.

Week 4

The third eastward reversal was recorded on 4 July by drifter 37 and drifter 40, during calm wind conditions. Drifter 37 turned east and inshore (Figure 3.15d), increasing its hourly drift velocity to a maximum of 36 $cm.s^{-1}$ as it entered the TNP. Drifter 37 washed ashore near the Tsitsikamma River on 9 July. The ADCP at Middelbank confirmed eastward flow throughout the water column between 4 – 9 July (Figure 3.16c). Drifter 40 turned east, 16 hours before drifter 37, in light offshore winds and continued moving east until 5 June (Figure 3.15d). Subsequently, drifter 40 zigzagged from east to west near Thyspunt, progressing further offshore with each change in direction (Figure 3.15d). The wind at Cape St. Francis was predominantly westwards during week 4, with gale force conditions on 8 July.

Drifter 227 moved further offshore following the 100 m depth contour onto the Agulhas Bank. Communication with drifter 227 was lost on 18 July, 35 days after deployment. Drifter 38 stayed inshore, southwest of Knysna (Figure 3.15d) until 13 July, when it moved offshore along the 100 m depth contour. The last report from drifter 38 was received on 25 July, just beyond the 200 m contour at the apex of the Agulhas Bank.

3.3.4 Deployment 4

Three drifters were released in November 2007; two at Middelbank and one in St. Francis Bay. Drifter 47 was deployed above the Middelbank ADCP on 17 November, and drifter 48, 7.4 km further offshore, fifteen minutes later. At the time of deployment, the wind was light (~ 2 $m.s^{-1}$) easterly (Figure 3.17), the water column above Middelbank was isothermal at 18 °C (Figure 3.19b), and the ADCP at Middelbank recorded weak (< 10 $cm.s^{-1}$) and variable currents (Figure 3.19 c and d). Drifter 41 was released in St. Francis Bay on 18 November, during light (~ 2 $m.s^{-1}$) south-westerly winds (Figure 3.17).

Drifters 47 and 48 followed distinctly different trajectories, despite being deployed only 7.4 km apart (Figure 3.17). The inshore drifter (47), stayed within a 2 km radius of Middelbank during the first 36 hours of its deployment, slowly moving west (average velocity < 5 $cm.s^{-1}$). At the same time, the offshore drifter (48) swiftly moved west and offshore (maximum velocity = 45 $cm.s^{-1}$) across the eastern Agulhas Bank (Figure 3.17). Drifter 48 stopped reporting on 20 November, three days after deployment. Drifter 41, deployed in St Francis Bay on 18 November, moved west around Cape St. Francis (Figure 3.17) at an average daily velocity of 36 $cm.s^{-1}$, against light (~ 3 $m.s^{-1}$) westerly winds (Figure 3.17 inset i). Drifter 41 stopped reporting on 19 November.

Drifter 47 changed direction to east and offshore on the afternoon of 20 November (Figure 3.17), during a period of gentle (4 – 7 $cm.s^{-1}$) northeasterly winds. The wind moderated with nightfall, and on 21 November the drifter turned onshore before resuming it's alongshore trajectory. The drifter again turned offshore as it crossed the eastern boundary of the TNP, on 23 November (Figure 3.17). The offshore movement coincided with moderate southeasterly winds at Cape St. Francis and at Tsitsikamma. The drifter (47) turned west when it reached the ~ 100 m isobath; at the same time accelerating to > 50 $cm.s^{-1}$. It continued west along the 100 m isobath, and reached the area where the cold ridge is normally located eight days after leaving the Tsitsikamma coast (Figure 3.17). The cold ridge was not identifiable from satellite imagery during this period. Drifter 47 left the study area on 30 November (Figure 3.17), but remained on the central Agulhas Bank during December 2007. It moved inshore, and onto the western Agulhas Bank, from where it left the shelf on 17 January 2008, and moved into the Atlantic Ocean. The last position from drifter 47 was received on 29 February 2008, 315 km off the southern Namibian coast.

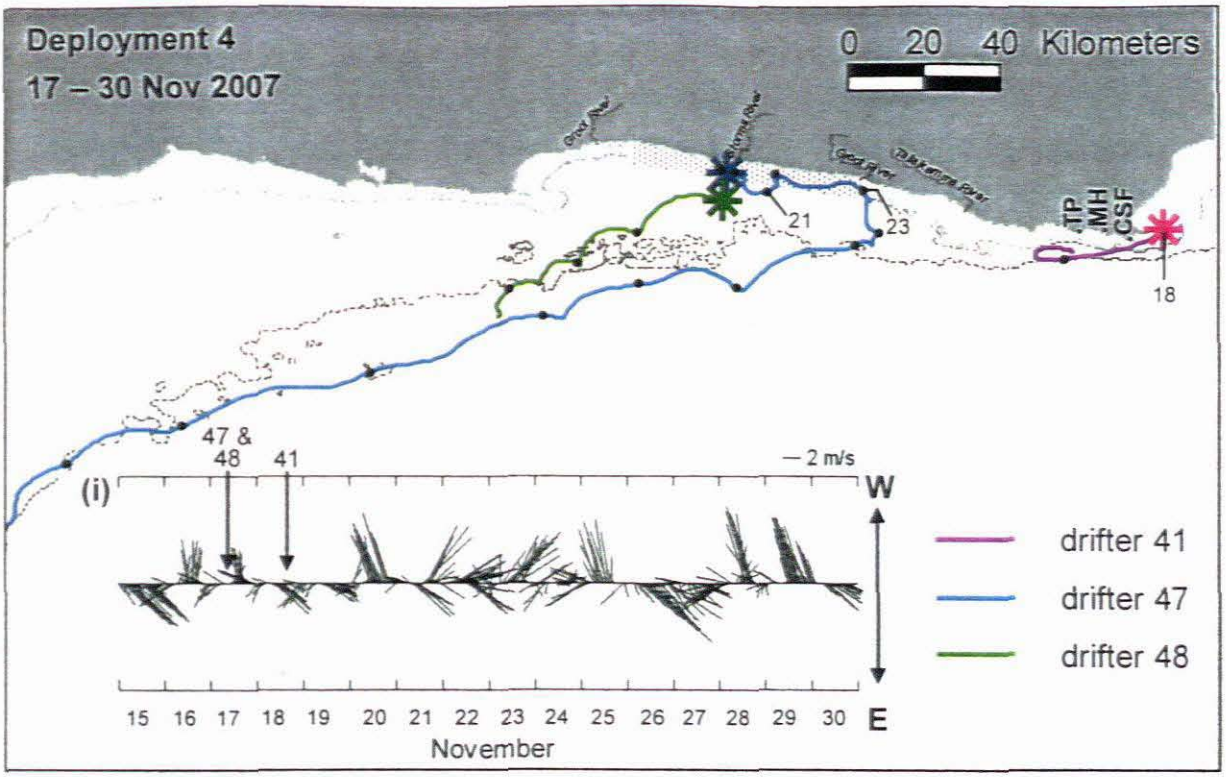

Figure 3.17: The trajectories of the drifters released during deployment 4 (November 2007). Drifter movement is away from the asterisk and black dots indicate daily ticks. Inset (i) shows unfiltered stick vectors of the wind at Tsitsikamma during drifter deployment 4. Abbreviated place names are: Thyspunt (TP), Mostert's Hoek (MH) and Cape St. Francis (CSF).

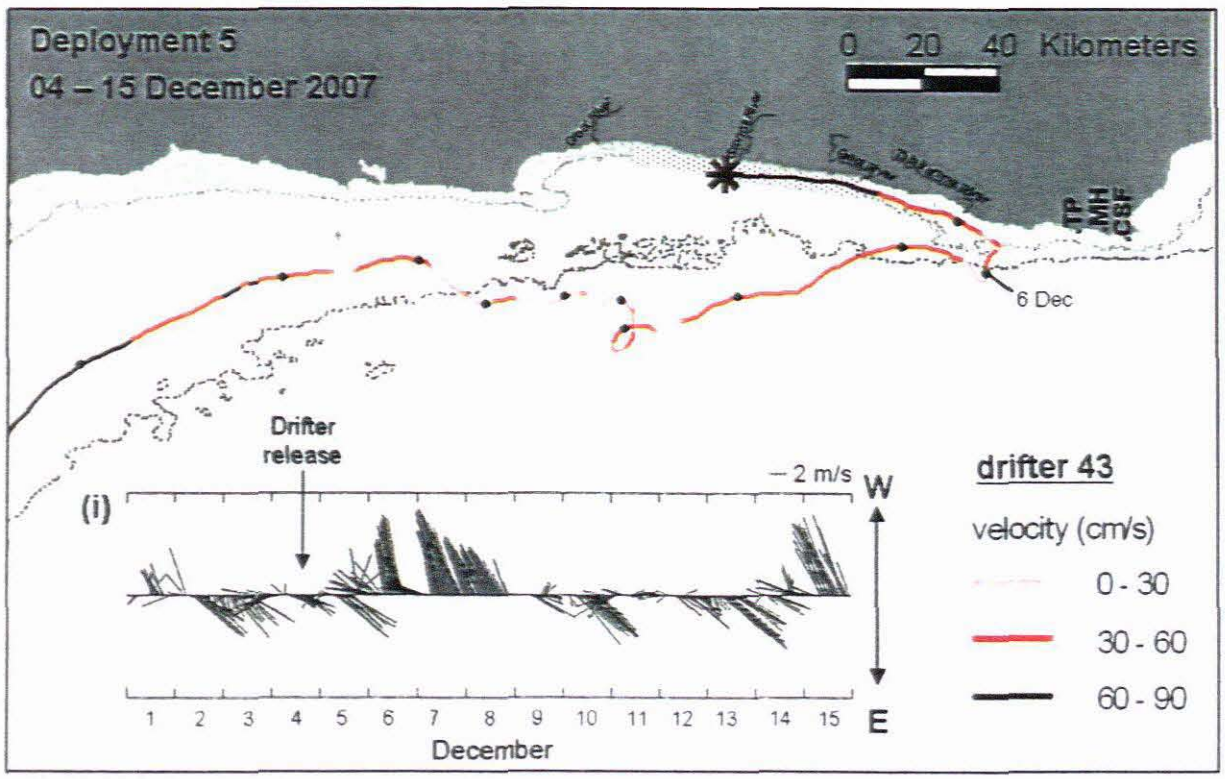

Figure 3.18: The trajectory of drifter 43 released during deployment 5 (December 2007). Drifter movement is away from the asterisk and black dots indicate daily ticks. Drift velocity is colour coded according to the legend. Inset (i) shows unfiltered stick vectors of the wind at Tsitsikamma during drifter deployment 5. Abbreviated place names are: Thyspunt (TP), Mostert's Hoek (MH) and Cape St. Francis (CSF).

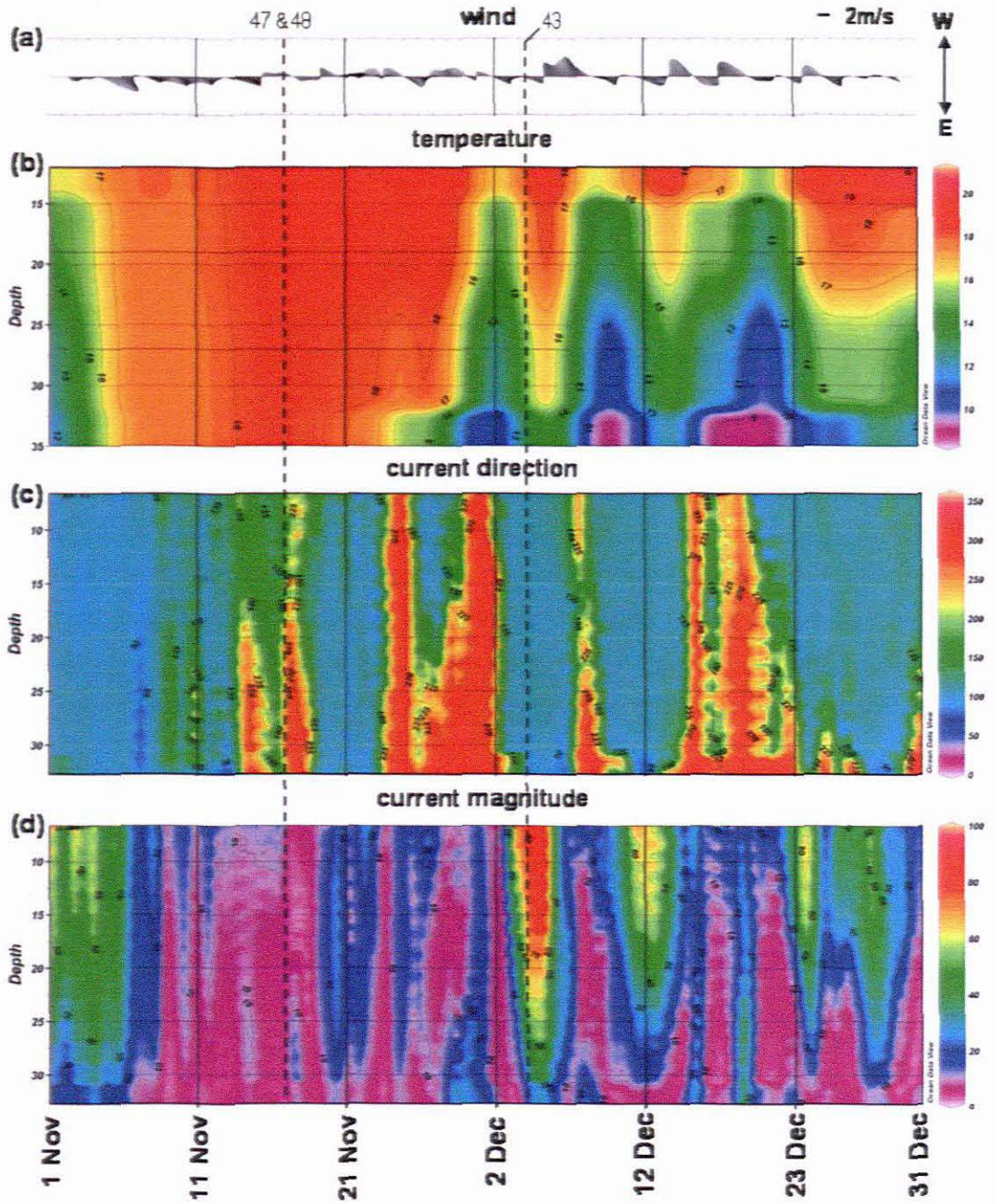

Figure 3.19: Data collected during November and December 2007 (deployments 4 and 5). (a) Filtered wind vectors from the Tsitsikamma weather station, (b) sea temperature measurements from the thermistor string at Middelbank, (c) current direction and (d) current magnitude measured by the ADCP at Middelbank. The dashed lines indicate the time of drifter deployment at Middelbank.

3.3.5 Deployment 5

Drifter 43 was released at Middelbank on 4 December, during light (~ 4 $m.s^{-1}$) southwesterly winds (Figure 3.19a), and downwelling conditions at Middelbank (Figure 3.19b). The drifter measured a strong (90 $cm.s^{-1}$) eastward current, confirmed by the Middelbank ADCP data (Figure 3.19 c and d).

The drifter stayed inshore, parallel to the coastline and maintained an hourly eastward velocity > 70 $cm.s^{-1}$, until it crossed the eastern boundary of the TNP (Figure 3.18), 12 hours after deployment. The wind changed direction from southwesterly to easterly on the afternoon of 5 December, and increased to fresh easterly by 7 December (Figure 3.18 inset i). Eastward drift velocity gradually decreased during this period of strengthening easterly winds, and the drifter turned west and offshore on 6 December, near Thyspunt (Figure 3.18). Drifter 43 moved west across the midshelf along the 100 m isobath (Figure 3.18), following a similar path to drifter 47 in deployment 4 (Figure 3.17). Upwelling was recorded by the inshore UTRs at Mostert's Hoek and Storms River Mouth on 7 and 8 December, respectively (Appendix C1). Drifter 43 left the study area on 15 December, 11 days after deployment at Middelbank The last successful report was received on 16 December, ~ 80 km south of Mossel Bay.

3.3.6 Deployment 6

Drifter 46 was deployed at Middelbank, on 11 March 2008, during a period of light to fresh southwesterly winds (Figure 3.20 inset i). The instruments at Middelbank recorded an eastward current (Figure 3.21 c and d) and a lowering of the thermocline (Figure 3.20c) at the time of deployment. Southwesterly winds strengthened to moderate gale force, with a maximum speed of 14.9 $m.s^{-1}$ recorded on 12 March at Cape St. Francis. The drifter behaved similarly to drifter 47 (Figure 3.17) and drifter 43 (Figure 3.18) in deployment 4 and 5, in that it rapidly moved east along the coast, crossing the eastern boundary of the TNP 16 hours after deployment. Drift velocity decreased with distance from Middelbank, and its daily average velocity was 55 $cm.s^{-1}$ and 22 $cm.s^{-1}$ on 11 and 12 March respectively. The southwesterly wind moderated on 13 March, and drifter 46, located near the Tsitsikamma River, moved offshore (Figure 3.20).

The drifter remained in the area between the Tsitsikamma River and Thyspunt until 16 March, alternating between eastward and westward drift. Moderate to strong easterly winds started on 15 March (Figure 3.20 inset i), and the drifter responded by turning west along the 100 m isobath. Upwelling started at Middelbank on 16 March and persisted for the duration of March 2008 (Figure 3.21b). During this upwelling event cold water (~13 °C) was also recorded at Mostert's Hoek and at Storms River Mouth on 18 and 19 March, respectively (Appendix C2).

Drifter 46 continued in a south-westward direction across the eastern Agulhas bank and left the study area 15 days after deployment. Drifter 46 remained on the Agulhas Bank for 84 days, moving as far west as Cape Agulhas, before turning east. The last report from drifter 46 was received on 3 June 2008, 28 km southeast of Knysna.

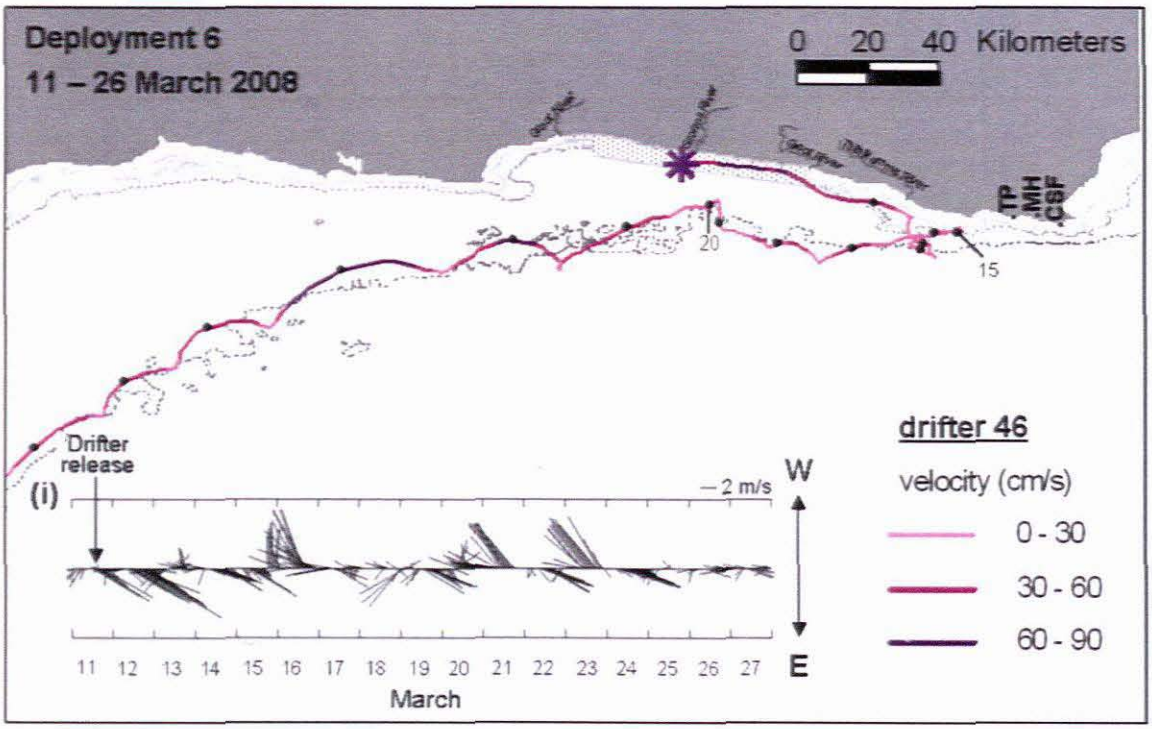

Figure 3.20: The trajectory of drifter 46, released during deployment 6 (March 2008). Drifter movement is away from the asterisk and black dots indicate daily ticks. Drift velocity is colour coded according to the legend. Inset (i) shows unfiltered stick vectors of the wind at Tsitsikamma during drifter deployment 6. Abbreviated place names are: Thyspunt (TP), Mostert's Hoek (MH) and Cape St. Francis (CSF).

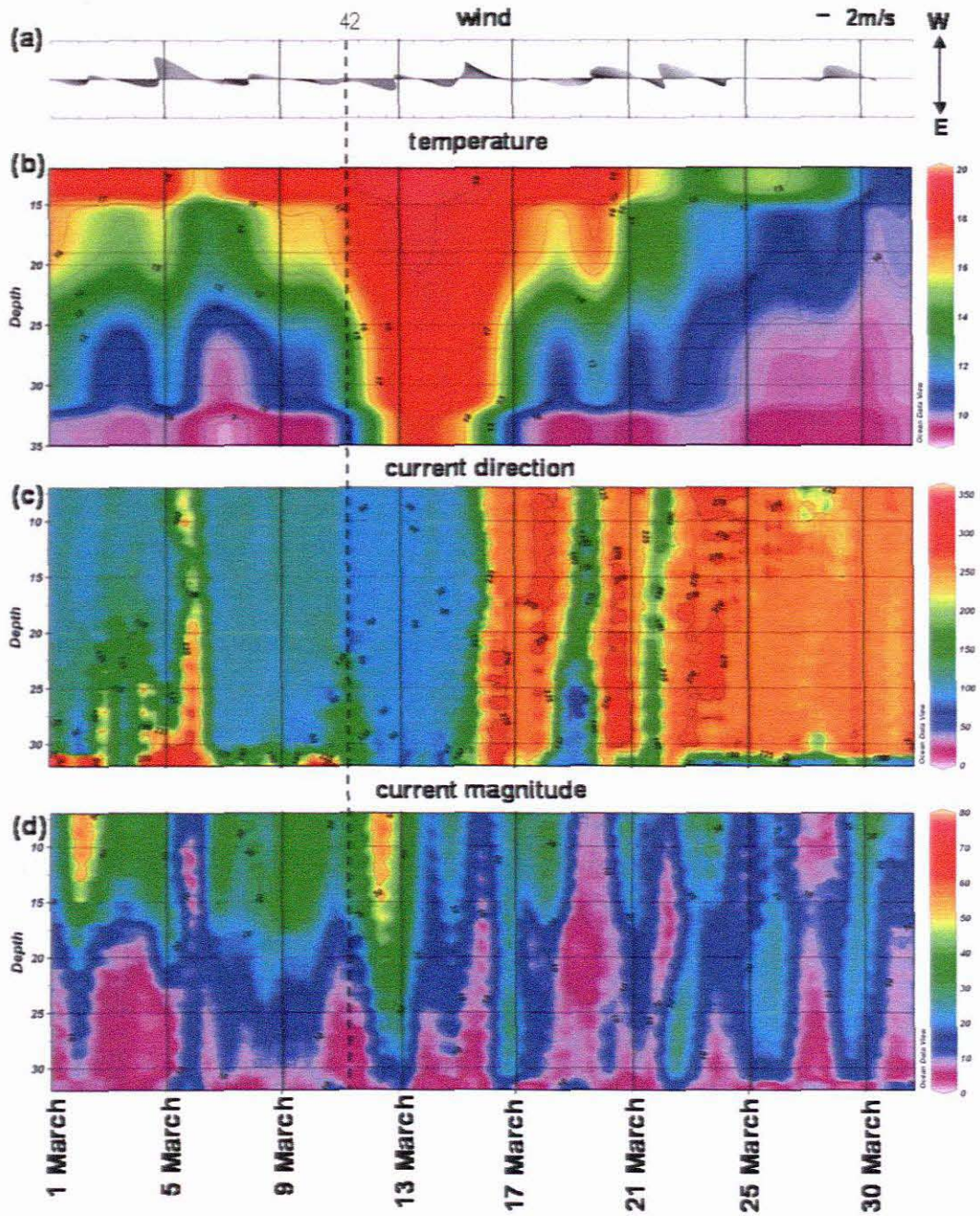

Figure 3.21: Data collected during March 2008 (deployments six). (a) Filtered wind vectors from the Tsitsikamma weather station, (b) sea temperature measurements from the thermistor string at Middelbank, (c) current direction and (d) current magnitude measured by the ADCP at Middelbank. The dashed line indicates the time when drifter 42 was deployed at Middelbank.

CHAPTER 4
DISCUSSION

The circulation off the Tsitsikamma coast have been investigated using various methods, including ship borne ADCPs (Boyd and Oberholster 1994, Boyd *et al.* 1992), fixed current meters (Tilney *et al.* 1996, Roberts and van den Berg 2005) and radio-tracked drifters (Attwood *et al.* 2002). The different methods have produced somewhat conflicting results, but all authors agreed that alongshore flow occurs inshore along the Tsitsikamma coast, and that the currents are strong enough to transport neutrally buoyant material, including eggs and larvae, beyond the boundaries of the TNP.

Tilney *et al.* (1996) measured only bottom currents (48 m) off the Elandsbos River and found the cross-shelf component to be dominant over the longshore component. Their data showed seasonal differences with alongshore barotropic oscillations in winter, and cross-shelf baroclinic oscillations in spring and summer. They proposed three theoretical current closure systems with the potential to transport eggs and larvae beyond the borders of the TNP. The first, an alongshore, barotropic reversal, occur year round and is associated with eastward moving weather systems that alter the sea level and generate barotropic coastal trapped waves (CTW). The second and third scenarios describe the offshore/onshore movement of surface water during small and large-scale upwelling and downwelling events, typical of spring and summer. All three scenarios suggest a closed circulation system with the potential to transport biotic material beyond the borders of the TNP, and the possibility of return to its point of origin with the prevailing shoreward or alongshore current.

A drogue study conducted by Attwood *et al.* (2002) showed the surface current to be mostly alongshore and westwards, with minor onshore and offshore components indicative of Ekman drift. They found no obvious seasonal trends and had difficulty differentiating between the winter and summer patterns observed by Tilney *et al.* (1996). Attwood *et al.* (2002) suggested that wind is not the primary driving force of the Tsitsikamma current and that alongshore reversals were caused by CTW. The radio-tracked drifters produced Lagrangian time series that were too short to test the current closure systems proposed by Tilney *et al.* (1996).

The analysis of 12 months of ADCP data from Middelbank (Roberts and van den Berg 2005), firmly established the presence of an alongshore current off the Tsitsikamma coast, and the dominance of eastward flow (68%) near the surface. In agreement with Tilney *et al.* (1996), who measured only bottom currents, Roberts and van den Berg (2005) found seasonal trends and transient current reversals. They also demonstrated how easterly winds and

resultant upwelling can interrupt an eastward current and turn the surface layer offshore, thus limiting eastward displacement near the surface. Roberts and van den Berg (2005) concluded that paralarvae spawned inshore, and caught up in an eastward flowing Tsitsikamma current, will be transported away from the copepod maximum at the cold ridge. This unexpected result required the following modification to the westward transport hypothesis (Roberts 2005): offshore displacement during upwelling implies that at least some of the paralarvae spawned inshore will end up on the midshelf from where they can be swept west, towards the cold ridge with the net flow (Boyd *et al.* 1992). Alternatively, onshore (surface) movement during downwelling provides a corridor for paralarvae on the midshelf to be returned inshore, thereby retarding eastward displacement and retaining paralarvae at the base of the cold ridge.

In this study, new data from a combination of Eularian and Lagrangian measurements provide the necessary spatial and temporal coverage to test the upwelling-driven current closures (Tilney *et al.* 1996, Roberts and van den Berg 2005), and the Western Transport Hypothesis, in its simple (Roberts 2005) and in its modified state (Roberts and van den Berg 2005). The dynamics of the Tsitsikamma current, including seasonality, driving forces and potential larval transport routes are discussed in more detail below.

The ADCP results confirm a predominantly longshore surface current, inshore along the Tsitsikamma Coast. Eastward flow was slightly dominant at Middelbank (58%) and at TNP-east (61%), while measurements at Thyspunt showed near-equal percentages of eastward (45%) and westward (55%) flow. This result is similar to the findings of Roberts and van den Berg (2005) who found 68% eastward flow near the surface at Middelbank in 1998/99. A longer time series is needed to determine inter-annual variability in the circulation off the Tsitsikamma Coast, and the influence of changes in the Southern Oscillation Index (ISO) that bring about El Niño and La Niña events.

The ADCP results show differences between surface and bottom currents in agreement with Roberts and van den Berg (2005), with eastward flow less dominant near the seabed. Longshore flow remained dominant near the seafloor at all three ADCP moorings sites, but the bottom currents at Thyspunt had a distinct onshore component. Progressive bottom displacement at Thyspunt was 192 km north in 111 days, compared to 167 km north at Middelbank during the same period. The increase in the cross-shelf component at Thyspunt supports the work of Tilney *et al.* (1996), who found onshore flow off the Elandsbos River Mouth to be the dominant component near the seabed. They measured a displacement of 187 km in 198 days, whereas the ADCP data from Roberts and van den Berg (2005) show a displacement of only 80 km for the same period at Middelbank. The discrepancies in bottom

displacement, between this study and previous current meter work (Tilney *et al.* 1996, Roberts and van den Berg 2005), can be attributed to seasonal and alongshore differences in the current, as measurements were made at different times of the year and at different locations. This result points to highly variable bottom currents off the Tsitsikamma coast, and the possibility of onshore feeder currents during upwelling as suggested by Tilney *et al.* (1996).

Currents were strongest during eastward flow, in summer. Velocities > 100 $cm.s^{-1}$ only occurred during eastward flow and made up ~ 1% of the total measurements. Current strength generally decreased with depth, and maximum surface velocity (141 $cm.s^{-1}$) coincided with the maximum velocity near the seafloor (59 $cm.s^{-1}$). Roberts and van den Berg (2005) observed the same pattern, but recorded a lower maximum surface velocity of 115 $cm.s^{-1}$, while the maximum velocity near the seabed was somewhat higher, at 65 $cm.s^{-1}$. Nevertheless, when averaged, velocities from this study and from Roberts and van den Berg (2005) are similar, with 27 $cm.s^{-1}$ vs. 24 $cm.s^{-1}$ and 9 $cm.s^{-1}$ vs. 10 $cm.s^{-1}$ near the surface and bottom at Middelbank, respectively.

The results further agree with Tilney *et al.* (1996) and Roberts and van den Berg (2005) in that eastward flow was sustained for longer periods (~ 4 weeks) than westward flow (~ 2 weeks). Above average velocities continued for 9 and 10 days, in the eastward and in the westward current respectively. In February 2008, velocities > 100 $cm.s^{-1}$ persisted for 31 hours at Middelbank (Appendix B1). The net eastward displacement during this period, 120 km east of Middelbank, highlights the importance of these jet-like eastward events in larval transport along the Tsitsikamma coast.

Results from the drifter study confirm the dominance of a longshore current off the Tsitsikamma Coast, and agree that the highest velocities occur inside the TNP, during eastward flow. Current velocity decreased east of the TNP and at Tsitsikamma Point several drifters moved offshore and onto the midshelf. Roberts (in prep) speculated that the Tsitsikamma current ends in a cyclonic lee eddy in the region off Tsitsikamma Point (Figure 4.2), but there was no evidence in this study to support this theory. The offshore movement at Tsitsikamma Point is likely a combination of bottom steering by the sloping bathymetry and wind-driven upwelling initiated at the capes, and is the apparent end of the main trajectory of the Tsitsikamma current. Further east, at Thyspunt, the current again aligned with the east-west axis along the steep nearshore bathymetry.

A dominant feature of the Tsitsikamma current is the occurrence of regular alongshore reversals (Tilney *et al.* 1996, Attwood *et al.* 2002, Roberts and van den Berg 2005). Attwood

et al. (2002) used radio-tracked drifters to study the circulation inside the borders of the TNP and observed that westward flow was mostly offshore and eastward flow mostly onshore. They attributed these cross-shelf movements to Ekman drift, related to wind-driven upwelling and downwelling. In this study, satellite tracking allowed the drifters to move beyond the borders of the TNP, which showed that the observed frequency of current reversals increased near the upwelling cells, west of Cape Seal and Seal Point. The drifters recorded alongshore oscillations near both capes that corresponded to changes in the wind direction. Westward and offshore drift occurred during upwelling favourable easterly winds; eastward and onshore drift during westerly winds and downwelling. The current along the straight part of the Tsitsikamma coast, between Cape Seal and Seal Point, was less affected by changes in wind direction. In agreement with Attwood *et al.* (2002), both eastward and westward currents were sometimes against the direction of the wind.

The trajectories of drifters deployed together off the Storms River Mouth, at Middelbank and further offshore, demonstrate that during eastward flow the Tsitsikamma current is a narrow counter current, less than 10 km wide. In deployment 1 (Figure 3.10) the drifters, released 4 km apart during downwelling, recorded a horizontal velocity shear, with the inshore drifter moving three times faster than the offshore drifter. In deployment 4 (Figure 3.17), the inshore drifter recorded a slack current at Middelbank, while the offshore drifter rapidly moved west and offshore. The exact width of the Tsitsikamma current could not be determined, as this would require the use of ship borne ADCP surveys.

4.1 Seasonality

Current measurements from Middelbank show seasonal trends, similar to those described by Tilney *et al.* (1996), and Roberts and van den Berg (2005). During spring, summer and autumn, net monthly displacement in the upper water column (< 19 m) was mostly eastward and offshore, while net monthly displacement near the seabed (31 m) was mostly westward and onshore (Figure 3.4). This baroclinic current structure is related to thermal stratification typically present during the summer season on the Agulhas Bank (Schumann and Beekman 1994), and is associated with wind-driven, coastal upwelling (Schumann 1999). In agreement with Roberts and van den Berg (2005), opposing surface and bottom currents were not always present during a thermal stratified water column. However, during the large upwelling event recorded in mid-March 2008 (Figure 3.21), baroclinic currents persisted for eight days at Middelbank, which resulted in surface and bottom displacement in opposite directions, with 223 km west and 45 km east of Middelbank respectively.

During summer upwelling, Ekman transport moves surface water west and offshore, while onshore compensation drift occurs near the seabed (Schumann *et al.* 1982). Tilney *et al.*

(1996) attributed the dominance of onshore flow near the seabed at Elandsbos River to this upwelling compensation current, and was uncertain whether it was a feeder current specific to the mooring location, or if onshore flow near the seabed was characteristic of the whole reserve area. The ADCP measurements collected in this study show that onshore (bottom) flow was more important at Thyspunt (71%) and Middelbank (68%) than at TNP-east (46%), suggesting that upwelling compensation currents along the Tsitsikamma coast are site specific, while alongshore flow dominates along other parts of the coast, even when upwelling is in progress.

During isothermal conditions typical of winter (Schumann and Beekman 1994), net monthly displacement was in the same direction at all depths, being mainly westward and onshore. A series of barotropic, alongshore reversals limited westward displacement in the current. Current speeds were generally lower during winter and exceeded the 75 $cm.s^{-1}$ threshold only on one occasion, during eastward flow near the surface (maximum = 107. 0 $cm.s^{-1}$). In the absence of upwelling in winter, offshore displacement at the capes was limited, and the drifter data indicate that current reversals caused by CTWs favours retention in the nearshore regions off the Tsitsikamma coast.

The dominance of westward flow during winter needs further investigation, as it could have been the result of anomalous conditions on the Agulhas Bank during June and July 2007. SST images from 13 – 29 June (Figure 4.1) show the presence of a large meander (A) on the shoreward border of the southern Agulhas Current. Meander A moved downstream, leaving behind a plume of warm water that turned towards the Agulhas Current to form a cyclonic border eddy in the lee of the Agulhas Bight. On 29 June another meander (B), possibly a Natal Pulse, can be seen southeast of Agloa Bay. Meander B moved onto the Bank and formed a second, larger cyclonic eddy that persisted throughout July 2007. The relationship between the circulation on the eastern Agulhas Bank and the Tsitsikamma current is further discussed in section 4.2.3

4.2 Driving forces of the Tsitsikamma current

4.2.1 Wind

Wind is not the primary driving force of the Tsitsikamma current (Attwood *et al.* 2002, Roberts and van den Berg 2005), but the Tsitsikamma current is affected by wind-driven processes (Tilney *et al.* 1996). Westerly winds generate CTWs throughout the year, but more frequently in winter (Schumann and Brink 1990), while easterly winds cause coastal upwelling, mainly in summer (Schumann *et al.* 1982). CTWs are sea level disturbances that propagate anticlockwise around the South African coast (Jury *et al.* 1990), causing

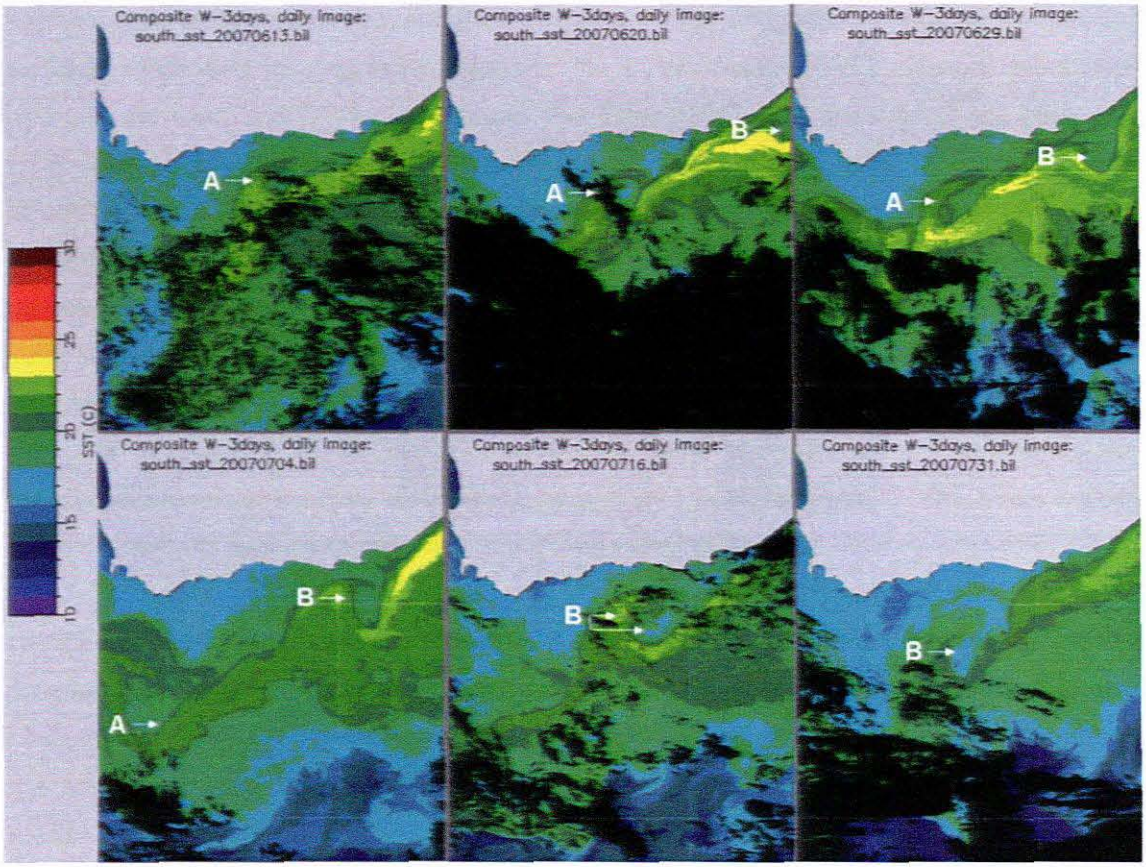

Figure 4.1: SST images show the downstream progression of two meanders (A and B) on the landward border of the southern Agulhas Current during June – July 2007.

nearshore barotropic current reversals (Tilney *et al.* 1996). A condition of resonance between westerly winds and the free-wave speed of the CTWs results in a consistent association between the wind and CTWs (Schumann and Brink 1990). The passage of the peak of a CTW (associated with westerly winds) turns the current eastwards, while the passage of the trough of the CTW (associated with easterly winds) turns the current westwards (Schumann and Brink 1990). Because of this association a certain degree of coherence can be expected between changes in wind direction and current direction along the Tsitsikamma coast. On several occasions in this study, an alongshore change in current direction was timed perfectly with an alongshore change in wind direction (Figure 3.12, Figure 3.14, Figure 3.16, Figure 3.19). Attwood *et al.* (2002) observed the same phenomenon and suggested that these synchronised reversals were likely caused by the passage of CTWs, since surface currents can not respond immediately to a change in wind direction.

On the south coast, upwelling is generally of short duration, as fluctuating alongshore winds produce cold water events over a typical period of a day; few events last more than four days (Schumann 1999). The upwelling process generates an alongshore current in the direction of the wind, i.e. south-westwards, that interrupts eastward flow in the Tsitsikamma current, thereby limiting displacement near the surface (Roberts and van den Berg 2005). Upwelling also alters the baroclinic structure of the water column (Tilney *et al.* 1996) and can cause surface and bottom currents to flow in opposite directions (Roberts and van den Berg 2005) as is demonstrated during the upwelling event recorded from 23 - 31 March 2008 (Figure 3.21).

At Middelbank, the westward upwelling current was relatively weak (< 50 $cm.s^{-1}$) and the current did not have a strong cross-shelf component. In contrast, the measurements made at Thyspunt showed stronger westward currents (> 50 $cm.s^{-1}$) during upwelling, with definite onshore compensation currents near the bottom. The same result can be expected in the upwelling zone west of Cape Seal i.e. strong westward currents during upwelling, with offshore flow near the surface and onshore flow near the seabed.

4.2.2 Coastal trapped waves, stratification and strong current events

Schumann and Brink (1990) showed the presence of large amplitude (~ 90 cm) sea level disturbances along the south coast, with current reversals during the peak of the wave. The exact mechanism of CTW forcing on the south coast remains uncertain, but the authors suggested that conditions of resonance or near-resonance, between coastal low pressure systems and their associated westerly winds and eastward moving CTWs, can increase the amplitude and the intensity of these waves. They found the propagating speed of CTW between Port Elizabeth and Cape Town to range between 5 – 9 $m.s^{-1}$. The large degree of

scatter in the propagating speed is indicative of the complex response of coastal waters to CTWs (Schumann and Brink 1990). Other factors that influence the propagation speeds of CTWs include thermal stratification, wave mode and bottom friction (Chapman 1987, Schumann and Brink 1990).

Measurements of sea level were not included in this study and the occurrence of CTWs at specific times could not be inferred. However, rotary analysis of the current at Middelbank (Figure 3.5) show significant peaks at 3.3 days and 4 days, which agree with the typical first mode (CTW) period of 4 days on the south coast (Tilney *et al.* 1996). The peaks at 8 days and 18 days are possibly related to longer period variations in the circulation on the eastern Agulhas Bank. Moreover, autospectra of the sea level at Knysna and Port Elizabeth related to the propagation of CTWs (Schumann and Brink 1990) show comparable peaks at 3.5 days, 5 days and 10 days.

The nearshore circulation on the south coast is influenced by CTWs (Schumann and Brink 1990, Tliney *et al.* 1996), which are associated with atmospheric low pressure systems that propagate anticlockwise around the South African coastline (Jury *et al.* 1990). The systems occur year round, but their frequency and intensity increase during winter months. In contrast, the ADCP data show that the occurrence of strong current episodes (> 75 $cm.s^{-1}$) increased during summer months. Strong current events are identified by the abnormally large velocity peaks that occur mostly during eastward flow (Appendix B1). Seven of the ten strong current events identified during the study period occurred in summer. All strong current events were found to be associated with a thermally stratified water column and, specifically, with the relaxation of the upwelling process and westerly winds.

Holland and Webster (1994) demonstrated that vertical stratification increases the phase speed of CTWs. There is also evidence that CTWs may be important in regulating the upwelling and downwelling processes in coastal oceans (Middelton and Leth 2004). Schumann (1999) suggested a consistent association between CTW and the wind, due to the condition of resonance. He showed that the peaks of CTWs tend to occur during westerly winds, and the troughs during easterly winds. Elevated sea levels at the coast during the peak of a CTW should therefore cause a strengthening of the downwelling process. Similarly, the passage of the trough of the CTW, which corresponds to easterly winds, should increase the effect of wind-driven upwelling, because a lower sea level already exists at the coast. Schumann *et al.* (1995) found that upwelling at the Tsitsikamma coast commenced and proceeded rapidly, even during relatively low easterly wind speeds. This rapid response is mainly a result of the steep bathymetry that allows cold bottom water to be present close to

the coast (Schumann 1999), but also suggests that CTWs may be important in controlling and enhancing the effects of upwelling and downwelling along the Tsitsikamma coast.

The data collected at Middelbank supports the theory that CTWs can regulate and amplify the effects of coastal upwelling and downwelling off the Tsitsikamma coast, and helps to explain the unusual cold water event recorded in July 2007. In the absence of data on sea level pressure, and following Schumann and Brink (1990), strong westerly wind conditions were used as a proxy for the passage of a CTW. The following description refers to the upwelling event recorded at Middelbank in July 2007 (Figure 3.16). Strong westerly winds were recorded at Tsitsikamma on 12 July (Figure 3.16a). A change to light easterly winds coincided with the onset of a strong westward current that persisted until 20 July (Figure 3.16 c and d). During this period of light easterly winds and strong westward flow, the thermocline was lifted (Figure 3.16b), and 11 °C water was recorded near the seafloor at Middelbank. The absence of strong easterly component winds suggests that the upwelling event was driven by another force, possibly the occurrence of a CTW, and more specifically the trough of the CTW. The upwelling event ended with the onset of strong westerly winds on 26 July. The downwelling process coincided with strong westerly winds (Figure 3.16a), possibly related to the peak of a CTW, and a strong eastward current (Figure 3.16 c and d).

The above example shows an association between the peak of a CTW, jet-like eastward pulses in the current, and intense downwelling; and the association between the trough of a CTW, westward flow, and the enhancement of upwelling. The relationship between CTWs, upwelling and the coastal currents deserve to be studied in more detail, given the importance of upwelling on productivity in the region.

4.2.3 Influence of shelf circulation on the Tsitsikamma current

The circulation on the eastern Agulhas Bank appears to be primarily controlled by the Agulhas Current that follows the nearby shelf break and, to a lesser extent, by local wind forcing (Schumann and Perrins 1983). Statistics indicate that the net flow on the eastern Agulhas Bank, between depths of 100 – 200 m, is in a south-westwards direction, parallel to the bathymetry and the southern Agulhas Current (Swart and Largier 1987, Boyd and Oberholster 1994).

Roberts (in prep) observed a cyclonic lee eddy and a localized sea level depression near the mouth of the Tsitsikamma River, and suggested that strong westward flow on the shelf, at Cape St. Francis, was responsible for removing water from the nearshore region, setting up the cyclonic lee eddy in the process. A similar situation occurs in the Natal Bight on the east coast where the Agulhas Current is responsible for creating the Durban cyclonic eddy

(Lutjeharms 2006). It is thought that this mechanism drives eastward flow in the Tsitsikamma current (Roberts pers comms). The cyclonic eddy was not observed during this study, but the trajectories of drifters near the mouth of the Tsitsikamma River (Figure 3.11, Figure 3.15, Figure 3.18 and Figure 3.20) may have been influenced by such a feature.

Variability in the circulation on the Agulhas Bank exists in the form of frontal instabilities on the shoreward border of the southern Agulhas Current (Lutjeharms 2000). These intrusions of Agulhas Current water onto the Bank have a marked influence on the shelf currents (Schumann and van Heerden 1988), and their presence is associated with eastward flow on the shelf (Lutjeharms *et al.* 1989). Given this, the large meanders present on the Agulhas Bank during the winter of 2007 (Figure 4.1) would have altered the flow of the shelf water to eastwards.

If westward flow on the shelf drives eastward flow along the Tsitsikamma coast (Roberts in prep), then how will eastward flow on the shelf influence the direction of the Tsitsikamma current? It is interesting that the anomalous westward flow, inshore along the Tsitsikamma coast, corresponded to the presence of two large cyclonic eddies on the eastern Agulhas Bank (Figure 4.1). The relationship between the Tsitsikamma current and the shelf circulation remains speculative, as it requires concurrent ADCP measurements across the width of the eastern Agulhas Bank.

4.3 Larval transport and connectivity to the cold ridge

Lagrangian drifters are designed to track two-dimensional flow in the oceans and are good indicators of the passive dispersion of particles (Lumpkin and Pazoz 2006). Surface drifters do not account for vertical migrations typical of many planktonic organisms, including chokka squid paralarvae. Martins *et al.* (in press) showed that the dispersal of squid paralarvae is affected by their biologically-mediated, vertical position in the water column. Such behaviour complicates the advection of paralarvae, especially when opposing surface and bottom currents exist. In this study, vertical migration could not be considered as the potential transport of paralarvae was estimated from a combination of surface drifter and ADCP measurements made along the Tsitsikamma coast.

The Western Transport Hypothesis (Roberts 2005) relies on a net westward shelf flow (Boyd and Oberholster 1994) to transport squid paralarvae from the coastal spawning grounds to the nursery area at cold ridge. The discovery of a predominantly eastward flowing Tsitsikamma current led to the modified Western Transport Hypothesis (Roberts and van den Berg 2005), which states that offshore flow during coastal upwelling moves particles onto the midshelf and simultaneously westward, from where they can either be transported to the cold ridge or returned to the coast, downstream of the eastward flowing Tsitsikamma current.

Roberts and van den Berg (2005) estimated monthly transport in the Tsitsikamma current at between 200 and 450 km east of Middelbank. They postulated that the eastward flowing Tsitsikamma current transports squid paralarvae towards Algoa Bay, and as far east as Port Alfred, from where paralarvae are likely entrained into the Agulhas Current (Goschen and Schumann 1988), and lost from the Agulhas Bank ecosystem. Roberts and van den Berg (2002) suggested that currents might pose a similar threat to the survival of squid paralarvae, and that shelf edge leakage could result in substantial losses of squid paralarvae from the Agulhas Bank to the oligotrophic open oceans.

Roberts and Mullon (2010), used a first version of Lagrangian IBM (Individually-Based Model) coupled to a ROMS (Regional Ocean Model System) model to show that the currents on the eastern Agulhas Bank were strongly influenced by the semi-permanent cyclonic gyre in the Agulhas Bight. Their simulations showed large losses of neutrally buoyant particles (i.e. squid paralarvae) from the eastern and western Agulhas Bank, while few particles were lost from the central Agulhas Bank. Data from the surface drifters support the findings of Roberts and Mullon (2010), as several drifters were retained on the central Agulhas Bank, even after they left the study area. Other trajectories highlight the possibility of shelf edge leakage, specifically at the southern and western extremities of the Agulhas Bank (pers obs).

A conceptual interpretation of potential surface transport off the Tsitsikamma coast derived from the combination current measurements and SST data collected in this study is presented in Figure 4.2. The daily displacement by drifters, 50 km east and 30 km west of Middelbank, demonstrate that particles near the surface are rapidly transported beyond the borders of the TNP. This confirms earlier findings by Tilney *et al.* (1996), Attwood *et al.* (2002), and Roberts and den Berg (2005) that the Tsitsikamma current has the potential to transport eggs and larvae to unprotected areas surrounding the TNP.

The drifter trajectories show that the progressive displacement estimates presented by Roberts and van den Berg (2005) were unrealistic, and that eastward flow in the Tsitsikamma current does not continue into Algoa Bay. Instead, drifters were either caught up in short reversals between Tsitsikamma Point and Cape St. Francis, or moved offshore into the westward shelf current. From the midshelf, drifters generally followed the 100 m isobath towards the cold ridge. This result strongly supports the Western Transport Hypothesis in its modified state (Roberts and van den Berg 2005), although the presence of the cold ridge could not be confirmed from satellite images during any of the drifter release periods.

During westward flow off the Tsitsikamma coast, when no counter current was present, the drifters highlighted a direct route for paralarvae from the spawning grounds to the cold ridge. In deployment 3 (Figure 3.15) several drifters followed the coast from Middelbank to Cape Seal and southwestwards along the 100 m isobath. This result supports the WTH in its simple state (Roberts 2005), even though the westward current was not associated with upwelling or the presence of the cold ridge on the central Agulhas Bank.

During upwelling drifters moved offshore at the capes and west with the midshelf currents. The return of drifters from the midshelf to the Tsitsikamma coast resulted in recirculation into the eastward flowing Tsitsikamma current, east of Middelbank, which supports the current closures proposed by Tilney *et al.* (1996) and Roberts and van den Berg (2005). However, the current closures recorded by drifter 38 and 227 in deployment 3 (Figure 3.15) were not associated with upwelling and was likely caused by the passage of a CTW or more remote influences on the Agulhas Bank. The large scale, upwelling-driven current closures (Tilney *et al.* 1996) could also not be confirmed as no drifters were deployed during the substantial upwelling events that took place in April 2007 and March 2008 (Appendix C2). The trajectories show that in winter, offshore displacement was limited and drifters were retained inshore for up to one month after deployment. In contrast, in summer, the combination of upwelling and CTWs favoured dispersion onto the Agulhas Bank.

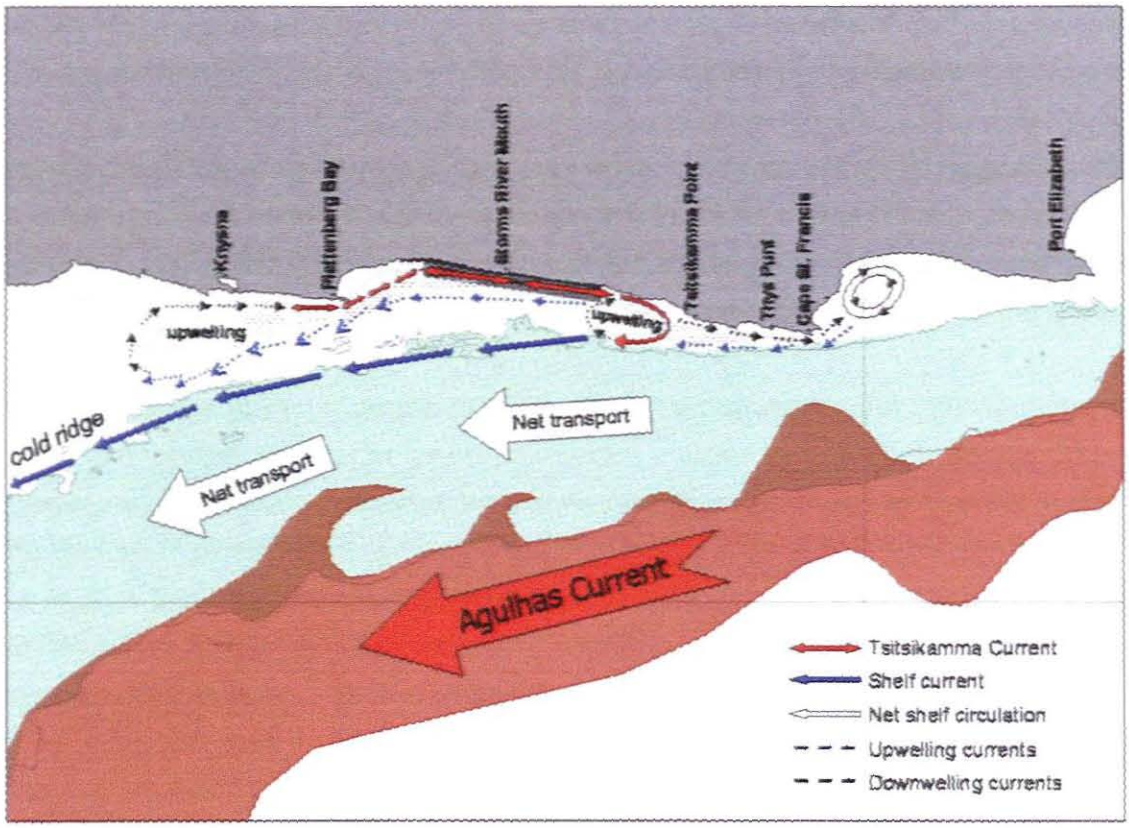

Figure 4.2: Conceptual drawing of currents along the Tsitsikamma coast. Solid red arrows indicate east-west flow in the Tsitsikamma current, dashed blue and black arrows are upwelling and downwelling currents respectively. Solid blue arrows show the current along the 100 m depth contour that leads to the cold ridge, and white arrows indicate net westward flow on the midshelf.

Results from the surface drifters therefore confirm that both eastward and westward currents have the ability to transport neutrally buoyant surface particles from the Tsitsikamma coast to the area of the cold ridge on the central Agulhas Bank. Drifters moved onto the midshelf, at the lee sides of Cape Seal and Seal Point, from where they reached the cold ridge in as little as eight days. Paralarvae of *Loligo reynaudii* can survive for 6 – 8 days without food at 16 °C (Vidal *et al.* 2005), and longer at lower temperatures and, in theory, this puts the cold ridge within reach for the successful recruitment of paralarvae spawned off the Tsitsikamma coast.

However, Martins *et al.* (in press), used an improved Lagrangian IBM (Individual-Based Model) that included the specific gravity of particles, coupled to a ROMS (Regional Ocean Modelling System) model, designed for the Agulhas Bank, and showed that the specific gravity of squid paralarvae may be important in enhancing their survival and recruitment on the Agulhas Bank. Laboratory experiments (Martins *et al.* in press) show that chokka squid paralarvae are always negatively buoyant, regardless of yolk content. The model results (Martins *et al.* in press) compare well with the Lagrangian trajectories recorded by the drifters in this study, and show that both neutrally and negatively buoyant particles released on the spawning grounds are dispersed west, across the Agulhas Bank to the cold ridge. However, the negative buoyancy of squid paralarvae was found (Martins *et al.* in press) to limit transport distance. This not only decreased losses of paralarvae from the Agulhas Bank, but also increased the time it took paralarvae to reach the cold ridge before starvation set in. The drifter data essentially complements the IBM-ROMS as it reveals details about the coastal circulation that is not yet possible in the model.

CHAPTER 5
CONCLUSIONS AND RECOMMENDATIONS

This work gives confirmation of a longshore and predominantly eastward current off the Tsitsikamma coast. The Tsitsikamma current is an intermittent current that starts west of Cape Seal and follows the coastline towards Tsitsikamma Point, where the main trajectory turns offshore and joins the circulation on the midshelf of the eastern Agulhas Bank. Some flow continues east past Thyspunt and towards St. Francis Bay.

The flow regime showed seasonal trends, but a longer time-series is needed to confirm seasonality in the Tsitsikamma current. During the summer upwelling season, the occurrence of jet-like, eastward currents increased and differences between surface and bottom currents were occasionally observed. In contrast, the current was weaker in winter months and flowed mostly westward throughout the water column. Barotropic alongshore reversals occurred frequently throughout the year and in the absence of upwelling, offshore flow was limited.

The Tsitsikamma current is influenced by wind-driven upwelling, CTWs and by the greater shelf circulation, which is in turn affected by the Agulhas Current. Surface currents were west and offshore during upwelling, while onshore compensation currents developed near the seafloor. The westward upwelling current was generally weak (< 40 $cm.s^{-1}$) and short-lived (1 – 2 days), reflecting the nature of upwelling on the south coast (Schumann 1999). The occurrence of CTWs seems to have a significant effect on the dynamics of the Tsitsikamma current, causing nearshore barotropic oscillations with alongshore dimensions of up to 100 km. The results suggest that a combination of CTWs and thermal stratification drives jet-like, eastward currents during the summer upwelling season, and that CTWs may be important in regulating upwelling and downwelling off the Tsitsikamma coast.

The dynamics of the Tsitsikamma current has important implications for the dispersal of squid paralarvae hatched in the TNP and in embayments along the Tsitsikamma coast. The combination of upwelling and strong eastward currents, during the main summer spawning season significantly increases transport potential. Paralarvae near the surface are likely dispersed onto the midshelf, from where the cold ridge can be reached within seven days. The position of paralarvae in the water column will ultimately determine their travel time from the Tsitsikamma coast to the cold ridge, with increased periods at greater depths. However, enhanced productivity during the post-upwelling period (Probyn *et al.* 1994) should increase paralarval survival rates, and starvation *en route* should not limit recruitment when upwelling occurs, in spring and summer. In winter, regular alongshore oscillations, without the offshore flow associated with upwelling, limits the dispersal of paralarvae onto the midshelf, which

suggests that paralarvae are retained inshore until they improve their swimming and their prey catching abilities.

This work demonstrates how variability in the Tsitsikamma current can influence the passive dispersal, and consequently, the recruitment of squid paralarvae. It is therefore important to gain a better understanding of the mechanisms that drive variability in the current; be it seasonal, long-term or anomalous. Future research should focus on the effect of CTWs on the Tsitsikamma current, and the role of CTWs in regulating upwelling and downwelling off the Tsitsikamma coast. In addition, the relationship between the shelf circulation and the inshore counter current needs to be established. This can be done by deploying a line of fixed ADCP moorings across width of the eastern Agulhas Bank, while ship-borne ADCP transects can determine the width of the counter current. The exact influence of wind on the Tsitsikamma current also needs to be established. Moreover, it is imperative to continue the long-term monitoring of currents and sea temperatures off the Tsitsikamma coast, as it offers a rare opportunity to examine the effects of climate change on this unique and productive coastal environment.

REFERENCES

Arkhiphin, A. I. (2000). Intrapopulation structure of winter-spawned Argentine short-finned squid *Illex argentinus* (Cephalopoda, Omastrephidae), during its feeding period over the Patagonian Shelf. *Fisheries Bulletin*, vol. 98, pp. 1-13.

Armstrong, D. A., Verheye, H. M., and Kemp, A. D. (1991). Short-term variability during an Anchor Station study in the southern Benguela upwelling system. *Progress in Oceanography*, vol. 28, pp. 167-188.

Attwood, C. G., Allen, J., and Claassen, P. J. (2002). Nearshore surface current patterns in the Tsitsikamma National Park, South Africa. *South African Journal of Marine Science*, vol. 24, pp. 151-160.

Augustyn, C. J. (1986).The squid jigging fishery on the South African south coast. *South African Shipping News Fishing Industry Review*, vol. 41, no. 5, pp. 24-26.

Augustyn, C. J. (1989). *Systematics, life cycle and resource potential of the chokker squid, Loligo vulgaris reynaudii.* Ph.D. Thesis, University of Port Elizabeth.

Augustyn, C. J. (1990). Biological studies on the chokka squid *Loligo vulgaris reynaudii* (Cephalopoda; Myopsida) on spawning grounds off the south-east coast of South Africa. *South African Journal of Marine Science*, vol. 9, pp. 11-26.

Augustyn, C. J., Lipinski, M. R., and Sauer, W. H. H. (1992). Can the *Loligo* squid fishery be managed effectively? A synthesis of research on *Loligo vulgaris reynaudii*. *South African Journal of Marine Science*, vol. 12, pp. 903-918.

Augustyn, C. J., Lipinski, M. R., Sauer, W. H. H., Roberts, M. J., and Mitchell-Inns, B. A. (1994). Chokka squid on the Agulhas Bank: life history and ecology. *South African Journal of Science*, vol. 90, no. 3, pp. 143-154.

Augustyn, C. J. and Roel, B. A. (1998). Fisheries biology, stock assessment, and management of the chokka squid (*Loligo vulgaris reynaudii*) in South African water: an overview. *California Cooperative Oceanic Fisheries Investigations Reports.*, vol. 39, pp. 71-80.

Bang, N. D. and Andrews, W. R. H. (1974). Direct current measurements of a shelf-edge frontal jet in the southern Benguela system. *Journal of Marine Research*, vol. 32, no. 3, pp. 405-417.

Barange, M., Pakhomov, E. A., Perissinotto, R., Froneman, P. W., Verheye, H. M., Taunton-Clarke, J., and Lucas, M. I. (1998). Pelagic community structure of the subtropical convergence region south of Africa and in the mid-Atlantic Ocean. *Deep Sea Research*, vol. 45, no. 10, pp. 1663-1687.

Beckley, L. E. (1988). Spatial and temporal variability in sea temperature in Algoa Bay, South Africa. *South Africa Journal of Science*, vol. 84, pp. 67-69.

Boyd, A. J. and Nelson, G. (1998). The variability of the Benguela Current off the Cape peninsula. *South African Journal of Marine Science*, vol. 19, pp. 27-39.

Boyd, A. J. and Oberholster, G. P. J. (1994). Currents off the west and south coasts of South Africa. *SA Shipping News and Fishing Industry Review*, Sept/Oct 1994, pp. 26-28.

Boyd, A. J., Taunton-Clark, J., and Oberholster, G. P. J. (1992). Spatial features of the near-surface and midwater circulation patterns off western and southern South Africa and their

role in the life histories of various commercially fished species. *South African Journal of Marine Science*, vol. 12, pp. 189-206.

Boyd, A. J. and Shillington, F. A. (1994). Physical forcing and circulation patterns on the Agulhas Bank. *South African Journal of Science*, vol. 90, pp. 114-122.

Brouwer, S. L., Griffiths, M. H., and Roberts, M. J. (2003). Adult movement and larval dispersion of *Argyrozona argyrozona* (Pisces: Sparidae) from a temperate marine protected area. *African Journal of Marine Science*, vol. 25, pp. 395-402.

Buxton, C. D. and Smale, M. J. (1984). A preliminary investigation of the marine ichthyofauna in the Tsitsikamma Coastal National Park. *Koedoe*, vol. 27, pp. 13-24.

Carter, R. A., McMurray, H. F., and Largier, J. L. (1987). Thermocline characteristics and phytoplankton dynamics in Agulhas Bank waters. *South African Journal of Marine Science*, vol. 5, pp. 327-336.

Chapman, D. C. (1987). Application of wind-forced, long, coastal trapped wave theory along the California Coast. *Journal of Geophysical Research*, vol. 92, pp. 1798-1816.

Cowley, P. D., Brouwer, S. L., and Tilney, R. L. (2002). The role of the Tsitsikamma national park in the management of four shore-angling fish along the South-Eastern Cape coast of South Africa. *South African Journal of Marine Science*, vol. 24, pp. 27-35.

de Ruitjer, W. P. M., van Leeuwen, P. J., and Lutjeharms, J. R. E. (1999). Generation and evolution of Natal Pulses: Solitary meanders in the Agulhas Current. *Journal of Physical Oceanography*, vol. 29, pp. 3043-3055.

Fisher, N. I. (1993). *Statistical analysis of circular data.* Cambridge University Press, Cambridge.

Flemming, B., Martin, K. and Akkers, W. (1986). *Agulhas Bank studies. Marine geology off the Tsitsikamma Coast.* Poster paper, Agulhas Bank Symposium, Cape Town.

Geyer, W.R. (1989). Field calibration of mixed layer drifters. *Journal of Atmospheric and Oceanic Technology*, vol. 6, pp. 333-342.

Gorden, A. L. (1985). Indian-Atlantic transfer of thermocline water at the Agulhas retroflection. *Science*, vol. 227, no. 4690, pp. 1030-1033.

Goschen, W. S. and Schumann, E. H. (1994). An Agulhas Current intrusion into Algoa Bay during August 1988. *South African Journal of Marine Science*, vol. 14, pp. 47-57.

Goschen, W. S. and Schumann, E. H. (1990). Agulhas current variability and inshore structures off the Cape province, South Africa. *Journal of Geophysical Research*, vol. 95, no. C1, pp. 667-678.

Goschen, W. S. and Schumann, E. H. (1994). An Agulhas Current intrusion into Algoa Bay during August 1988. *South African Journal of Marine Science*, vol. 14, pp. 47-57.

Griffiths, M. H. and Wilke, C. G. (2002). Long-term movement patterns of five temperate reef fishes (Pisces: Sparidae): implications for marine reserves. *Marine and Freshwater Resources*, vol. 53, pp. 233-244.

Gründlingh, M. L. (1979). Observation of a Large Meander in the Agulhas Current. *Journal of Geophysical Research*, vol. 84, no. C7, pp. 3776-3778.

Gründlingh, M. L. (1983). On the course of the Agulhas Current. *South African Geographical Journal*, vol. 65, no. 1, pp. 49-57.

Gründlingh, M. L. (1986). Features of the northern Agulhas Current in spring 1983. *South African Journal of Science*, vol. 82, no. 1, pp. 18-20.

Harris, T. F. W., Legeckis, R., and van Forest, D. (1978). Satellite infra-red images in the Agulhas Current System. *Deep-Sea Research*, vol. 25, pp. 543-548.

Hatanaka, H., Lange, A. M. T., and Amaratunga, T. (1985). Geographical and vertical distribution of larval short-finned squid (*Illex illecebrosus*) in the Northwest Atlantic. *Northwest Atlantic Fisheries Organization Scientific Council Studies*, vol. 9, no. 93, p. 99.

Holland, D. M. and Webster, I. T. (1994). The effects of stratification and alongshore currents on the propagation of coastal-trapped waves. *Continental Shelf Research*, vol. 14, no. 1, pp. 57-78.

Hsueh, Y. and O'Brien, J. J. (1971). Steady coastal upwelling induced by an along shore current. *Journal of Physical Oceanography*, vol. 1, no. 3, pp. 180-186.

Hutchings, L. (1994). The Agulhas Bank: a synthesis of available information and a brief comparison with other east-coast shelf regions. *South Africa Journal of Science*, vol. 90, no. 3, pp. 179-185.

Hutchings, L., Beckley, L. E., Griffiths, M. H., Roberts, M. J., Sundby, S., and van der Lingen, C. (2002). Spawning on the edge: spawning grounds and nursery areas around the southern African coastline. *Marine Freshwater Resources*, vol. 53, pp. 307-318.

Jury, M. R., MacArthur, C. I., and Reason, C. J. C. (1990). Observations of coastal trapped waves in the atmosphere and ocean along the coast of Southern Africa. *South African Geographical Journal*, vol. 72, pp. 33-46.

Jury, M. R. and Levey, K. (2006). The climatology and characteristics of drought in the eastern Cape of South Africa. *International Journal of Climatology*, vol. 13, no. 6, pp. 629-641.

Jury, M. R. (1994). A review of the meteorology of the eastern Agulhas Bank. *South Africa Journal of Science*, vol. 90, no. 3, pp. 109-113.

Largier, J. L. and Swart, V. P. (1987). East-west variation in thermocline breakdown on the Agulhas Bank. *South African Journal of Marine Science*, vol. 5: The Benguela and Comparable Ecosystems, pp. 263-272.

Lipinski, M. R. (1987). Food and feeding of *Loligo vulgaris reynaudii* from St Francis bay, South Africa, *South African Journal of Marine Science*, vol. 5, pp. 557-564.

Lipinski, M. R. (1992). Cephalopds and the Benguela ecosystem: Trophic relationships and impact. *South African Journal of Marine Science*, vol. 12, pp. 791-802.

Lumpkin, R. and Pazoz, M. (2006) Measuring surface currents with Surface Velocity Program drifters: the instrument, its data, and some recent results. Griffa, A., Kirwan, A. D., Mariano, A. J., Ozgokmen, T. and Rossby, T. (Eds). Chapter 2 of *Langrangian Analysis and Prediction of Coastal and Ocean Dynamics (LAPCOD)*.

Lutjeharms, J. R. E., Bang, N. D., and Valentine, H. R. (1981). Die fisiese oseanologie van die Agulhasbank. 1. Vaart 170 van die N.S. Thomas B. Davie. South African Council for Scientific and Industrial Research *CSIR Researsch Report*, vol. 386, pp 1-38.

Lutjeharms, J. R. E. (1981). Features of the southern Agulhas Current circulation from satellite remote sensing. *South Africa Journal of Science*, vol. 77, pp. 231-236.

Lutjeharms, J. R. E. and Van Ballegooyen, R. C. (1988). The retroflection of the Agulhas Current. *Journal of Physical Oceanography*, vol. 18, pp. 1570-1583.

Lutjeharms, J. R. E. and Roberts, H. R. (1988). The Natal Pulse: an extreme transient on the Agulhas Current. *Journal of Physical Oceanography*, vol. 93, pp. 631-645.

Lutjeharms, J. R. E., Catzel, R., and Valentine, H. R. (1989). Eddies and other border phenomena of the Agulhas Current, *Continental Shelf Research*, vol. 9, no. 7, pp. 597-616.

Lutjeharms, J. R. E., Cooper, J., and Roberts, M. J. (2000). Upwelling at the inshore edge of the Agulhas Current. *Continental Shelf Research*, vol. 20, pp. 737-761.

Lutjeharms, J. R. E. (2006). *The Agulhas Current*. Springer.

Martins, R. S., Roberts, M. J., Chang, N., Verley, P., Moloney C. L., and Vidal, E. A. G. (in press). Effect of yolk utilization on the specific gravity of chokka squid (*Loligo reynaudii*) paralarvae: implications for dispersal on the Agulhas Bank, South Africa. ICES Journal of Marine Science.

Melo, Y. C. and Sauer, W. H. H. (1999). Confirmation of serial spawning in the chokka squid *Loligo vulgaris reynaudii* off the coast of South Africa. *Marine Biology*, vol. 135, pp. 307-313.

Middelton, J. F. and Leth, O. K. (2004). Wind-forces setup of upwelling, geographical origins and numerical models: The role of bottom friction. *Journal of Geophysical Research*, vol. 109, no. C12, pp. 1-12.

Mooers, C. N. K. (1973). A technique for the cross spectrum analysis of pairs of complex-valued time-series, with emphasis on properties of polarized components and rational invariants. *Deep-Sea Research*, vol. 20, pp. 1129-1141.

Morgan, T. (2010). *South African Nautical Almanac*, 9th edition. On Board Publications. ISBN 978-0-620-43853-7.

Niiler, P. P., Davis, R. E., and White, H. J. (1987). Water-following characteristics of a mixed layer drifter. *Deep Sea Research*, vol.34, no. 10, pp. 1867-1881.

Niiler, P. P., and Paduan, J. D. (1995). Wind-driven motions in the Northeast Pacific as measured by Lagrangian drifters. *Journal of Physical Oceanography* vol. 25, no. 11, pp. 2819-2830.

Niiler, P.P., Andrew, S., Kenkong, B., Poulain, P. M., and Bitterman, D. (1996). Measurements of the water-following capability of Holey-Sock and Tristar drifters. *Deep Sea Research*, Part I, vol. 42, pp. 951–964.

Nerheim, S. (2004). Shear-generating motions at various length scales and frequencies in the Blatic Sea - an attempt to narrow down the problem of horizontal dispersion. *Oceanologia*, vol. 46, no. 4, pp. 477-503.

Oosthuizen, A., Roberts, M. J., and Sauer, W. H. H. (2002a). Early post-cleavage stages and abnormalities identified in the embryonic development of chokka squid eggs *Loligo vulgaris reynaudii*. *South African Journal of Marine Science*, vol. 24, pp. 379-382.

Oosthuizen, A., Roberts, M. J., and Sauer, W. H. H. (2002b). Temperature effects on embryonic development and hatching success of the squid *Loligo Vulgaris Reynaudii*, *Bulletin of Marine Science*, vol. 71, pp. 619-632.

Oosthuizen, A. and Roberts, M. J. (2009). Bottom temperature and *in situ* development of chokka squid eggs (*Loligo vulgaris reynaudii*) on the deep spawning grounds, South Africa. *ICES Journal of Marine Science*, vol. 66, no. 1967, p. 1971.

Pazan, S. E. and Niiler, P. P. (2001). Recovery of near-surface velocity from undrogued drifters. *Journal of Atmospheric and Oceanic Technology*, vol. 18, no. 3, pp. 476-489.

Parrish, R. H., Bakun, A., Husby, D. M., and Nelson, C. S. (1983).Comparative climatology of selected environmental processes in relation to eastern boundary current pelagic fish production. In *Proceedings of the Expert Consultation to Examine Changes in Abundance and Species Composition of Neritic Fish Resources*, San Jose, Costa Rica, April 1983. Sharp, G. D. and Csirke, J., (Eds), *F.A.O Fisheries Reproduction*, vol. 291, no. 3, pp. 731-777.

Preston-Whyte, R. A. and Tyson, P. D. (1988). *The atmosphere and weather of southern Africa.* Oxford University Press.

Probyn, T. A., Mitchell-Innes, B. A., Brown, P. C., Hutchings, L., and Carter, R. A. (1994). A review of primary production and related processes on the Agulhas Bank. *South African Journal of Science, vol. 90, no. 3, pp. 166-173.*

Roberts, M. J. (2005). Chokka squid (*Loligo vulgaris reynaudii*) abundance linked to changes in South Africa's Agulhas Bank ecosystem during spawning and the early life cycle. *ICES Journal of Marine Science, vol. 62, no. 1, pp. 33-55.*

Roberts, M. J. and Sauer, W. H. H. (1994). Environment: the key to understanding the South African chokka squid (*Loligo vulgaris reynaudii*) life cycle and fishery. *Antarctic Science, vol. 6, no. 2, pp. 249-258.*

Roberts, M. J. and Mullon, C. (2010). First ROMS–IBM simulations indicate poor recruitment in the South African squid fishery (*Loligo vulgaris reynaudii*) is caused by off-shelf losses of paralarvae. *African Journal of Marine Science, 32.*

Roberts, M. J., and van den Berg, M. (2002). Recruitment variability of chokka squid - role of currents on the Agulhas Bank (South Africa) in paralarvae distribution and food abundance. Part II. *Bulletin of Marine Science, vol. 71, pp. 691-710.*

Roberts, M. J., and van den Berg, M. (2005). Currents along the Tsitsikamma coast, South Africa, and potential transport of squid paralarvae and ichthyoplankton. *African Journal of Marine Science*, vol. 27, no. 2, pp. 375-388.

Robinson, G. A. and De Graaff, G. (1994). *Marine protected areas of the Republic of South Africa.* Council for the Environment. IUCN.

Sale, P. F., Cowen, R. K., Danilowicz, B. S., Jones, G. P., Kritzer, J. P., Lindeman, K. C., Planes, S., Polunin, V. C., Russ, G. R., Sadovy, Y. J., and Steneck, R. S. (2005). Critical science gaps impede use of no-take fishery reserves. *Trends in Ecology and Evolution*, vol. 20, no. 2, pp. 74-80.

Sanders, B. F. and Chrysikopoulos, C. V. (2004). Longitudinal interpolation of parameters characterizing channel geometry by piece-wise polynomial and universal kriging methods: effects on flow modeling. *Advances in Water Resources*, vol. 27, pp. 1061-1073.

SANParks. (2005). *Tsitsikamma National Park Management Plan.* Version 1. Ref 16/1/5/1/5/6/2 31/10/2006.

Sauer, W. H. H. and Lipinski, M. R. (1990). Histological validation of morphological stages of sexual maturity in chokka squid *Loligo vulgaris reynaudii* D'Orb (Cephalopoda; Loliginidae). *South African Journal of Marine Science*, vol. 9, pp. 189-200.

Sauer, W. H. H. (1991). *Population characteristics of the chokker squid, Loligo vulgaris reynaudii, and its distribution in the Algoa Bay-St Francis Bay area in relation to environmental conditions.* M.Sc. Thesis, University of Port Elizabeth.

Sauer, W. H. H., Smale, M. J., and Lipinski, M. R. (1992). The location of spawning grounds, spawning and schooling behavior of the squid *Loligo vulgaris reynaudii* (Cephalopoda: Myopsida) off the Eastern Cape coast, South Africa. *Marine Biology*, vol. 112.

Sauer, W. H. H. 1995, South Africa's Tsitsikamma National Park as a protected breeding area for the commercially exploited chokka squid *Loligo vulgaris reynaudii. South African Journal of Marine Science*, vol. 16, pp. 365-371.

Schumann, E. H. (1981). Low frequency fluctuations off the Natal coast. *Journal of Geophysical Research*, vol. 86, no. c7, pp. 6499-6508.

Schumann, E. H., Perrins, L. A., and Hunter, I. T. (1982). Upwelling along the south coast of the Cape Province, South Africa. *South Africa Journal of Science*, vol. 78, pp. 238-242.

Schumann, E. H. and Beekman, L. J. (1984). Ocean temperature structures on the Agulhas Bank. *Transactions of the Royal Society of South Africa*, vol. 45, no. 2, pp. 191-203.

Schumann, E. H. (1987). The coastal ocean off the east coast of South Africa. *Transactions of the Royal Society of South Africa*, vol. Part 3, pp. 215-229.

Schumann, E. H., Ross, G. J. B., and Goschen, W. S. (1988). Cold water events in Algoa Bay and along the Cape south coast, South Africa in March/April 1987. *South African Journal of Marine Science*, vol. 84, pp. 579-584.

Schumann, E. H. and van Heerden, I. L. (1988). Observations of Agulhas Current frontal features south of Africa, October 1983. *Deep-Sea Research*, vol. 35, no. 8, pp. 1355-1362.

Schumann, E. H. (1989). The propagation of air pressure and wind systems along the South African coast. *South Africa Journal of Science*, vol. 85, pp. 382-385.

Schumann, E. H. and Brink, K. H. (1990). Coastal-trapped waves off the coast of South Africa: Generation, propagation and current structures. *Journal of Physical Oceanography*, vol. 20, pp. 1206-1218.

Schumann, E. H. and Martin, J. A. (1991). Climatological aspects of the coastal wind field over Algoa Bay, South Africa. *South African Geographical Journal*, vol. 73, pp. 48-51.

Schumann, E. H., Cohen, A. L., and Jury, M. R. (1995). Coastal sea surface temperature variability along the south coast of South Africa and the relationship to regional and global climate. *Journal of Marine Research*, vol. 53, pp. 231-248.

Schumann, E. H. (1999). Wind-driven mixed layer and coastal upwelling processes off the south coast of South Africa. *Journal of Marine Research*, vol. 57, pp. 671-691.

Schumann, E. H. and Perrins, L. A. (1982).Tidal and inertial currents around South Africa. In *Proceedings of the 18th Coastal Engineering Conference*. Cape Town. South Africa, no. 14-19, pp. 2562-2580.

Shannon, L. V. (1970) Oceanic circulation off South Africa. *South African Fisheries Bulletin*, vol. 6, no. 27, p. 33.

Shannon, L. V. (1985). The Benguela Ecosystem. 1. Evolution of the Benguela, physical features and processes. In *Oceanography and Marine Biology. A Annual Review*, vol. 23. Barnes, M. (Ed). Aberdeen University Press. pp. 105-182.

Shannon, L. V. (2001). The Benguela Current. In *Encyclopedia of Ocean Science*, 1st ed. Steele, J., Thorpe, S. and Turekian, K. (Eds). Academic Press London, pp. 255-267.

Shannon, L. V. and Nelson, G. (1996). The Benguela: Large-scale features and process and system variability. *The South Atlantic: Present and Past Circulation,* G. Wefer, W. H. Berger, G. Siedler, and D. J. Webb, (Eds), Springer-Verlag, pp. 162–210.

South Africa. Department of Environmental Affairs and Tourism. (2005). *Policy for the allocation and management of commercial fishing rights in the squid fishery.*

South Africa. Department of Environmental Affairs and Tourism. (2008). *Marine Living Resources Act (18/1998): Amendment of regulations.* Government Gazette 8860(30907), 2.

Swart, V. P. and Largier, J. L. (1987). Thermal Structure of Agulhas Bank water. *South African Journal of Marine Science*, vol. 5, no. The Benguela and Comparable Systems, pp. 243-253.

Sybrandy, A. L. and Niiler, P. P. (1992). *WOCE/TOGA Lagrangian drifter construction manual.* Scripps Institute of Oceanography, La Jolla, California, 63.

Sybrandy, A. L., Niiler, P. P., Martin, S., Scuba, W., Charpentier, E., and Meldrum, D. T. (2005). *Global Drifter Programme: barometer drifter design reference.* Data Buoy Co-operation Panel, Report no. 4.

Taljaard, J. J. (1972). Synoptic meteorology of the southern hemisphere. *Meteorological Monographs*, vol. 13, pp. 139-213.

Tilney, R. L., Nelson, G., Radloff, S. E., and Buxton, C. D. (1996). Ichthyoplankton distribution and dispersal in the Tsitsikamma National Park marine reserve, South Africa. *South African Journal of Marine Science*, vol. 17, pp. 1-14.

Toerien, D. K. (1976). Geologie van die Tsitsikamma kusstrook. *Koedoe*, vol. 19, pp. 31-41.

van der Lingen, C., Hutchings, L., Merkle, D., van den Westhuizen, J. J., and Nelson, J. (2001). Comparative spawning habitats of anchovy (*Engraulis capensis*) and sardine (*Sardinops sagax*) in the southern Benguela upwelling ecosystem. In *Spatial Processes and Management of Marine Populations*. Kruse, G. H., Bez, N., Booth, T., Dorn, M., Hills, S., Lipcius, R. N., Pelletier, D., Roy, C., Smith, S. J. and D. Witherell (Eds). University of Alaska Sea Grant College Programme, AK-SG-01-02, Fairbanks, pp. 185-209.

Venter, J. D., van Wyngaardt, S., Verschoor, J. A., Lipinski, M. R., and Verheye, H. M. (1999). Detection of zooplankton prey in squid paralarvae with immunoassay. *Journal of Immunoassay and Immunochemistry*, vol. 20, pp. 127-149.

Verheye, H. M., Hutchings, L., Hugget, J. A., Carter, R. A., Peterson, W. T., and painting, S. J. (1994). Community structure, distribution and trophic ecology of zooplankton on the Agulhas Bank with special reference to copepods. *South African Journal of Science*, vol. 90, pp 154-165.

Vidal, E. A. G., DiMarco, F. P., Wormuth, J. H., and Lee, P. G. (2002). Influence of temperature and food availability on survival, growth and yolk utilization in hatchling squid. *Bulletin of Marine Science*, vol. 7, no. 2, pp. 915-931.

Vidal, E. A. G., Roberts, M. J., and Martins, R. S. (2005). Yolk utilization, metabolism and growth in reared *Loligo vulgaris reynaudii* paralarvae. *Aquatic Living Resources*, vol. 18, pp. 385-393.

Walker, N. D. (1986). Satellite observations of the Agulhas Current and episodic upwelling south of Africa. *Deep-Sea Research*, vol. 33, no. 8, pp. 1083-1106.

Wells, N. C., Ivchenko, V., and Best, S. E. (2000). Instabilities in the Agulhas retroflection current system - A Comparative model study, *Journal of Geophysical Research*, vol. 105, no. c2, pp. 3233-3241.

Wood, A. D., Brouwer, S. L., Cowley, P. D., and Harrison, T. D. (2000). An updated checklist of the ichthyofaunal species assemblage of the Tsitsikamma National Park, South Africa. *Koedoe*, vol. 43, no. 1, pp. 83-95.

APPENDICES

Appendix A

A1: The wind distribution at three weather stations along the Tsitsikamma coast during the months of spring (September, October, November). Direction is given in the meteorological standard.

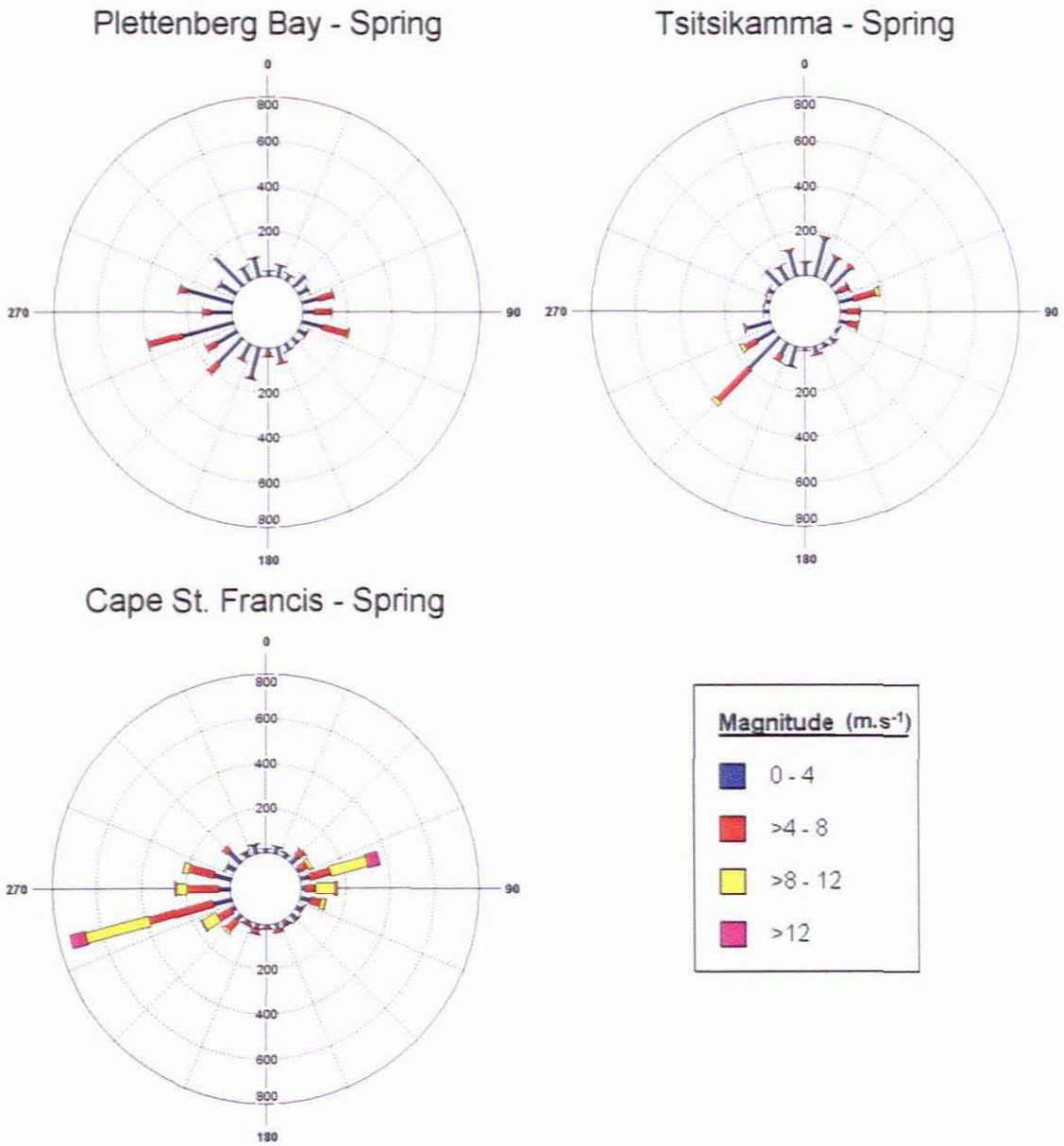

A2: The wind distribution at three weather stations along the Tsitsikamma coast during summer months (December, January, February). Direction is given in the meteorological standard.

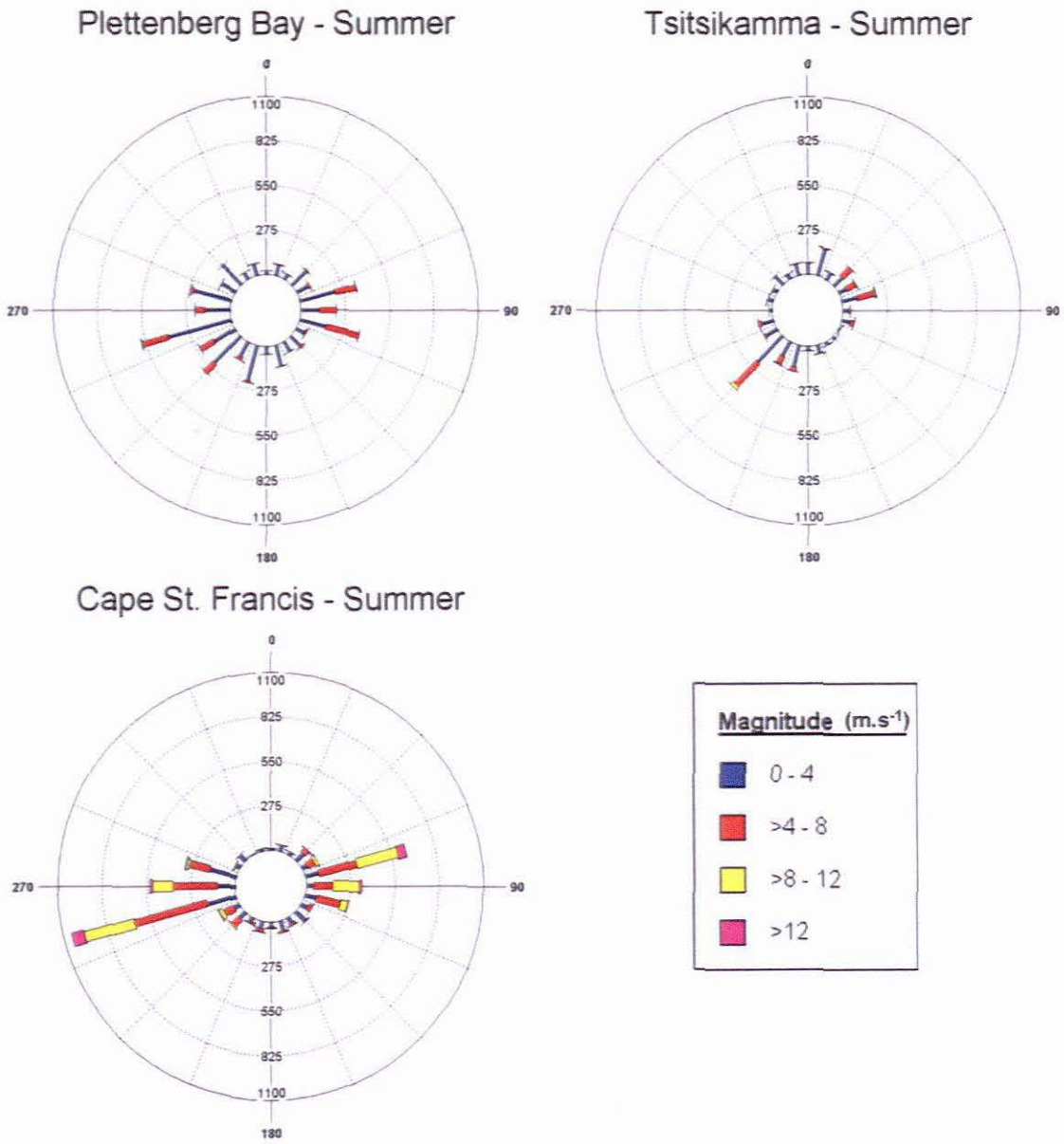

A3: The wind distribution at three weather stations along the Tsitsikamma coast during autumn months (March, April, May). Direction is given in the meteorological standard.

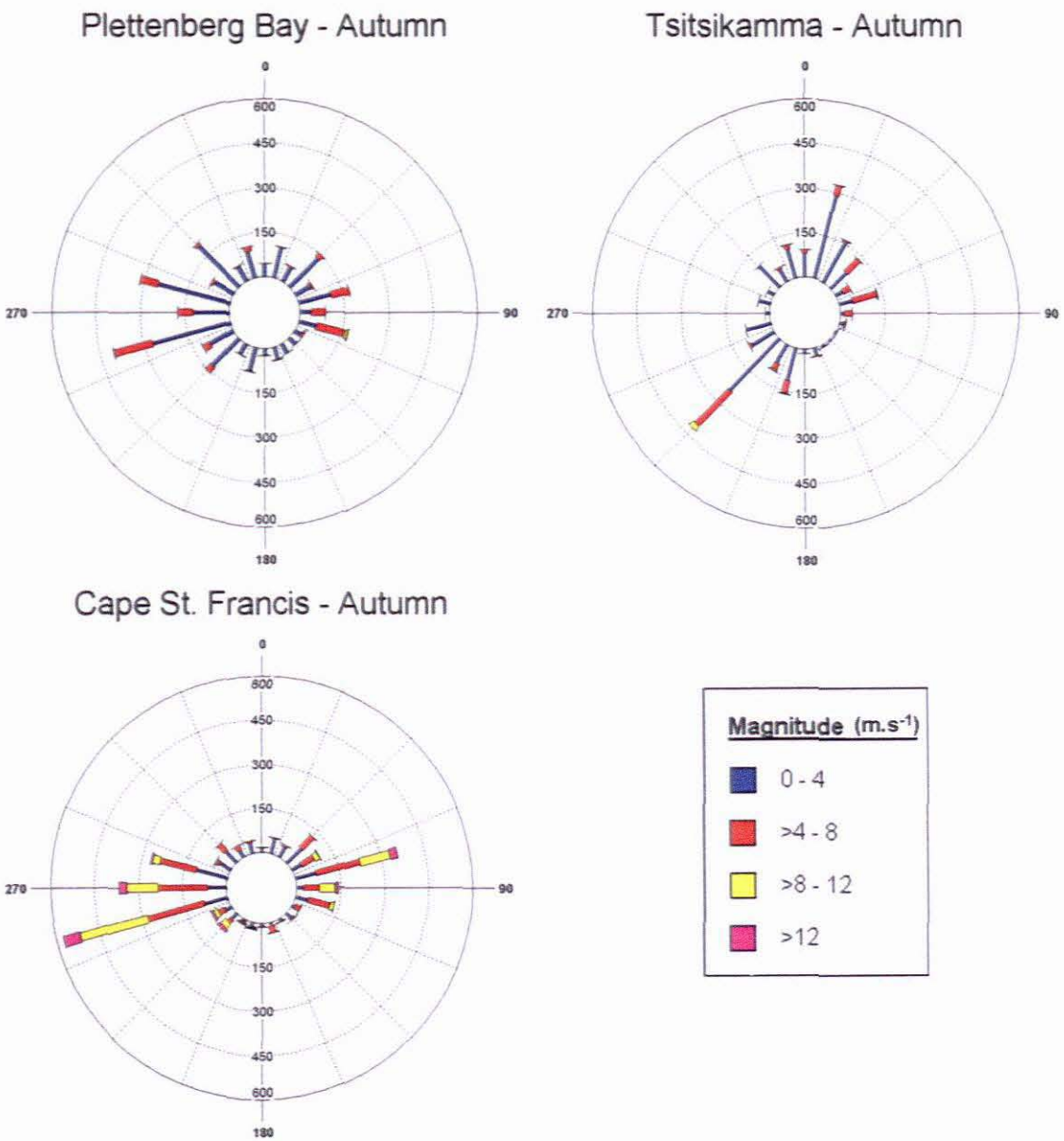

A4: The wind distribution at three weather stations along the Tsitsikamma coast during winter months (June, July, August). Direction is given in the meteorological standard.

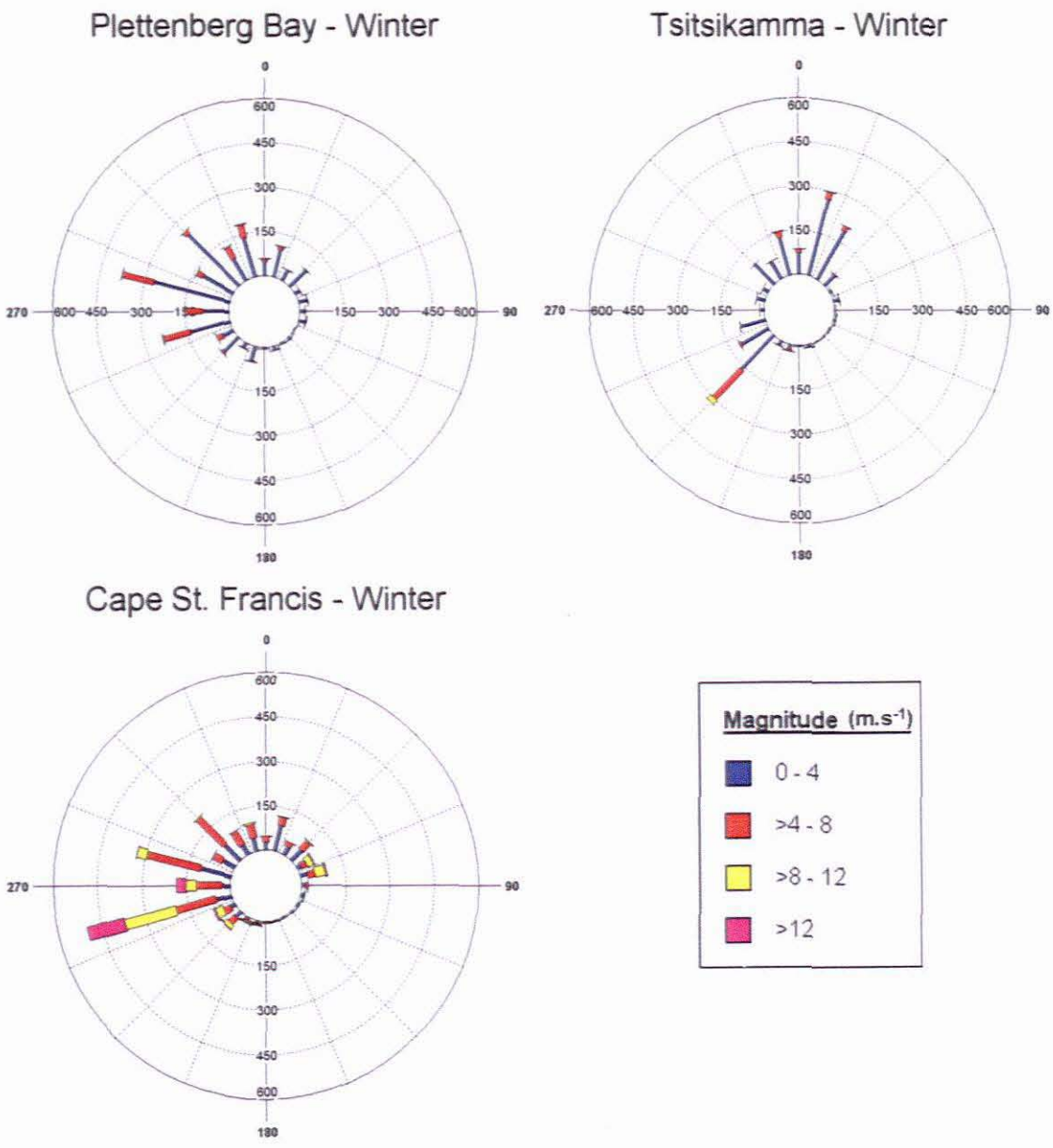

Appendix B

B1: East-west velocity of the ADCP measured surface currents at Middelbank (black), Groot River East (red) and Thyspunt (blue). Positive y-axis values denote eastward flow and negative values denote westward flow. Average velocities are represented by the dotted lines and shaded areas indicate strong eastward pulses in the current.

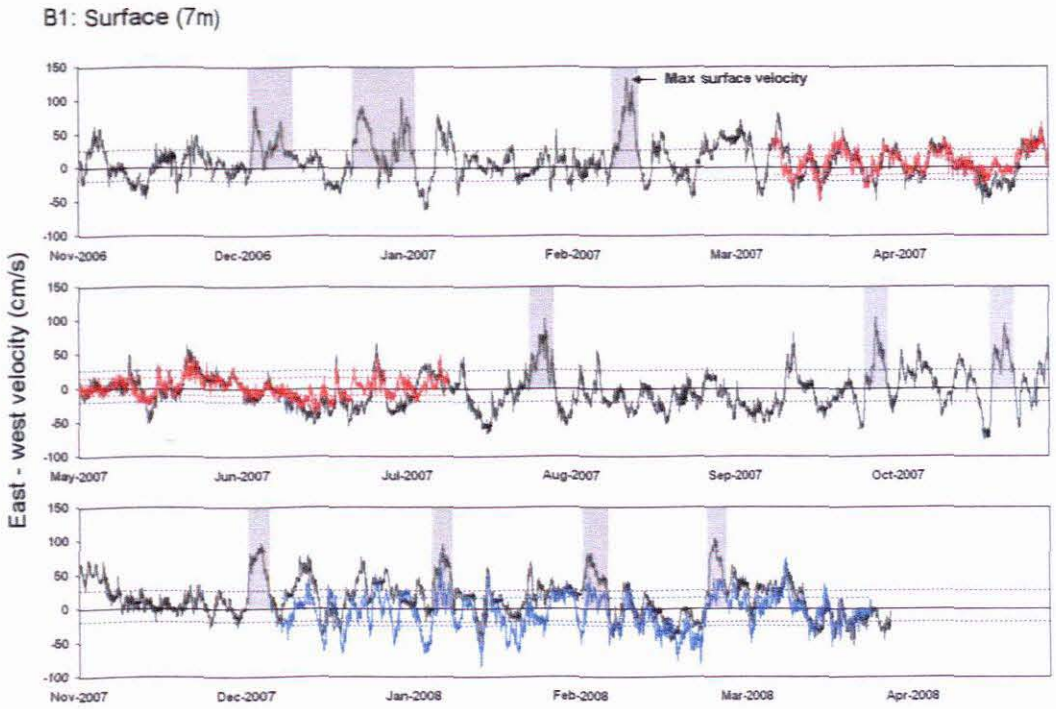

B2: East-west velocity of the ADCP measured bottom currents at Middelbank (black), Groot River East (red) and Thyspunt (blue). Positive y-axis values denote eastward flow and negative values denote westward flow. Average velocities are represented by the dotted lines.

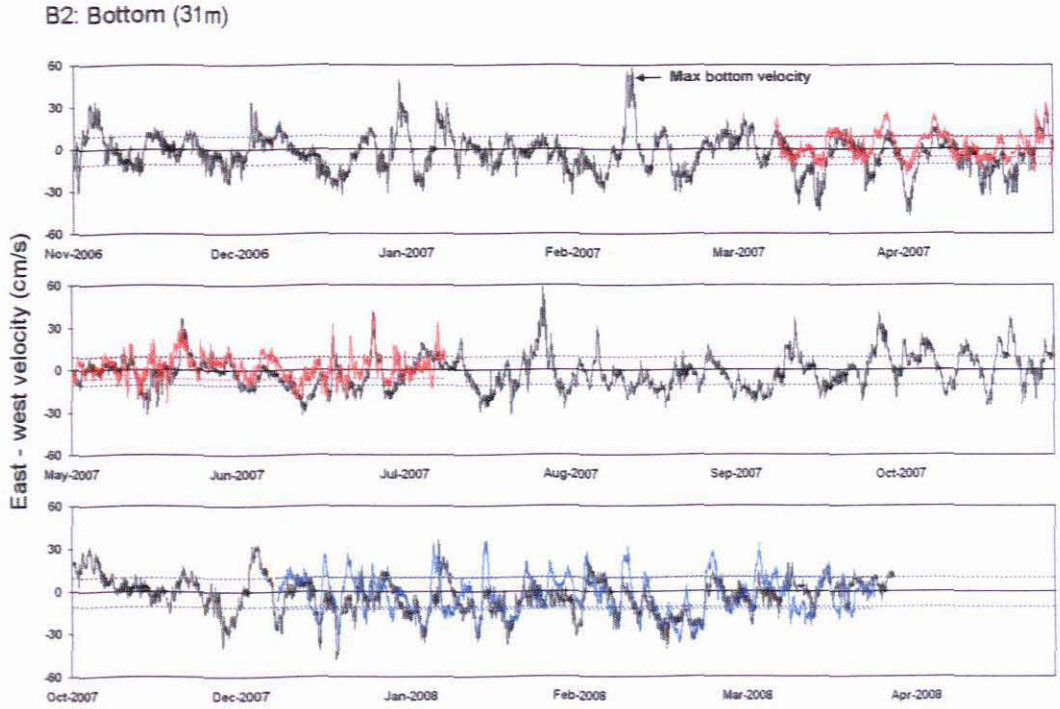

B3: North-south velocity of the ADCP measured surface currents at Middelbank (black), Groot River East (red) and Thyspunt (blue). Positive y-axis values denote eastward flow and negative values denote westward flow. Average velocities are represented by the dotted lines.

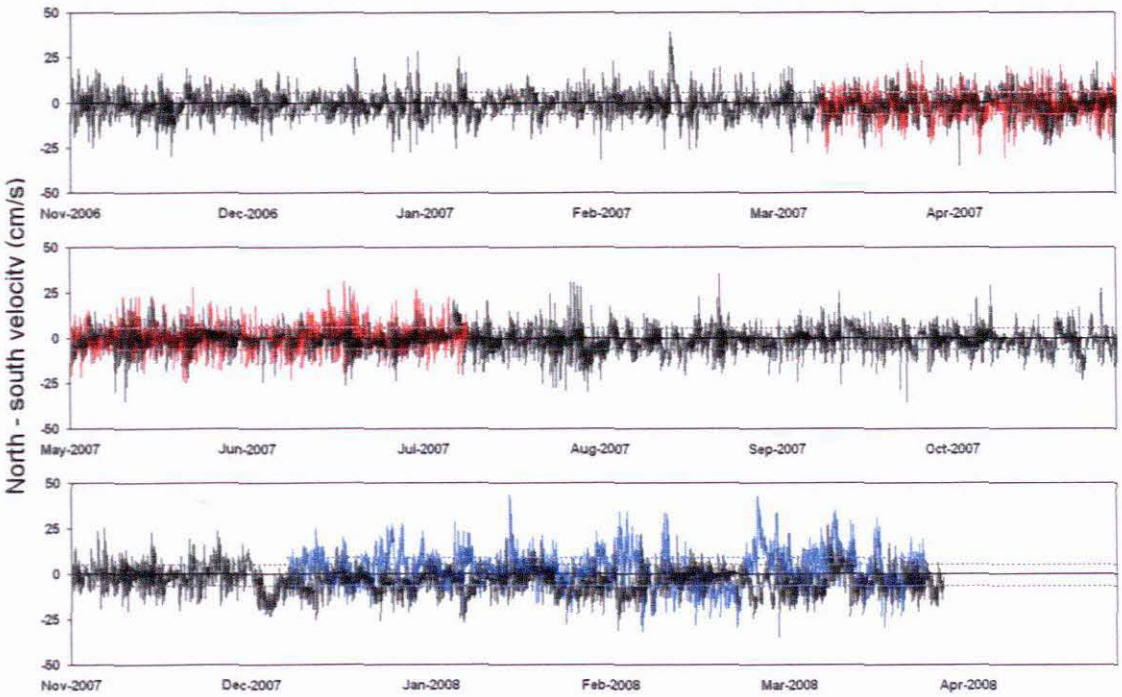

B4: North-south velocity of the ADCP measured bottom currents at Middelbank (black), Groot River East (red) and Thyspunt (blue). Positive y-axis values denote eastward flow and negative values denote westward flow. Average velocities are represented by the dotted lines.

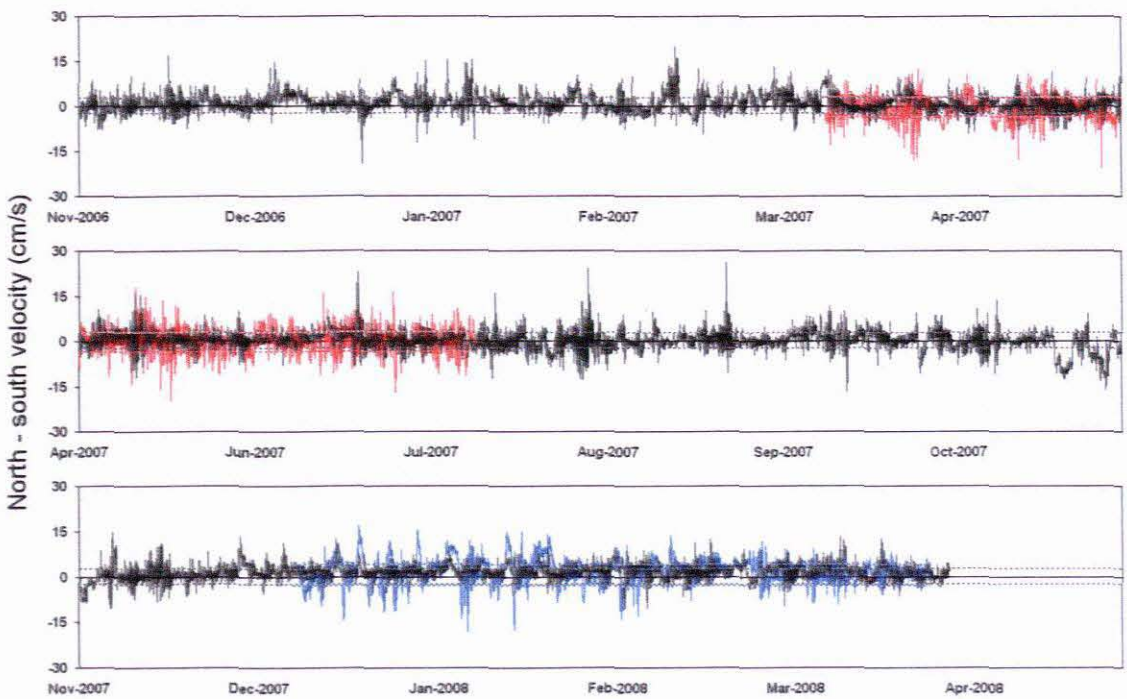

Appendix C

C1: Sea surface temperature at (7 m) recorded at Storms River Mouth (black) and Moster's Hoek (red) between November 2006 and March 2008.

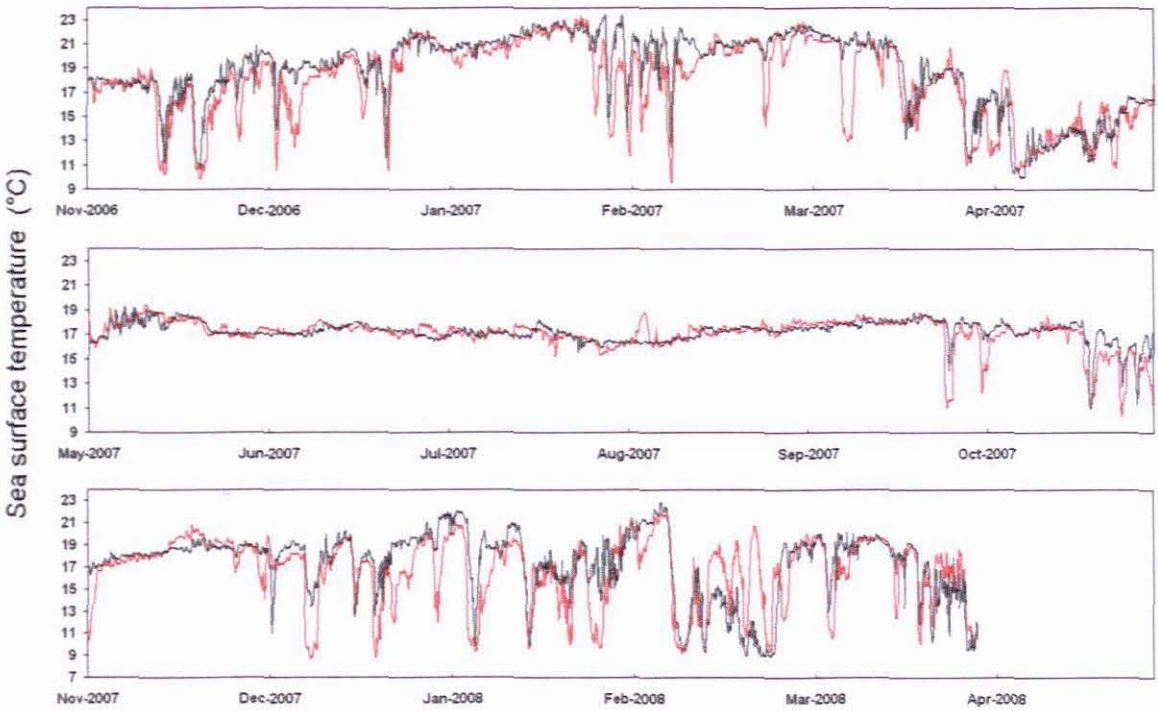

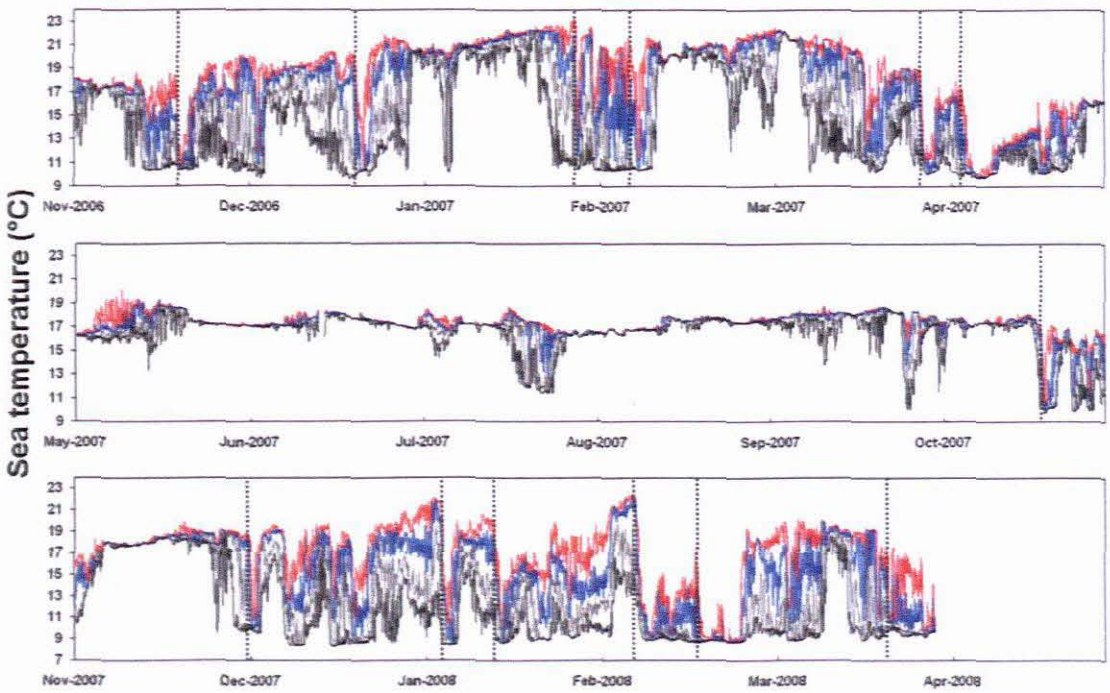

C2: Vertical profile of the sea temperature recorded at Middelbank between November 2006 and March 2008. Approximate depths of the measurements are 35 m (black), 27 m (grey), 19 m (blue) and 12 m (red). Surface and bottom currents were investigated during the upwelling events indicated by the dashed lines.

Appendix D
D1: Beaufort wind scale

Beaufort number	Beaufort description	Sea conditions	wind speed $m.s^{-1}$	wind speed knots
0	Calm	Sea like a mirror.	< 0.3	< 1
1	Light air	Ripples without crests.	0.3 – 1.5	1 – 2
2	Light winds	Small wavelets. Crests of glassy appearance, not breaking.	1.6 – 3.4	3 – 6
3	Gentle winds	Large wavelets. Crests begin to break; scattered whitecaps.	3.4 – 5.4	7 – 10
4	Moderate winds	Small waves with breaking crests. Fairly frequent white horses.	5.5 – 7.9	11 – 15
5	Fresh winds	Moderate waves, taking a more pronounced long form. Many white horses. Small amount of spray.	8.0 – 10.7	16 – 20
6	Strong winds	Long waves begin to form. White foam crests are very frequent. Some airborne spray is present.	10.8 – 13.8	21 – 26
7	Moderate gale	Sea heaps up. Some foam from breaking waves is blown into streaks along wind direction. Moderate amounts of airborne spray.	13.9 – 17.1	27 – 33
8	Gale	Moderately high waves with breaking crests forming spindrift. Well-marked streaks of foam are blown along wind direction. Considerable airborne spray.	17.2 – 20.7	34 – 40
9	Strong Gale	High waves whose crests sometimes roll over. Dense foam is blown along wind direction. Large amounts of airborne spray may begin to reduce visibility.	20.8 – 24.4	41 – 47
10	Storm	Very high waves with overhanging crests. Large patches of foam from wave crests give the sea a white appearance. Considerable tumbling of waves with heavy impact. Large amounts of airborne spray reduce visibility.	24.5 – 28.4	48 – 55
11	Violent storm	Exceptionally high waves. Very large patches of foam, driven before the wind, cover much of the sea surface. Very large amounts of airborne spray severely reduce visibility.	28.5 – 32.6	56 – 63
12	Hurricane	Huge waves. Sea is completely white with foam and spray. Air is filled with driving spray, greatly reducing visibility.	> 32.7	> 4